OPTIMAL PROTECTION MEASURES FOR CONTROLLING RIVER BANK EROSION

A thesis submitted

in partial fulfillment of the requirements for the award of the degree of

DOCTOR OF PHILOSOPHY

By

Hriday Mani Kalita

DEPARTMENT OF CIVIL ENGINEERING
INDIAN INSTITUTE OF TECHNOLOGY GUWAHATI
GUWAHATI-781039, ASSAM, INDIA
JULY, 2014

Dedicated to my

beloved

parents & family

Certificate

It is certified that the work contained in the thesis entitled "**Optimal protection measures for controlling river bank erosion**" by Hriday Mani Kalita, Roll Number 10610417, a student in the Department of Civil Engineering, Indian Institute of Technology Guwahati for the award of the degree of Doctor of Philosophy has been carried out under our supervision and that this work has not been submitted elsewhere for a degree.

Arup Kumar Sarma
Professor
Department of Civil Engineering
Indian Institute of Technology Guwahati
Guwahati-781039, Assam, India
July, 2014

Rajib Kumar Bhattacharjya
Associate Professor
Department of Civil Engineering
Indian Institute of Technology Guwahati
Guwahati-781039, Assam, India
July, 2014

Acknowledgements

I would like to place on record my deep sense of gratitude and sincere thanks to my thesis supervisors **Dr. Arup Kumar Sarma**, **Professor, Department of Civil Engineering,** Indian Institute of Technology Guwahati and **Dr. Rajib Kumar Bhattacharjya, Associate Professor, Department of Civil Engineering,** Indian Institute of Technology Guwahati for their invaluable guidance and full hand cooperation throughout the all aspects of this research work. I also admire their patient explanation of the concepts and basic principles.

I would also like to put on record my heartfelt thanks and reverence to the chairman of the Doctoral Committee, **Dr. Sudip Talukdar, Professor, Department of Civil Engineering,** Indian Institute of Technology Guwahati, for his valuable suggestions and help at various stages of this research work. I am indebted to **Dr. Suresh A. Kartha, Associate Professor, Department of Civil Engineering,** Indian Institute of Technology Guwahati and **Dr. Sashindra K. Kakoty, Professor, Department of Mechanical Engineering,** Indian Institute of Technology Guwahati, for their keen interest, valuable suggestions and guidance provided to complete this work as members of the Doctoral Committee.

My sincere thanks are also due to all the **Faculty members** of **Water Resources Engineering and Management,** Indian Institute of Technology Guwahati for their keen interest and suggestions.

I would also like to acknowledge the help and logistic support provided by **Water Resources Department, Govt. of Assam** during the field investigation.

I express my sincere thanks to the **staff members** of the **Civil Engineering Department,** Indian Institute of Technology Guwahati for their kind cooperation during my work.

It is virtually impossible to name all my friends and well wishers with whom I shared many happy moments during my stay at Indian Institute of Technology Guwahati, but I would be failing in my duty, if do not take the names of **Rajib Lochan Deka, Wazir Alam, Nabarun Debsharma, Sandeep Chaurasia, Rajesh Kumar Paswan, Vishal Deshpande, Sudarshan Patowary, Ratan Sarmah, Debraj Biswas, and Abhijit Deka** for their good wishes, help and support at various phases of this study.

I would also like to offer my love, admiration and respect to **my parents** and **other family members** for their love, blessings and moral support without which this work probably would not have seen the light of the day. I have great pleasure to convey sincere thanks and gratitude to my wife **Mainu** for her continuous support, patience and encouragement throughout my thesis period.

Finally, to the Almighty God who has seen me this far!

Hriday Mani Kalita

Indian Institute of Technology Guwahati

Abstract

Use of structural measures for controlling a river to minimize its devastating effect and to utilize the river for the benefit of mankind is a common practice all over the world. These structures are generally called river training works. Spur dike or groyne is one of the important river training structures generally applied to train the flow with various objectives. Some of such objectives are, reduction of flow velocities at certain location to promote sedimentation or to protect river bank from erosion, deflecting or repelling the flow away from the bank for its safety, increasing flow depth to facilitate navigation, to create recreational reach and achieving vibrant but stable near-bank channel for river front development. As groynes are very expensive, their optimal combination in terms of number, position and length should be taken up to reduce the total construction cost of the project. It necessitates an optimization model to determine the optimal combination of groynes to have desired training on a river reach at minimum total construction cost.

For obtaining the optimal combination of groynes, it is necessary to incorporate the hydrodynamic flow model with the optimization model. For selecting the best numerical technique in terms of stability, robustness, accuracy and computational complicacy and computational time, four different finite difference based numerical techniques have been considered in the study. The four methods considered are, Lax diffusive explicit scheme, MacCormack explicit predictor corrector scheme, Modified predictor corrector explicit scheme and implicit Beam and Warming scheme. The governing equations are solved on a boundary fitted coordinate system leading to accurate simulation in case of non rectangular flow domain at less computational effort. The results obtained with all the schemes are compared with several experimental and hypothetical results. From the comparisons of results, it appears that though the Beam and Warming scheme takes more computational time it can precisely simulate various flow scenarios including hydrograph routing, subcritical flow, supercritical flow, mixed flow and flow around groynes.

The optimization model developed in this study determines the optimal combination of groynes leading to minimum total construction cost to achieve a desired target speed value on a predefined area within a river. One of the formulations of this optimization model can also minimize the flow speed on a predefined area within a river for known number of groynes. To

handle the integer nature of the variables in the present non linear non convex optimization model, the model is solved using binary coded Genetic Algorithm.

The present methodology is developed by linking the hydrodynamic flow simulation model with the binary coded Genetic Algorithm. To evaluate the performance of the proposed model, it is applied for three different test problems which include a straight hypothetical channel, a meandering hypothetical channel and a hypothetical braided channel. The evaluation of results shows that the model is capable to handle diverse situations and has the potential for field applications.

To evaluate the field applicability of the proposed model, it is applied on a vulnerable river reach of Brahmaputra. The results of the proposed model are compared with the results obtained from traditional iterative based approach for determination of optimal groyne combination. The comparison has revealed the potential applicability and the advantage of the proposed model over traditional approach.

Though computational time required for such Genetic Algorithms based linked simulation-optimization model is high, this may not be considered as a limitation, as number of alternatives tested during the computational procedure is enormous. Test of such large alternatives would have otherwise taken much more time and effort as compared to the time required by the model.

Contents

List of figures

List of tables

List of notations

A = Area of flow

A1 = Jacobian of flux matrix for 1D governing equation

A2 = Jacobian of flux matrix in flow direction for 2D transformed governing equation

b = Width of Rozovskii channel

B1 = Jacobian of source matrix for 1D governing equation

B2 = Jacobian of flux matrix across flow direction for 2D transformed governing equation

C = Total construction cost of groyne system

Cz = Chezy roughness coefficient

CN = Courant number

CS = Artificial viscosity coefficient for predictor corrector schemes

CT = Artificial viscosity coefficient for Beam and Warming scheme

C1 = Per meter run construction cost of groyne

D = Artificial viscosity parameter for predictor corrector schemes

E1 = Flux matrix in flow direction for 1D governing equations

E2 = Flux matrix in flow direction for 2D governing equations

F2 = Flux matrix across flow direction for 2D governing equations

g = Acceleration due to gravity

h = Water depth

H = Water level

i = Grid points in flow direction

I1 = Identity matrix of size 2 by 2

I2 = Identity matrix of size 3 by 3

j = Grid points in transverse to flow direction

K = Source matrix for 2D transformed governing equations

k = Grid points in time direction

L = Matrix of conserved variables for 2D transformed governing equations

Lc = Corrected conserved flow variables for 2D transformed governing equations

Llg = Length of groyne on left bank

Lp = Predicted conserved flow variables for 2D transformed governing equations

Lrg = Length of groyne on right bank

L* = Intermediate increment of conserved flow variables in Beam and Warming scheme for 2D transformed governing equations

L** = Final increment of conserved flow variables in Beam and Warming scheme for 2D transformed governing equations

M = Flux matrix in flow direction for 2D transformed governing equations

n = Manning's roughness coefficient

nn = Computational flow direction in MIKE21C

N = Flux matrix across flow direction for 2D transformed governing equations

Ng = Total number of groyne

p = Mass fluxes in flow direction in MIKE21C

P = Wetted perimeter of flow area

Plg = Position of groyne on left bank

Prg = Position of groyne on left bank

q = Mass fluxes in transverse direction in MIKE21C

Q = Discharge

Q2 = Jacobian of source matrix for 2D transformed governing equation

RHS = Right hand side of force balance equation in MIKE21C containing Reynolds stress, Coriolis force and Atmospheric pressure

R_{nn} = Radius of curvature of computational direction

R_{ss} = Radius of curvature of computational direction

s = Distance along center line for Rozovskii channel

ss = Computational flow direction in MIKE21C

S_{fx} = Friction slope on x direction

S_{fy} = Friction slope in y direction

S_{ox} = Bed slope in x direction

S_{oy} = Bed slope in y direction

S1 = Source matrix for 1D governing equations

S2 = Source matrix for 2D governing equations

t = time

u = Velocity component in flow direction in Cartesian coordinate

U = Velocity component in flow direction in boundary fitted coordinate

UU = Maximum flow speed on the predefined area

U1 = Vector of conserved variables for 1D governing equations

U1* = Increment of conserved flow variables in Beam and Warming scheme for 1D governing equations

U1c = Corrected conserved flow variables for 1D governing equations

U1p = Predicted conserved flow variables for 1D governing equations

U2 = Vector of conserved variables for 2D governing equations

v = Velocity component in transverse direction in Cartesian coordinate

V = Velocity component in transverse direction in boundary fitted coordinate

W = Resultant velocity

x = Cartesian coordinate

y = Cartesian coordinate

$\bar{\mathbf{y}}$ = Distance from the top water surface to the centroid of the flow area

J = Jacobian of coordinate transformation

Δt = Time step

Δx = Grid spacing in x direction

$\Delta \eta$ = Grid spacing in η direction

$\Delta \xi$ = Grid spacing in ξ direction

γ = Parameters of Beam and Warming scheme

θ = Parameters of Beam and Warming scheme

ε = Artificial viscosity parameter for predictor corrector schemes

η = Body fitted coordinate

ξ = Body fitted coordinate

ω = Artificial viscosity parameter for predictor corrector schemes

Ω = Target speed value

List of abbreviations

1D = One Dimensional

2D = Two Dimensional

3D = Three Dimensional

ADI = Alternate Direction Implicit

CFL = Courant Friedrichs Lewy

FDM = Finite Difference Method

FEM = Finite Element Method

FVM = Finite Volume Method

GA = Genetic Algorithm

GIS = Geographical Information System

GPS = Geographical Positioning System

LP = Linear Programming

MSL = Mean Sea Level

NLP = Non Linear Programming

PSO = Particle Swarm Optimization

QP = Quadratic Programming

SLP = Successive Linear Programming

TVD = Total Variation Diminishing

CHAPTER 1

INTRODUCTION

1.1 Purpose of study

Engineering measures taken up for guiding flow of a river in a manner beneficial to mankind are referred as river training work. Structures like spur dikes, groyne, and bandelling are generally applied to train the flow with various objectives, which include reduction of flow velocities at certain location to promote sedimentation or to protect river bank from erosion, deflecting/repelling the flow away from the bank for its safety, increasing flow depth to facilitate navigation and achieving vibrant but stable near-bank channel for river front development. To attain the targeted velocity or depth at a given location spur dikes or groynes can be arranged in numerous combinations in terms of their number, length and spacing. As these structures are costly, most optimal combinations should ideally be used. Recourse is generally made to mathematical model study to arrive at the best combination, as physical model study has limited scope of testing large number of alternatives because of time and cost constraints. Though mathematical model study has a better opportunity of studying more alternatives compared to physical model, yet cannot give a true optimal solution. Generally some potential alternatives are chosen on the basis of experience and tested by mathematical simulation to compare their relative performance. Based on such comparative study the combination that satisfies the required constraints of velocity/depth at minimum cost is selected from the chosen alternatives for implementation. This approach therefore does not guarantee the most optimal solution and chance of arriving at a near optimal solution depends a lot on the modeler's experience. To avoid such subjectivity, it is intended to develop an optimization model which can automatically evaluate the optimal combination of groynes for achieving control over a river reach at minimum cost. The main aims of the project can be briefly summarized as given below:

i. To develop mathematical models capable of simulating free surface flow using different numerical methods and to apply them for analysing performance of river training work, more precisely the groyne, to select the best one.
ii. To develop a linked simulation-optimization model that can automatically determine the most optimal combination of groynes for achieving control over a river reach.

iii. To assess applicability of the proposed linked simulation-optimization model in a large braided river for determining optimal combination of groynes to protect its vulnerable bank and to compare its performance with traditional iterative approach.

1.2 Organization of the thesis

The entire work has been divided into several phases and is presented in different chapters as given below.

In chapter 2, a brief review on the past works done on solution of the unsteady free surface flow equations along with various studies for flow simulation around groyne are presented. It also contains some of the past studies done on application of optimization models to various water resources related problems.

Chapter 3 contains details of the governing equations used in this study for simulating 1D and 2D unsteady open channel flow. The transformation of the 2D governing equations to a general coordinate system for their application in complex flow domains is also presented in this chapter.

Performance of different numerical schemes in solving the governing equations both in 1D and 2D cases are analyzed and presented in chapter 4. Applicability of these models for analyzing performance of river training work, more precisely the groyne, has also been shown in this chapter.

Chapter 5 contains the details of the linked simulation optimization model developed using binary coded Genetic Algorithm (GA) for determining optimal combination of groyne leading to minimum construction cost subject to some given constraint.

Chapter 6 presents the practical application of the linked simulation-optimization model for protecting a vulnerable reach of river Brahmaputra and the results obtained are compared with the results obtained from iterative approach of finding best solution from some chosen alternatives.

A general discussion and conclusion on the entire research work along with some outline for future study, are presented in the last chapter, i.e., in the chapter 7.

CHAPTER 2

LITERATURE REVIEW

2.1 Introduction

Research work envisaged in this study will basically involve modeling of unsteady free surface flow for analyzing effect of groyne on the flow and application of optimization technique to determine optimal combination of groyne to have the desired effect at minimum cost. Therefore, knowing past research works done on free surface flow modeling along with groyne simulation and application of optimization technique in the field of water resources is essential for taking this study forward in a right direction. Review of the past work has therefore been grouped into three parts:

i. Review of work on mathematical modelling of free surface flow.
ii. Review of work on flow simulation around groyne.
iii. Review of work on application of optimization technique in the field for water resource engineering.

2.2 Past works on modeling unsteady free surface flow

The governing equations of unsteady free surface flow is a set of conservation of mass and momentum equations first proposed by Saint Venant in 1871 (Chaudhry 2008). These equations, also called shallow water wave equations, are a set of non-linear first order hyperbolic partial differential equations. Since these equations are very complex and difficult to solve analytically without large number of approximations, they are generally solved using numerical techniques.

2.2.1 Method of characteristics

The method of characteristics is a technique for solving partial differential equations of first order. It is also applicable for hyperbolic partial differential equation. In this method the partial differential equations are first reduced to some algebraic equations and then solved from some initial data.

Starting from the characteristics equations, Ritter (1892) made the first attempt to solve the Saint Venant's equations analytically for a frictionless horizontal channel for simulation of dam break flow (Saikia 2007). Ritter gave explicit expressions for water depth and velocity of flow from a dam site. An attempt was made by Dressler (1952) for solution of the combined Saint Venant's equations along with Chezy resistance equation using method of characteristics for simulation of flood wave due to braking of a dam in a horizontal rectangular channel. A series of experiments were conducted in National Hydraulic Laboratory in Washington to check the performance of the proposed model and it performed well. Isaacson et al. (1954) extended the method of characteristics for routing hydrograph in a real field problem. They solved the 1D unsteady free surface flow equations to simulate the unsteady flow in Ohio River and the confluence of Ohio River and Mississippi river in USA. They assumed that the slope and width of the rivers is constant and the bed is horizontal conforming to the actual values. Using this simplified assumptions they routed hydrographs through the rivers and the confluences. Leendertse (1967) first used the method of characteristics for the solution of 2D unsteady free surface flow equations. The main objective of that study was to simulate the water wave propagation generated by large nuclear explosions near the surface of the ocean or under water. He applied this model for the Tokyo Bay in Japan and Haringvliet estuary of Rhine River in Netherland to assess the tide levels. When compared with known measured tide levels on those areas it was observed that the proposed model has ability to produce good results. Method of characteristics was modified by Huang and Charles (1985) to solve the Saint Venant's equations for the simulation of unsteady open channel flow. After comparing with the experimental results it was concluded that the stability increases as the energy slope term is treated more implicitly and more fully. Another very important outcome of the study was that the most stable scheme is not necessarily the most accurate.

2.2.2 Finite difference method

Method of characteristics was used extensively by many researchers in 1960s. However when some bores or shocks are present in the flow, method of characteristics fails. To overcome this problem, finite difference method was introduced. It consists of approximating the differential operator by replacing the derivatives in the governing equation using differential quotients. At

the same time the domain is partitioned in space and time and approximations of the solution are computed at the space or time points.

Hughton and Kasahara (1967) introduced one of the first mathematical models; using finite difference method for solution of the 1D unsteady free surface flow equations. They simulated the steady flow over a ridge by solving the governing equations using Lax Wendroff finite difference scheme. By varying the ridge height and the approach velocity they obtained three different zones in the graph of approach velocity versus ridge height. In the zone where ridge height is less and approach velocity is more and in the zone where ridge height is less and the approach velocity is also less they did not observe any hydraulic jump. Sharp and Moore (1976) gave the step by step solution procedure for solution of the Saint Venant's equations using three different finite difference schemes namely, Leap Frog, Lax Diffusive and Lax Wendroff schemes.

Kalkwijk and Devriend (1980) are one of the first researchers, who used the finite difference method for solution of the 2D depth averaged steady flow equations to simulate low depth steady flow in a bend channel. The governing equations were transformed into curvilinear coordinate system for easy application in bend channel. The simulated results were validated with experimental study done in Delft Hydraulics Laboratory of Delft University of Technology in Netherland. Three second-order accurate explicit finite difference schemes named MacCormack predictor corrector, Lambda, and Gabutti were introduced by Fennema and Chaudhry (1986) for the analysis of unsteady, free-surface flows in 1D having shocks or bores. They showed the need of artificial viscosity for removal of the numerical oscillations near the shock. They observed that Preissmann implicit scheme takes four to eight times the CPU time taken by these explicit schemes which are even easy to program. Bellos and Sakkas (1987) employed explicit predictor corrector scheme to solve the Saint Venant's equations in conservation form to compute the flood wave resulting from the total and instantaneous collapse of a dam in a broad rectangular channel. They compared the experimental and computational results in terms of wave front advance and stage hydrographs and observed a good agreement between these.

To overcome the stability problem associated with explicit scheme, Fennema and Chaudhry (1989) first used Beam and Warming scheme for solution of the 2D unsteady free surface flow equations. This implicit scheme was proposed by Beam and Warming (1976) for solution of the

2D inviscid Euler equation. This Alternate Direction Implicit (ADI) finite difference scheme is non iterative and is second order accurate in time. Using this implicit scheme, they simulated the bore formed due to partial breaching of dam and obtained very good results.

Miller and Chaudhry (1989) compared the results obtained by conservation and non conservation form of 1D Saint Venant's equations in simulating the bend channel flow. They used Lax diffusive scheme for the integration of the governing equations. To account for the super elevation of the water surface in the bend portion they used a formula based on absolute velocity of the wave, radius of curvature of the channel centerline and acceleration due to gravity. Comparison of results with experimental data showed that conservative form can produce better results.

Fennema and Chaudhry (1990) adopted the MacCormack predictor corrector scheme and the Gabutti scheme for solution of unsteady free surface flow equations in 2D. To demonstrate the application of these two schemes in hydraulic engineering, two typical problems were solved by them. In one of these problems, a strong bore is formed by partial breach of dam. While the second problem deals with gradually varied flows by allowing flood propagation through a channel contraction. The results obtained were compared with results of Beam and Warming scheme (Fennema and Chaudhry 1989) and good conformity was observed. Bellos et al. (1991) examined the 2D flood waves resulting from the instantaneous break of dams. The governing equations were transformed into an equivalent square grid to overcome the difficulties associated with determination of flow characteristics near the boundary. They adopted MacCormack predictor corrector scheme for the integration of the governing equations. They compared the computed results with experimental data and observed good conformity between them. Bhallamudi and Chaudhry (1992) solved the 2D depth averaged unsteady free surface flow equations in a transformed coordinate system by using the predictor corrector scheme to analyze flows in channel expansions and contractions. The unsteady flow model was used to obtain steady flow solutions by treating the time variable as an iteration parameter and letting the solution converge to the steady state. They compared the computed and measured results and observed that in cases where the assumption of hydrostatic pressure distribution is valid it can produce very good results.

Navarro et al. (1992) modified the popular MacCormack predictor corrector scheme for solution of 1D unsteady free surface flow equations. They added one extra step based on theory of total variation diminishing (TVD) which is capable of capturing sharp discontinuities without generating the spurious oscillations, the usual characteristics of second order schemes. They validated this methodology for various test cases containing hydraulic jump and bore, for which analytical solutions were available. Trapezoidal formulation of Beam and Warming scheme was first used by Molls and Chaudhry (1995) for solution of 2D unsteady free surface flow equations in boundary fitted coordinate system. They compared the results obtained with and without the effective stresses and observed that in many cases the effective stresses do not significantly affect the converged solution.

Simulation of channel flow along with floodplain flow was attempted by Rashid and Chaudhry (1995). The governing Saint Venant's equations were solved using the unconditionally stable Preissmann four point implicit finite difference scheme. For approximating the channel cross section they adopted two procedures. In the first approximation the flood plain was taken as storage only and in the second case it was assumed that entire channel section contributes to momentum flux. They applied this model for evaluation of time varying water depth along an experimental channel due to an upstream hydrograph and observed that first approximation gives better results.

Jin and Fread (1997) developed a characteristics based, upwind, finite difference explicit numerical scheme for solution of the Saint Venant's equations. After comparing it with the four point implicit scheme they found that this new scheme has advantages over the four point implicit scheme for some special unsteady flow situations having subcritical/supercritical and supercritical/subcritical interface. Molls and Zhao (2000) compared the explicit predictor corrector and implicit Beam and Warming schemes in simulation of supercritical flow in a channel with wavy sidewall. To accurately simulate the wavy sidewall, both models solved the 2D governing equations in transformed computational coordinates. Bottom friction was computed using the manning formula and the effective stresses were modeled with a constant eddy-viscosity turbulence model. Both the models were giving results having good agreements with experimental data. It was observed that, in Beam and Warming Scheme Courant number can be set up to 2.5; however in predictor corrector scheme it is limited to 1 only.

Wang et al. (2006) solved the Saint Venant's equations using a new technique called 4 point finite difference form of Muskingum Method for the simulation of open channel flow. In this method at first a nonlinear convection diffusion equation based on the Saint Venant's equations of continuity and momentum were discretized by mixing cell method. After that an iterative procedure was adopted for obtaining the flow discharge. The method developed was tested with both synthetic numerical examples and observed events and the results were compared with those of the Lambda scheme and the method of characteristics and it was observed that by this new scheme a good accuracy can be obtained. The simple kinematic and diffusive formations of the Saint Venant's equations in 1D were solved by Alhan and Medina (2007) using MacCormack predictor corrector scheme. The results obtained from this scheme were compared with the results of a modeling tool named SWMM (Storm Water Management Model), and good agreement between them was observed. Finally it was concluded that this method is excellent for discrete storm events because of its efficiency and accuracy.

Siviglia et al. (2008) proposed a new methodology for solution of the Saint Venant's equations along with Exner equation of sediment transport. They took a quasi conservative formation and solved the resulting governing equations using MacCormack predictor corrector scheme. They applied this proposed methodology for some cases including dam break flow for inviscid shallow water equations with available analytic solution, experimental mobile bed case and natural mobile bed case and good results were observed.

Bellos and Hrissanthou (2011) simulated the flood wave propagation due to break of a reinforced concrete dam. For this case, they solved the Saint Venant's equations using two second order accurate schemes named Lax Wendroff scheme and MacCormack predictor corrector scheme. The model was validated with results from an experimental dam break study. A triangular hump was placed on the channel bed just downstream of the dam to check the performance of the present model in case of undulating bed and it was observed that the model can reproduce the actual surface elevation favorably. The popular explicit predictor corrector scheme has been modified by Tsakiris and Bellos (2014) by incorporating artificial viscosity through a diffusion factor in order to avoid numerical oscillations. In the same model, a threshold of water depth is introduced in order to distinguish the wet and dry cells of the computational domain. The

presented model was validated with analytical solution, experimental results and with the output of another software package in real world flood simulation studies.

2.2.3 Finite element method

To overcome the problem of handling complex flow domain, finite element methods were proposed. The finite element method is a numerical technique for finding approximate solutions of partial differential equations. The solution approach is based either on eliminating the differential equation completely (steady state problems), or rendering the partial differential equation into an approximating system of ordinary differential equations, which are then numerically integrated using standard techniques such as Euler's method, Runge-Kutta method, etc. The finite element methods have the advantage of applicability in non rectangular complicated flow domain.

Katopodes (1984a) developed one of the earliest models employing Galerkin finite element method for solution of the Saint Venant's equation. The resulting model was second order accurate with respect to the time step and produces a clean, sharp jump structure that agrees favorably with the exact solution of some test problems. The same model was extended for 2D unsteady free surface flow equations by Katopodes (1984b). In this scheme central differencing was used in the time direction which makes the scheme second order accurate in time. This method was based on discontinuous weighing function which introduces upwind effect in the solution. The performance of the scheme was verified with various test problems. To effectively handle the dry bed case, Akanbi and Katopodes (1988) developed a finite element model for solution of the 2D unsteady free surface flow equations. They developed this numerical technique to simulate the flood wave propagation on initially dry land. The governing equations are transformed to an equivalent system valid on a deforming coordinate system and are solved by a dissipative finite element technique. The accuracy and the stability of the model were examined by comparing the results of the model with observed data from an experimental field test.

A modified version of Galerkin finite element scheme was proposed by Hicks and Steffler (1992) for simulation of open channel flow by solving the Saint Venant's equation. In this scheme, the spatial discretization of the system of equations was achieved through the use of

linear interpolation functions to approximate the behavior of the solution over each element. A stability analysis was done and it was observed that this scheme gives very high phase accuracy for a courant number 0.5 or less than it. Numerical tests were carried out to see the performance of this scheme and it responded well. Ambrosi et al. (1996) developed an unconditionally stable fractional finite element scheme to solve the unsteady depth averaged free surface flow equations in 2D conservative form. The unconditional stability was achieved by employing fractional step method to advance the time. They applied this model to the simulation of the flow of the Po River and satisfactory results were observed. Tisdale et al. (1998) attempted a comparative study between the kinematic and shallow water wave equations using stream line upwind and Galerkin finite element methods. From the study they observed that, streamline upwind and Galerkin solutions of the kinematic wave equation exhibited good agreement with an analytic solution for flow over an inverted cone. However, Galerkin solutions of the shallow water wave equations for inverted cone and bowl-shaped surfaces displayed oscillations in time and space, while the streamline upwind method exhibited no oscillatory behavior. Moreover, results generated by the streamline upwind method also agreed well with experimental datasets and MacCormack finite difference results.

Khan (2000) applied the finite element technique for dam break flow simulation. He solved the 1D unsteady flow equations to simulate the flow resulting from a sudden removal of a dam over an initially dry downstream bed. The governing Saint Venant's equations were solved using a Petrov Galerkin finite element scheme, where a Courant number of about 0.5 was suggested by the author to balance space and time errors. The proposed numerical scheme was verified against analytical and as well as experimental results.

Jia et al. (2001) extended the finite element model for 3D flow simulation in plunge pools. The k-ε turbulence model was used for modeling the turbulence process. The results simulated by the model proposed here agree reasonably well with experimental data.

Schwanenberg and Harms (2004) used Runge-Kutta discontinuous Galerkin finite element method for solution of 2D depth averaged shallow water equations. The major advantage of this scheme was that, the explicit time integration, which makes the method for the investigated flows computationally as efficient as comparable finite volume schemes. To confirm the accuracy of the proposed scheme they applied it for several steady transcritical and transient

flows and the results showed excellent agreement with analytical solutions. A modified version of Galerkin finite element scheme was proposed by Chen et al. (2007) for solution of Saint Venant's equations. In this scheme, the fully conservative form was developed by revising the boundary pressure term accounting for the topographic variation in the momentum equation. The proposed model showed good results when applied for steady flow in a diverging channel with hydraulic jump, dam break flow in a converging diverging channel and for unsteady flow in Oldman River in southern Alberta.

A comparison between the Runge-Kutta discontinuous Galerkin finite element method and the second order accurate finite volume method was done by Ghostine et al. (2010) for simulation of supercritical flow through crossroads of a city during flood time. Three key processes observed in that study were, prediction of the water depths, location of the right and oblique hydraulic jumps in the crossing and distribution of the flow discharges in the downstream branches. The proposed model was found to give better results than finite volume method by validating with experimental results. A numerical model based on finite element solution of kinematic wave and diffusion wave approximations of Saint Venant's equations, Geographical Information System (GIS) and Remote Sensing (RS) was developed by Shahapure et al. (2011) to simulate urban flooding process. The proposed model was applied for a catchment of Navi Mumbai in India for some known rainfall events for which measured data were available, and the model results were satisfactory.

A modified shock capturing upwind finite element method was proposed by Ali and Steffler (2012) for friction dominated steady state flow in 1D. For abruptly changing river bed, a modified combined friction parameter was proposed by them for practical application. They showed that, using this modified version the problem of abrupt change of water surface elevation due to non uniform bed can be avoided.

More recently, Rossell and Ting (2013) extended the finite element model for evaluation of contraction scour on the areas near the James River bridges near Mitchell in USA. From the study they observed that, channel meandering, the no-flow boundary condition imposed by the walls of the river valley and skewed roadway embankment, and the dense trees along the left bank are the three main factors that create the unique hydraulic conditions at the bridge site.

They also found that, the predicted scour depth was very sensitive to the critical shear stress and slope of the curve of erosion rate versus shear stress.

2.2.4 Finite volume method

To achieve the advantages of simplicity of finite difference and capability of handling complicated flow domain of finite element methods together, application of finite volume methods have been attempted recently for solving shallow water equations. The finite volume method is a method for representing and evaluating partial differential equations in the form of algebraic equations. "Finite volume" refers to the small volume surrounding each node point on a mesh. In the finite volume method, first of all volume integrals in a partial differential equation term are converted to surface integrals, using the divergence theorem. These terms are then evaluated as fluxes at the surfaces of each finite volume. Because the flux entering a given volume is identical to that leaving the adjacent volume, these methods are conservative.

Zhao et al. (1994) proposed a finite volume model for solution of the 2D unsteady free surface flow equations. The considered finite volume scheme was based on characteristic theory, first order accurate, and also shock capturing in nature. They applied it for two dam break problems and obtained satisfactory results. They also applied this model to a portion of the Kissimmee River basin in Florida for flow simulations and the results agreed well with the field data and laboratory data in a physical model study of this river reach conducted at the University of California, Berkeley. The viscous terms of the shallow water equations have first been considered in finite volume technique in the model developed by Anastasiou and Chan (1997). They implemented the solver on unstructured triangular meshes and the solution methodology was based upon Godunov type second order upwind finite volume formulation. The proposed model was validated for various example problems published in some journals and very good results were observed. Another second order accurate Godunov type finite volume scheme has been proposed by Mingham and Causon (1998) to solve the unsteady free surface flow equations. In this technique, the Riemann problem was solved using the two step Runge-Kutta time stepping scheme. They applied this method for several dam break problems including 1D dam break, circular dam break, oblique bore formation and partial dam break cases and very good quality results were observed.

Bradford and Katopodes (2001) developed a robust, efficient, and accurate model for computing 2D shallow water flow over initially dry, rough, porous and arbitrary terrain. In that model a predictor corrector type of time stepping was used in that model to make it second order accurate and the fluxes were computed with Roe's approximate Riemann solver. The proposed model was compared with various experimental data for 1D and 2D problems involving rough, impermeable, and permeable beds, including a poorly leveled basin and very good results were observed. In a river flow, lateral movement of boundaries take place due to flooding and erosion. To model this phenomenon, Bradford and Sanders (2002) extended the finite volume method for solution of unsteady free surface flow equations in 2D to simulate moving lateral boundaries caused by flooding or recession. The major advantage of this scheme was that it does not need artificial viscosity and is capable of handling moving boundaries. The proposed model has been successfully applied to the dry bed dam break problem as well as long wave run up in one and two dimensions. Wu (2004) solved the 2D governing equations of unsteady free surface flows along with the equation of non uniform sediment transport using finite volume approach. In that model, they incorporated the turbulent stresses using the depth averaged parabolic eddy viscosity model and the standard k-ε turbulence model. The proposed model was applied for various cases like channel aggregation, channel degradation, basin erosion and the east Fork River in Western United states and fine results were observed. Utilizing finite volume method in transformed non orthogonal curvilinear coordinate system Zarrati et al. (2005) developed a 2D hydrodynamic model, which is very good in handling complex mesh arrangements with high skewness in grid size. The proposed model was applied for three experimental meandering channels. The comparison of results with experimental data revealed that the predicted water surface elevation and the velocity distribution were well agreeing.

Nguyen et al. (2006) developed a 2D shallow water numerical model, which is based on the resolution of the shallow water equations using the unstructured finite volumes method, combined with Green's theorem technique. As the model was based on the Green's theorem, which is very suitable for resolving the shallow water equations with the presence of important source terms subjected to the bottom variation it was quite applicable for the calculation of river, estuarine, and coastal flows in which geometry, bathymetry, and diffusion effects, as well as Coriolis and wind forcing. The proposed model was validated for various experimental and actual field problems.

Blade et al. (2008) solved the Saint Venant's equations in 1D using finite volume technique, to correctly simulate the steady state water resting on irregular geometries. For the numerical technique they used Roe TVD type of finite volume technique. Results obtained were compared with experimental results and good resemblances were observed.

Kuiry et al. (2010) developed a coupled 1D-2D flood inundation model on unstructured triangular grids for representation of the slow rising river floods. The channel flow was assumed to be 1D and modeled by solving the Saint Venant's equations using finite volume scheme. Spread of excess flood water spilling over bank from the river onto the floodplains was assumed as 2D and computed using a storage cell model discretized into an unstructured triangular grid. Finally, the predicted extent of inundation for a flood event on a stretch of River Severn, United Kingdom, was found out using this model and found to have good resemblance with the actual one. Lai (2010) developed another 2D depth averaged unsteady free surface flow model using finite volume technique where the mass conservation is satisfied both locally and globally. The main advantage of the model was its hybrid mesh strategy. In this strategy, the main channel and important areas were represented with quadrilateral cells and the rest of areas were represented with triangular cells. Another advantages associated with this proposed methodology were that it can simulate steady and unsteady flows and is also applicable for subcritical, supercritical and transcritical flows. The model was validated for various analytical and experimental cases including subcritical flow in 1D, transcritical flow in 1D, flow diversion in 2D, flow in meandering channel and flow simulation in Sandy River Delta in Portland. Finite volume method was used for simulation of 2D dam break flow by Singh et al. (2011). The main advantage of this scheme was that no Riemann solution is needed here leading positivity of the flow depth over complex topography if the Courant number is kept less than 0.25. The model was verified against analytical results for water surface elevation and discharge for three benchmark test cases. A good agreement between analytical solutions and computed results was observed.

In a more recent study, Zhang et al. (2013) solved the coupled 1D Saint Venant's equation and solute transport equation for simulation of basin fertigation process. The advection upstream splitting method (AUSM) and central finite volume method were used for solution of the equations. The proposed model was validated with three field experiments. From the excellent

results they concluded that this type of model can be used as research and practical tool for the design and management of basin fertigation.

2.3 Modeling tools available for unsteady flow simulation

Some user friendly modeling tools have also been developed by various organizations and Institutes across the worlds in the past to simulate the channel flow by solving the unsteady free surface flow equations. Some of them are discussed briefly in the following paragraphs.

HEC-RAS is a computer program that models the hydraulics of water flow through natural rivers and other channels. The program was developed by the US Department of Defense, Army Corps of Engineers. For unsteady flow, HEC-RAS solves the full, dynamic, 1D Saint Venant's equations using an implicit finite difference method. It has found wide acceptance, since its public release in 1995. Ackerman and Brunner (2006) used HEC-RAS to find the inundation mapping of water surface profile results from a dam failure and hence to provide a preliminary assessment of the flood hazard for the South Fork Dam, Pennsylvania. Aggett and Wilson (2009) used HEC-RAS to find the inundation potential, the avulsion hazard potential and spatial distribution of other hydrologic and fluvial geomorphic processes for different flood events for the Naches River in Washington State, in USA. Adams et al. (2010) used modeling tool HEC-RAS for the generation of real time flood inundation maps and to improve visualization capabilities of flow dynamics for the mainstream of the Ohio River in North America.

MIKE11 is a 1D software package developed by Danish Hydraulic Institute (DHI), Denmark for simulation of flow, sediment transport and water quality in estuaries, river, irrigation system and similar water bodies. It solves the full Saint Venant's equations in 1D using finite difference implicit scheme. Many investigators have been using MIKE 11 for simulation of open channel flow. Stronska et al. (1999) developed a flood forecasting tool for the Odra River in Poland by simulating the flow using modeling tool MIKE11. Sole and Zuccaro (2005) simulated the flood wave propagation process for the city of Albenga in Italy by using MIKE 11. Cat and Duong (2007) used MIKE 11 to develop an unsteady model to assess the hydraulic regimes and flood mapping due to construction of a thermal power station at the Mong Duong estuary in Vietnam.

CCHE2D is a 2D hydrodynamic model for unsteady turbulent open channel flow and sediment transport simulations developed at the National Centre for Computational Hydro science and

Engineering (NCCHE), the University Of Mississippi School Of Engineering. It solves the full 2D Reynolds Averaged Navier Stokes equations using finite element technique. Duan et al. (2001) developed a methodology for the simulation of the alluvial channel migration process in a river bend using the depth averaged CCHE2D modeling tool. Hasan et al. (2007) simulated the flow process for the Muda River in Kedah, Malaysia using the 2D depth averaged mathematical model CCHE2D to find optimal design cross section of river, economic main river channel alignment and an environmentally sound river. Negm et al. (2010) used CCHE2D modeling tool to predict the life span of high Aswan dam reservoir in Egypt by studying the silting and scouring processes.

RIVER2D is a 2D depth averaged hydrodynamic and fish habitat model developed specifically for use in natural streams and rivers, developed at the University of Alberta with funding provided by: the Natural Sciences and Engineering Research Council of Canada, the Department of Fisheries and Oceans, Government of Canada, Alberta Environmental Protection, and the United States Geological Survey. It solves the 2D unsteady free surface flow equations using finite element technique based on a conservative Petrov-Galerkin up winding formulation. Koopaei et al. (2003) used the 2D depth averaged mathematical modeling tool RIVER2D to calculate the local shear velocity and roughness length for a reach of river Severn in U.K. by utilizing the velocity and turbulence measured at the actual field. Vasquez et al. (2005) used the 2D mathematical model RIVER2D, for transcritical flow, which has been coupled with a sediment transport model to simulate bed elevation changes in alluvial beds. Cubanova (2009) used the modeling tool RIVER2D, for designing of geometry of standard fish passes at any water structure for the streams of Slovak Republic.

MIKE21C is a 2D software package developed by the Danish Hydraulics Institute, in Denmark, used for simulating free surface flows, water quality, sediment transport and waves in rivers, lakes, estuaries, bays, coastal seas and other water bodies. It solves the 2D depth averaged unsteady free surface flow equations in curvilinear coordinates by finite difference implicit method. Hassan and Dibike (2000) used MIKE21C to simulate the confluence of the rivers Ganges and the Yamuna, situated in Bangladesh and showed its potential in river dredging and navigation studies. Hye and Jahan (2001) used MIKE21C to simulate Meghna River in Bangladesh to investigate the response to flow and sediment regime changes due to construction

of a road bridge upstream of an existing railway bridge. Beck and Basson (2008) used MIKE21C to determine the effectiveness of flushing of sediments during breaching, by investigating the breaching process at different water levels for the Klein river estuary in South Africa.

2.4 Past works on flow simulation around groyne

Groyne sometimes also called spur dike is a type of river protection measure generally made from the bank and towards central portion of a river for various purposes. Such purposes may be like prevention of bank erosion, creation of recreational zone by lowering the flow speed, guiding the flow to some desired direction etc. Inclusion of groyne in a flow field leads to many influences to the hydrodynamics and morphology of the river. Therefore the modeling of flow around groynes is a very important topic.

2.4.1 Experimental flow simulation around groyne

As reported by Molls et al. (1995), Mushtaq Ahmad in 1953 conducted one of the first experimental studies concerning flow around a groyne. He measured only the water levels around the groyne and reported a constant water level upstream of the groyne, a sudden drop at the nose, followed by a gradual recovery along the downstream side. Rajaratnam and Nwachukwu (1983) are the first researchers who measured flow velocity near the groyne in an experimental study conducted for observing turbulent flow near groynes. Conducting different cases by varying parameters like depth of flow, shape of the groyne etc. they observed that when a groyne is placed in a channel, it causes a significant disturbance to the flow for a short distance upstream and for a longer distance downstream. For all of the test cases it was observed that the maximum bed shear stress occurs near the nose of the groyne.

For mobile bed channel, Kuhnle et al. (1999) conducted a physical model study to predict the volume and geometry of the scour hole associated with a groyne. They varied the groyne length, flow depth, and shear velocity ratio in the experiments and found that these parameters significantly influence the volume of the scour hole. For overtopping flows, at higher flow depth to spur dike height ratios, the location of the maximum depth of scour changed from the upstream point of the groyne toward the channel bank and caused a secondary scour zone to form downstream of the groyne. For comparing scour associated with different angled groynes, Kuhnle et al. (2002) did an experimental study by considering groynes angled at 45^0, 90^0, and

135^0 to the downstream channel sidewall with contraction ratios of 0.125 and 0.250. Out of the three angles that they considered it was observed that, least erosion of the bed in the near bank region took place with groynes 90^0 angles, while the greatest volume of the scour hole was associated with the 135^0 groynes. Giri et al. (2004) did an experimental study in a meandering channel with smooth rigid bed channel to observe the flow and turbulence processes associated with groynes. In their study, they considered five different cases by changing the number, location and bearing of groynes and for all of them numerical models were also developed which later gave same results.

Uijttewaal (2005) did a comparative study between submerged and nonsubmerged groyne. Four different types of combination like, standard reference groynes, groynes with a head having a gentle slope and extending into the main channel, permeable groynes consisting of pile rows, and hybrid groynes consisting of a lowered impermeable groyne with a pile row on top were taken. From the study they observed that, the turbulence properties near and downstream of the groyne changes with respect to the changes with permeability and slope of the groyne head. It was further observed that, in case of submerged groyne, the flow becomes 3D in nature which will make it difficult to predict by applying depth averaged numerical models or by 3D models with a coarse resolution in the vertical direction.

Fazli et al. (2008) developed a physical model to study the scour and flow pattern around a groyne located in a 90° channel bend. They conducted different experiments by considering different locations, different lengths of the groynes with different values of discharge. After conducting the model study they observed that, the depth of scour hole is largely affected by the value of Froude numbers, lengths and the locations of groyne in the bend. Duan et al. (2009) did an experimental study to compare the flow simulation around groyne for rigid bed and mobile bed case. From the results they observed that the length of flow separation zone is lesser in case of scouring bed than that of rigid bed. For the scouring bed case it was observed that the scour is initiated at the areas near the upstream side of the groyne and advance in the zone of high shear stress induced by horse shoe vortices. The maximum scour depth was observed to be occurred on the areas where the shear stress is highest. For both erodible and non erodible beds the maximum bed shear stress was 6 to 8 times of the approaching flow.

Yossef and Vriend (2010) first did an experimental study to observe the sediment exchange between river and groyne field. They took both submerged and emerged groynes for investigation. In case of emerged groyne, it was observed that sediment is transported from the main channel to the groyne field due to the circulating flow. However, the sediment is transported from the main channel toward the groyne through the mixing layer in case of submerged groyne.

Vaghefi et al. (2012) conducted an experimental study to observe the geometry of the scour hole and topography of the bed around a T-shaped unsubmerged groyne. They conducted their experiments on a 90° bend channel. They observed the effects of various parameters like the length of groyne, the wing length of groyne, the location of groyne in the bend and the radius of bend on the bed topography of the channel and finally developed a equation for computing the scour parameters because of a T-shaped groyne.

In a more recent study, Dehghani et al. (2013) conducted experimental study in a straight channel for studying the scour depth associated with straight and L head groynes. From the results they observed that the maximum scour depth with L head groynes in upstream direction is less than that of with L head groynes in downstream direction and straight groynes. The distance of thalweg line from the L head groyne was observed less than straight groyne. At the same time the optimal angles of L head groyne with parallel wall in downstream direction and parallel wall in upstream directions were found as 110^0 and 60^0 respectively leading to less bed scouring.

2.4.2 Numerical flow simulation around groyne

Due to the advancements in computer power in the recent decades, mathematical modeling of groyne simulation has got attentions by many researchers. Tingsanchali and Maheswaran (1990) developed one of the first mathematical models capable of simulating flow around groyne. They used a hybrid finite difference scheme and an iterative method to solve the governing equations of flow and k-ε turbulence model. They observed that a correction factor is needed to be incorporated into the k-e turbulence model to improve the agreement between the computed and experimental data for a simulation study around groyne. A comparison between the Beam and Warming ADI scheme and MacCormack predictor corrector explicit scheme in case of 2D flow simulation around groyne was done by Molls et al. (1995). The effective stresses were modeled

by applying a constant eddy viscosity model. By comparing the results obtained with experimental data they observed that if the eddy viscosity can be estimated near the groyne, the constant eddy viscosity model produces results similar to those obtained with more advanced turbulence models.

Ouillon and Dartus (1997) simulated the three dimensional (3D) steady, shallow turbulent flow around a groyne in a rectangular channel by solving the Reynolds's equation along with k-ε turbulence model. The governing equations were solved using a hybrid finite volume method. Results of experimental studies done in Delft Hydraulic Laboratory in Netherland, Franzius Institute and the Institute for Fluid Mechanics and Computer Application in Civil Engineering at the University of Hannover in Germany were used to validate the present model. Comparisons in terms of water depth, reattachment length and resultant shear stress revealed the capability of the model.

Jia and Wang (1999) used the 2D modeling tool CCHE2D for simulation of hydrodynamic and morphologic processes around a groyne placed in a straight rectangular channel. To appraise the model applicability, they compared the results obtained by the model with the experimental results of Rajaratnam and Nwachukwu (1983) and obtained very conforming results. Eddy viscosity model of Smagorisky along with depth averaged 2D unsteady free surface flow equations was first tested by Bo et al. (2002) to numerically simulate the flow process around a non submergible groyne. For this case, the governing equations were solved using explicit finite volume Method. For validation of the model the computed results were compared with the experimental results done in Changsha Communication University in China and a good resemblance was observed.

Giri et al. (2004) developed an earlier 2D numerical model for simulation of flow process around groynes for meandering channel with rigid bed. The results were compared with experimental results and the effected flow property and turbulence property due to the groyne were well predicted by the mathematical model at less computational time. Hydrodynamic process along with suspended sediment concentration distribution in a groyne field was modeled by Duan and Nanda (2006). For simulation of the depth averaged suspended sediment concentration they solved the depth averaged 2D convection and diffusion equation. The validated model was applied in a practical case and it was observed that the depth averaged, 2D model can

approximately simulate the flow hydrodynamic field and concentration of suspended sediment near a groyne.

The 3D large eddy simulation model has been applied by McCoy et al. (2008) for simulation of flow hydrodynamics in a groyne system placed on a straight channel on one side. The proposed model was validated by comparing mean velocity and turbulent fluctuations data collected at the free surface for a previous experimental study. From this study they observed that, the transverse velocity distribution is strongly nonuniform over the depth at the groyne channel interface. Strong vertical eddies were also observed to be formed on both side of the interface. Yazdi et al. (2010) developed another 3D hydrodynamic model to observe the effect of groyne length on recirculation zone size and also to study the effect of bearing of groynes on maximum bed shear stress. The 3D flow process around groynes were studied using the 3D mathematical model FLUENT. By comparing the results with the data obtained from a flume, they observed that groyne of higher length produces larger recirculation zone. However maximum bed shear stress was observed in vertical groyne rather than groynes oriented upstream and downstream.

Mukherjee and Sarma (2010) determined the optimal combination of groynes in terms of their length, position and numbers, required for a vulnerable reach of river Brahmaputra in India. They took some predecided combinations and for each of the combinations they observed the hydrodynamic and morphologic effects on the river by simulating the combination using the modeling tool MIKE21C. Finally they found out the best combination out of all those predefined combinations from a comparative study of all of them. A similar type of study was also done by Alauddin and Tsujimoto (2012) to determine optimal configuration of groynes. For the simulation purpose, they used the 2D modeling tool RIC-Nays. They considered three different configurations of groyne system and observed three processes, erosion in channel bed, deposition in groyne field and the scour near groynes for all the configurations. Finally they found out the best configuration out of those three configurations for maintenance of navigation channel at low flow and bank protection at high flood as well.

Fredrik et al. (2013) conducted numerical simulation of groyne using 3D modeling code OpenFOAM to meet the ecological, economical and safety goals along with prevention of bank erosion and channel maintenance. They considered three different types of submerged groyne

such as, vertical groyne, L shaped groyne and wedge shaped groyne and observed that, wedge shaped groynes can perform very well in minimizing the flood depth.

2.5 Past works on optimization in the field of Water Resource Engineering

Optimization is the process of maximization of benefit from the available resources at minimum efforts. Research on applying optimization technique for obtaining optimal combination of river bank projection system is yet to take momentum. However, various optimization techniques have been applied by many researchers in the past for solving diverse problems related to water resource management. Some of such past works are presented in the following paragraphs.

Hall and Buras (1961) first proposed the application of dynamic programming to the optimization of serial reservoir system planning. They gave simple and general expressions for the highly complex problem of optimization of reservoir systems by casting the main problem into a series of far less complex problems. However in actual river system, the main and tributary channels always lead to non serial or branched reservoir systems. To overcome this problem Meier and Beightler (1967) attempted new optimization technique for branched reservoir system planning. In this technique the complex non linear optimization problem is decomposed into a sequence of simpler problems and then solved repeatedly. They observed that the proposed technique is less complex than the nonlinear programming formulation and is applicable to large scale system planning. Since then many optimization models have been developed for various problems in the diverse field of water resources engineering. Some of them are presented in the subsequent paragraphs.

Kleinecke (1971) used linear programming for estimation of the Geohydrologic parameters such as permeability and storage capacity for simulation of groundwater basin. In his model he minimized the maximum absolute value of error in the water balance given by Darcy's law. The estimated values of the preceding two parameters using the present technique were compared with the historical data for 11 years obtained by California State Department of Water Resources for Chino-Riverside basin. The comparison showed a good agreement though for better prediction they concluded that the historical data should cover a time span of 25 to 30 years.

Johnston and Pilgrim (1976) compared Direct Search Technique and Steepest Descent Technique for optimization of some watershed parameters in rainfall runoff simulation model of

watershed. The eight different parameters taken under considerations were capacity of interception store, capacity of upper soil store, capacity of drainage store, capacity of lower soil store, maximum evapotranspiration rate when the relevant soil store is full, fraction of evapotranspiration from upper soil store, daily infiltration rate when lower soil store is empty and empirical constant in the infiltration function. Their main objective was to minimize the sum of the squares of the differences between the total monthly computed and observed runoff values. Comparison of the assigned optimization techniques revealed that the Direct Search Technique is less susceptible to the non uniformity of the response surface than that of Steepest Descent Technique.

Nov and Golany (1979) proposed Dynamic Programming for optimal design of dam systems in rivers of arid and semiarid areas for recharging runoff water into the ground. In their study the objective was to maximize the volume of recharged water at minimum total construction cost of the system. The proposed model was aimed from the point of view of water scarcity in arid and semiarid climates, where the principal need is for water and not for flood control.

Gorelick et al. (1983) used multiple linear regression and linear programming for identification of locations and magnitudes of aquifer pollutant sources. In both the methodologies the objectives were to minimize various functions of differences between measured and simulated concentrations. For simulation of pollutant transport they used the governing equations of groundwater flow and solute transport. The proposed model was applied for two different hypothetical cases one being steady state and the remaining being unsteady case and for both the cases the performance of the model was observed satisfactory.

Guo and Hughes (1984) suggested a graphical method for determining optimal cross section of trapezoidal channel with consideration of freeboard. They gave some graphs relating the parameters like freeboard to water depth ratios, water depth, discharge values and side slope values. Using these graphs the corresponding water depth required for best hydraulic section can be computed from a given discharge for a trapezoidal channel of known side slope and freeboard to water depth ratios.

A new algorithm called Genetic Algorithm (GA), based on the mechanics of natural genetics was first introduced by Goldberg and Kuo (1987) to optimize both the design and operation of

pipeline systems. In the formulation of the optimization problem, their objective was to minimize the total power consumed by pumps maintaining discharge pressure and suction pressure within allowable limits. They applied GA for a hypothetical test case of 40 pumps in 10 pump stations along a serial pipeline and very good results were obtained. They further claimed that, GAs have a more global perspective than many engineering optimization procedures and can be extended to more complex, highly dimensional problems in the near future.

Lansey and Mays (1989) proposed a new methodology for determination of optimal design of water distribution system leading to minimum total construction cost. In this methodology they coupled nonlinear programming techniques with existing water distribution simulation models. In their optimization model they minimized the total cost by optimizing different decision variables such as head, diameter of pies, pump size, valve setting and tank volume. They applied this methodology for two different water distribution networks and showed the potential applicability of the model.

Kacimov (1992) applied a complex-variable method for minimization of seepage loss from trapezoidal and rectangular channels. He plotted some graphs between various channel and flow characteristics, which can help in designing channels for minimum values of seepage loss or minimum cost function for specified hydraulic characteristics such as area of cross section, hydraulic radius, and discharge.

Simpson et al. (1994) applied GA for optimization of pipe networks and the results obtained were compared with results from enumeration technique and non linear programming. They considered a case study network having some interesting features, including selection of diameters of five new pipes; three existing pipes may be cleaned or left alone; three demand patterns must be satisfied; and with two available supply sources. From comparison of the results they observed that GA technique is very effective in finding near optimal or optimal solutions in relatively few evaluations.

Liong et al. (1995) applied GA for accurate prediction of peak flows and/or runoff volumes from a catchment by evaluating optimal values of some catchment calibration parameters. The parameters that they considered are the overland flow, the depression storage, the initial infiltration rate, the ultimate infiltration parameters, the infiltration decay rate, the catchment

width, the percentage of the impervious area, and the catchment slope. They applied the model for Upper Buklt Tlmah Catchment in Singapore and good predictions were observed.

Reis et al. (1997) used GA for determining appropriate location of control valves in a water supply pipe network and their settings to have minimum leakage. Along with the objective of minimizing the leakage, the various constraints were; nodal mass balance, minimum acceptable head for the nodes, upper and lower bounds for valve openings and the Hazen-Williams equation that relates flow-head loss and pipe characteristics. The proposed model of valve location was used for a problem of 25 node network with 37 pipes. At first they minimized the leakage to obtain the valve settings for given valve locations, and then they maximized the leakage reduction to determine the optimal location of these valves. The results obtained from this study were validated with results from complete enumeration.

Wardlaw and Sharif (1999) applied GA for optimal reservoir system operation. The objective is to maximize the benefits from a reservoir system over 12 two hour operating periods. The corresponding constraints were the storage constraints, release constraints and continuity constraints. They applied this approach for example problems involving 4 and 10 reservoir, deterministic and finite horizon problems and obtained the optimal operating policies for these systems.

Das (2000) used optimization techniques for evaluation of optimal open channel cross sections with composite roughness leading to minimum construction cost. The constraints of the nonlinear optimization problem were the Manning's equation, positive values for design variables, and specified values of side slopes or top width. The constrained problem was transformed into an unconstrained problem using the Lagrangian multipliers and solution was obtained using the first-order necessary conditions for optima.

Barros et al. (2003) used non linear programming (NLP) for optimization of Large-Scale Brazilian hydropower system operations. Six different objective functions were; minimizing the loss of the stored potential energy; minimizing storage deviations from targets; maximizing total energy production; minimizing spilled energy; minimizing energy complementation and maximizing the profit derived from secondary energy. The performance of the NLP model was compared against the historical operational records. The results obtained were compared with the

results from linear programming (LP) and successive linear programming (SLP). It was observed that for planning purposes, the LP and the SLP models are sufficient. However the NLP model is the most accurate and particularly suitable for real-time operation.

Cho et al. (2004) applied GA to develop a water quality management model to achieve the water quality goals as well as to minimize the waste water treatment cost. The proposed management model was an integrated model where the water quality was simulated using the modeling tool Qual2e and the optimization model was developed using GA. They applied this water quality management model for the Youngsan River in South Korea to evaluate the treatment type and cost of the thirteen existing and thirteen planned plants in the river basin. From the result they observed that, advanced treatment must be carried out in five planned plants and nine existing plants and out of the thirteen planned plants, it is unnecessary to construct six and secondary treatment is sufficient for two other plants.

Ahmed and Sarma (2005) applied GA model for finding the optimal operating policy of a multi-purpose reservoir, located on the river Pagladia, a major tributary of the river Brahmaputra in India. The objective function considered in this study is minimization of squared deficit from demand. And the constraints were reservoir storage constraints, constraints of release from the reservoir and continuity constraints of the reservoir. The results were compared with the results obtained from Stochastic Dynamic Programming model and it was observed that GA performs better than Stochastic Dynamic Programming model in many aspects.

Bhattacharjya (2006) developed a nonlinear optimization model for evaluation of optimal channel cross section incorporating the critical flow condition at minimum construction cost. Manning's equation was used as constraint to specify the uniform flow condition in the channel. Another constraint was applied to prevent the flow from being critical. The developed non linear optimization model was solved by sequential quadratic programming using MATLAB. The proposed model was applied for a trapezoidal channel and good results were obtained.

Park et al. (2006) proposed a new integrated technique combining GA and Geographic Information System (GIS) for the design of an effective water quality monitoring network in a large river system. For selection of effective monitoring network five selection criteria such as representativeness of a river system, compliance with water quality standards, supervision of

water use, surveillance of pollution sources and examination of water quality changes were chosen and fitness levels were obtained through a series of calculations of the fitness functions using GIS data. By applying the proposed methodology to the design of water quality monitoring networks in the Nakdong River system, in Korea, they observed that only 35 out of 110 stations currently in operation coincide with those in the new network design. This study indicated that the effectiveness of the current monitoring network for that river system should be re-examined carefully.

Singh and Datta (2006) applied GA based linked simulation optimization approach for optimal identification of unknown groundwater pollution sources for simple as well as complex scenarios of multiple unknown groundwater pollution sources. For simulation of the physical flow and transport process an external model was linked to the GA based optimization model. The objective of optimal identification was achieved by minimizing the weighted sum of absolute differences between the observed and estimated concentrations in the system of interest. The developed model was applied for three different hypothetical test cases and it was observed that GA has a very good capability for these types of complex cases.

Travis and Mays (2008) developed a new methodology using dynamic programming to determine the optimal sizing and location of retention basins in a watershed leading to minimum construction cost of the project. The different types of constraints were incorporated in terms of minimum flow depth, area of retention basin, maximum permissible volume of water and infiltration characteristics. To check the applicability of the proposed model they applied it to a hypothetical watershed and the results showed that this methodology could allow substantial cost savings.

Pan and Kao (2009) applied optimization technique for evaluation of optimal sewer system at minimum construction cost. The proposed model was an integrated model of quadratic programming (QP) and GA. The decision variables were the diameter of the pipes and pumping station locations. However pipe slopes and pipe buried depths of each generated chromosome were determined using the QP model. Two associated constraints were the diameter must be large enough to transport the accumulated flow from the upstream pipes and the diameter of a downstream pipe must be larger than or equal to the diameter of its upstream counterpart. They applied the proposed model for a case study and obtained very good design alternatives.

Tang et al. (2010) used GA optimization technique for parameter optimization in simulating 1D river network flow using solution of Saint Venant's equation. The optimization method they developed minimizes the difference between the observed and predicted values of hydrodynamic parameters and simultaneously finds the optimal set of Manning's n values for the river network system considered. They applied the optimized parameters into a hydrodynamic numerical model, and a good agreement was attained between the simulated results and the field data.

Nicolini et al. (2011) used GA optimization technique for calibration and optimal leakage management for water distribution network. A multi objective approach was proposed where the first objective was to minimize the number of pressure release valves, while the second was to minimize the total leakage in the system. The main advantage of the model was that, one run of the model results in optimal set of parameters where both the cost of pressure valve installation is minimized as well as leakage from the system is minimized. By applying the developed model for a hypothetical case very good results were observed.

Qureshi et al. (2012) used LP for determination of optimum cropping pattern for available monthly canal water discharges and tube well pumpages to achieve maximum net benefits. Various constraints associated with this model are, net water requirements for crop, effective rainfall, canal water availability and tube well pumpages. They applied this methodology for an area near Jamal Shah secondary canal from Rohri main canal located in Nawabshah, Pakistan and established the potentiality of the model.

In a recent study Chang et al. (2013) developed a multi-objective optimization model for optimal utilization of water resources of the Tao River basin in China using a hybrid technique composed of particle swarm optimization and genetic algorithm (PSO-GA). The proposed model minimizes the water shortage and maximizes the hydro power production. Equality constraint for the model was obtained from water balance equation of the reservoir. However the bound constraints were reservoir storage, reservoir discharge and output power production. The results showed that the proposed hybrid algorithm can simultaneously obtain a promising solution and speed up the convergence.

2.6 Conclusions

From the review of the past works following observations have been made.

1. Solution of the governing equations of unsteady free surface flows remains a topic of continued interest since its development and quite a number of investigators have worked on various numerical techniques for solution of these equations for mathematical simulation of unsteady flow.
2. Out of the various available methods, finite difference method is one of the most popular and widely used methods for simulation of unsteady flow. Transformation of the governing equations to a boundary fitted coordinate system can result in efficient simulation in case of non regular flow domain.
3. A number of commercially/freely available softwares have been developed in the past for simulation of unsteady free surface. These softwares basically solve the governing equations describing unsteady free surface flow using different numerical techniques. Use of appropriate model parameter is essential for getting reliable results using these softwares. Therefore before applying these softwares emphasis should be given on calibration and validation of these models.
4. A large number of studies have been conducted in the past for simulation of flow process around groynes both numerically and experimentally. Similarly enormous literatures are also available for different optimization models developed for various aspects of water resources engineering. It has been observed that limited efforts have been made towards determination of optimal combination of groynes for various purposes.
5. A few studies have been obtained in the literature where some investigators have tried to determine the optimal combination of groynes. However, in all of these studies performances of some pre decided combinations have been tested by simulating the flow scenarios numerically/experimentally with each combination separately. Finally the best combination was found out by comparing the results of each combination. No literature has been found so far where effort is made for finding a true optimal combination of groynes by utilizing optimization model.
6. From the literature review it is found that, researchers are yet to put effort towards applying optimization technique for developing optimal river training system. Therefore, this research work is oriented towards developing a linked simulation

optimization model that can automatically determine the most optimal combination of river training works for achieving control over a river reach

CHAPTER 3

GOVERNING EQUATIONS

3.1 Introduction

The governing equations of gradually varied unsteady free surface flow are a set of hyperbolic partial differential equations and are extensively used for hydrodynamic simulations in rivers, lakes, estuaries and floodplains. These are basically continuity and momentum equations expressed in one dimensional, two dimensional or three dimensional forms depending on the situation to be modeled. To express the complex physical processes mathematically, several assumptions are made. Details of different forms of these governing equations along with the assumptions made in their derivation are presented in this chapter.

3.2 Assumptions made in the governing equations

Following assumptions are made in derivation of the equations describing unsteady free surface flows.

i. Flow is assumed to vary gradually along the channel so that the pressure distribution is hydrostatic and vertical acceleration can be neglected.
ii. The bottom slope of the channel bed is small so that the flow depth measured normal to the channel bottom and measured vertically are approximately the same.
iii. The channel bed is fixed. The effect of scour and deposition are negligible.
iv. The head losses in unsteady flow may be simulated by using steady state resistance laws, such as the Manning or Chezy equation .i.e. head losses for a given flow velocity during unsteady flow are the same as that during steady flow.
v. Fluid is incompressible and of constant density throughout the flow.
vi. Wind shear force caused by frictional resistance of wind against the free surface of water is negligible.

3.3 One dimensional (1D) representation

For prismatic channels having no lateral inflow or outflow the governing equations in 1D (Saint Venant's equation) can be written in matrix form as (Chaudhry 2008),

$$U1_t + E1_x + S1 = 0 \quad (3.1)$$

Where,

$$U1 = \begin{Bmatrix} A \\ Q \end{Bmatrix}$$

$$E1 = \begin{Bmatrix} Q \\ \frac{Q^2}{A} + gA\bar{y} \end{Bmatrix}$$

$$S1 = \begin{Bmatrix} 0 \\ -gA(S_o - S_f) \end{Bmatrix}$$

A is area of flow, Q is discharge, g is acceleration due to gravity, $\bar{y}$ is distance from the top water surface to the centroid of the flow area, S_o is bed slope, S_f is friction slope. Friction slope S_f is generally calculated using Manning's equation as given below,

$$S_f = \frac{Q^2 n^2 P^{\frac{4}{3}}}{A^{\frac{10}{3}}} \quad (3.2)$$

Where, P is wetted parameter of the flow area and n is Manning's roughness value.

For rectangular channel, equation (3.1) can be modified as,

$$U1_t + E1_x + S1 = 0 \quad (3.3)$$

Where,

$$U1 = \begin{Bmatrix} h \\ hu \end{Bmatrix}$$

$$E1 = \begin{Bmatrix} hu \\ hu^2 + \frac{gh^2}{2} \end{Bmatrix}$$

$$S1 = \begin{Bmatrix} 0 \\ -gh(S_o - S_f) \end{Bmatrix}$$

h is flow depth, u is velocity, g is acceleration due to gravity, S_o is bed slope and S_f is friction slope. Equation (3.3) is also valid for wide rectangular channel provided the friction slope is modified as,

$$S_f = \frac{n^2 u^2}{h^{\frac{4}{3}}} \tag{3.4}$$

3.4 Two dimensional (2D) representation

Using vertically depth averaged velocity, neglecting vertical acceleration, lateral inflow, wind shear, eddy loss and assuming that effective shear stress is dominated by bottom shear stress & small channel bottom slope, 2D governing equations of unsteady free surface flows can be derived from three dimensional Navier Stokes equation. These equations in matrix form can be written as (Chaudhry 2008),

$$U2_t + E2_x + F2_y + S2 = 0 \tag{3.5}$$

Where,

$$U2 = \begin{Bmatrix} h \\ hu \\ hv \end{Bmatrix}$$

$$E2 = \begin{Bmatrix} hu \\ hu^2 + \frac{gh^2}{2} \\ huv \end{Bmatrix}$$

$$F2 = \begin{Bmatrix} hv \\ huv \\ hv^2 + \frac{gh^2}{2} \end{Bmatrix}$$

$$S2 = \begin{Bmatrix} 0 \\ -gh(S_{ox} - S_{fx}) \\ -gh(S_{oy} - S_{fy}) \end{Bmatrix}$$

h is flow depth, u is velocity component in x direction, v is velocity component in y direction, g is acceleration due to gravity, S_{ox} & S_{oy} are the bed slopes in x direction and y direction

respectively, S_{fx} & S_{fy} are the friction slopes in x direction and y direction respectively. The friction slopes S_{fx} & S_{fy} are computed using Manning's equation as given below,

$$S_{fx} = \frac{n^2 u\sqrt{u^2+v^2}}{h^{\frac{4}{3}}} \tag{3.6}$$

$$S_{fy} = \frac{n^2 v\sqrt{u^2+v^2}}{h^{\frac{4}{3}}} \tag{3.7}$$

3.5 Governing equations in boundary fitted coordinate system

In real field problem, many a time the computational domain is irregular in shape. To handle the irregular shape of the domain, a body fitted coordinate system is needed. This greatly simplifies the application of boundary conditions in the numerical model used to solve the equations.

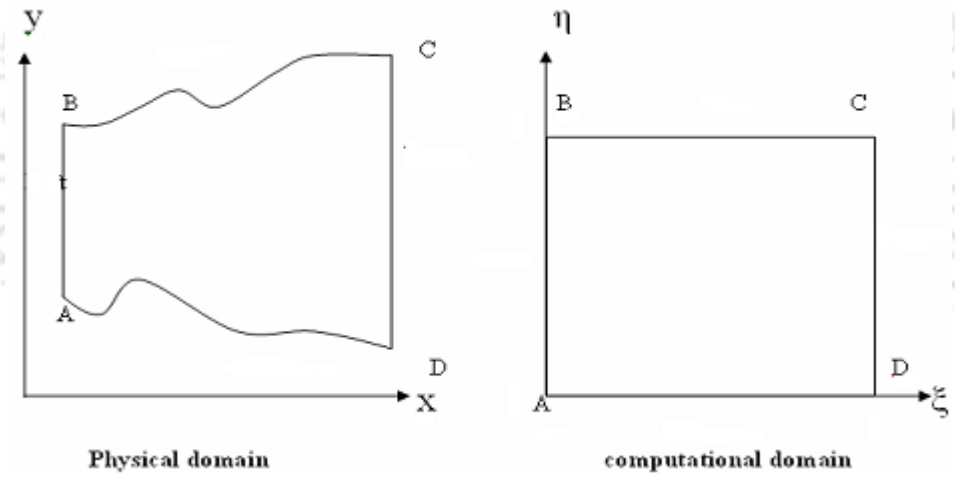

Figure 3.1 Physical and computational domain

Let us consider a simply connected irregular physical domain as shown in the figure 3.1 with physical coordinates (x, y). Let the computational domain be in coordinates (ξ, η). The transformations process given by Anderson et al. (1984) is applied in this project as given below,

For two dimensional unsteady flow the independent variables in physical space will be (x, y, t) and these are to be transformed to another set of independent variable (ξ, η, τ),

Where,

$\xi = \xi(x, y)$ (3.8)

$\eta = \eta(x, y)$ (3.9)

$\tau = (t)$ (3.10)

The equations (3.8), (3.9) and (3.10) represent the transformation. For practical application the transformation given by above equations must be given some type of specific analytical relation or sometimes a specific numerical relation. In the above equation τ is considered to be a function of t only and here it is given by $\tau = t$. From equations (3.8) and (3.9) writing the exact differential,

$$d\xi = \frac{\partial \xi}{\partial x} dx + \frac{\partial \xi}{\partial y} dy \tag{3.11}$$

$$d\eta = \frac{\partial \eta}{\partial x} dx + \frac{\partial \eta}{\partial y} dy \tag{3.12}$$

The equations (3.11) and (3.12) in matrix form are,

$$\begin{bmatrix} d\xi \\ d\eta \end{bmatrix} = \begin{bmatrix} \frac{\partial \xi}{\partial x} & \frac{\partial \xi}{\partial y} \\ \frac{\partial \eta}{\partial x} & \frac{\partial \eta}{\partial y} \end{bmatrix} \begin{bmatrix} dx \\ dy \end{bmatrix} \tag{3.13}$$

Now considering the inverse transformation,

$x = x(\xi, \eta)$ (3.14)

$y = y(\xi, \eta)$ (3.15)

Taking exact differential from equations (3.14) and (3.15),

$$dx = \frac{\partial x}{\partial \xi} d\xi + \frac{\partial x}{\partial \eta} d\eta \tag{3.16}$$

$$dy = \frac{\partial y}{\partial \xi} d\xi + \frac{\partial y}{\partial \eta} d\eta \tag{3.17}$$

The equations (3.16) and (3.17) can be written as,

$$\begin{bmatrix} dx \\ dy \end{bmatrix} = \begin{bmatrix} \frac{\partial x}{\partial \xi} & \frac{\partial x}{\partial \eta} \\ \frac{\partial y}{\partial \xi} & \frac{\partial y}{\partial \eta} \end{bmatrix} \begin{bmatrix} d\xi \\ d\eta \end{bmatrix} \tag{3.18}$$

From equations (3.13) and (3.18),

$$\begin{bmatrix} \frac{\partial \xi}{\partial x} & \frac{\partial \xi}{\partial y} \\ \frac{\partial \eta}{\partial x} & \frac{\partial \eta}{\partial y} \end{bmatrix} = \begin{bmatrix} \frac{\partial x}{\partial \xi} & \frac{\partial x}{\partial \eta} \\ \frac{\partial y}{\partial \xi} & \frac{\partial y}{\partial \eta} \end{bmatrix}^{-1}$$

$$=> \begin{bmatrix} \frac{\partial \xi}{\partial x} & \frac{\partial \xi}{\partial y} \\ \frac{\partial \eta}{\partial x} & \frac{\partial \eta}{\partial y} \end{bmatrix} = \frac{\begin{bmatrix} \frac{\partial y}{\partial \eta} & -\frac{\partial x}{\partial \eta} \\ -\frac{\partial y}{\partial \xi} & \frac{\partial x}{\partial \xi} \end{bmatrix}}{\begin{vmatrix} \frac{\partial \xi}{\partial x} & \frac{\partial \xi}{\partial y} \\ \frac{\partial \eta}{\partial x} & \frac{\partial \eta}{\partial y} \end{vmatrix}}$$

$$=> \begin{bmatrix} \frac{\partial \xi}{\partial x} & \frac{\partial \xi}{\partial y} \\ \frac{\partial \eta}{\partial x} & \frac{\partial \eta}{\partial y} \end{bmatrix} = \frac{1}{J} \begin{bmatrix} \frac{\partial y}{\partial \eta} & -\frac{\partial x}{\partial \eta} \\ -\frac{\partial y}{\partial \xi} & \frac{\partial x}{\partial \xi} \end{bmatrix} \tag{3.19}$$

Where,

$$\begin{vmatrix} \frac{\partial x}{\partial \xi} & \frac{\partial x}{\partial \eta} \\ \frac{\partial y}{\partial \xi} & \frac{\partial y}{\partial \eta} \end{vmatrix} = \begin{vmatrix} \frac{\partial x}{\partial \xi} & \frac{\partial y}{\partial \xi} \\ \frac{\partial x}{\partial \eta} & \frac{\partial y}{\partial \eta} \end{vmatrix} = J \tag{3.20}$$

From equation (3.19) following relation exists,

$$\frac{\partial \xi}{\partial x} = \frac{1}{J} \frac{\partial y}{\partial \eta} \tag{3.21}$$

$$\frac{\partial \xi}{\partial y} = -\frac{1}{J} \frac{\partial x}{\partial \eta} \tag{3.22}$$

$$\frac{\partial \eta}{\partial x} = -\frac{1}{J}\frac{\partial y}{\partial \xi} \tag{3.23}$$

$$\frac{\partial \eta}{\partial y} = \frac{1}{J}\frac{\partial x}{\partial \xi} \tag{3.24}$$

In the equations (3.21) to (3.24) the jacobian J and the matrices $\partial y/\partial \eta$, $\partial x/\partial \eta$, $\partial y/\partial \xi$ and $\partial x/\partial \xi$ are results of grid transformation and they are computed numerically from the known coordinates (x, y). Now from equation (3.5)

$$=> \frac{\partial U2}{\partial t} + \frac{\partial E2}{\partial x} + \frac{\partial F2}{\partial y} = S2$$

$$=> \frac{\partial U2}{\partial t} + \frac{\partial E2}{\partial \xi}\frac{\partial \xi}{\partial x} + \frac{\partial E2}{\partial \eta}\frac{\partial \eta}{\partial x} + \frac{\partial F2}{\partial \xi}\frac{\partial \xi}{\partial y} + \frac{\partial F2}{\partial \eta}\frac{\partial \eta}{\partial y} = S2 \tag{3.25}$$

Multiplying both sides of equation (3.25) by J,

$$=> J\frac{\partial U2}{\partial t} + J\frac{\partial E2}{\partial \xi}\frac{\partial \xi}{\partial x} + J\frac{\partial E2}{\partial \eta}\frac{\partial \eta}{\partial x} + J\frac{\partial F2}{\partial \xi}\frac{\partial \xi}{\partial y} + J\frac{\partial F2}{\partial \eta}\frac{\partial \eta}{\partial y} = JS2 \tag{3.26}$$

Again, it can be written that,

$$\frac{\partial}{\partial \xi}\left[E2\left(J\frac{\partial \xi}{\partial x}\right)\right] = J\left(\frac{\partial \xi}{\partial x}\right)\frac{\partial E2}{\partial \xi} + E2\frac{\partial}{\partial \xi}\left(J\frac{\partial \xi}{\partial x}\right)$$

$$=> J\left(\frac{\partial \xi}{\partial x}\right)\frac{\partial E2}{\partial \xi} = \frac{\partial}{\partial \xi}\left[E2\left(J\frac{\partial \xi}{\partial x}\right)\right] - E2\frac{\partial}{\partial \xi}\left(J\frac{\partial \xi}{\partial x}\right) \tag{3.27}$$

Similarly,

$$J\left(\frac{\partial \eta}{\partial x}\right)\frac{\partial E2}{\partial \eta} = \frac{\partial}{\partial \eta}\left[E2\left(J\frac{\partial \eta}{\partial x}\right)\right] - E2\frac{\partial}{\partial \eta}\left(J\frac{\partial \eta}{\partial x}\right) \tag{3.28}$$

$$J\left(\frac{\partial \xi}{\partial y}\right)\frac{\partial F2}{\partial \xi} = \frac{\partial}{\partial \xi}\left[F2\left(J\frac{\partial \xi}{\partial y}\right)\right] - F2\frac{\partial}{\partial \xi}\left(J\frac{\partial \xi}{\partial y}\right) \tag{3.29}$$

$$J\left(\frac{\partial \eta}{\partial y}\right)\frac{\partial F2}{\partial \eta} = \frac{\partial}{\partial \eta}\left[F2\left(J\frac{\partial \eta}{\partial y}\right)\right] - F2\frac{\partial}{\partial \eta}\left(J\frac{\partial \eta}{\partial x}\right) \tag{3.30}$$

Using equations (3.27) to (3.30), the equation (3.26) can be rewritten as,

$$=> J\frac{\partial U2}{\partial t} + \frac{\partial}{\partial \xi}\left[E2\left(J\frac{\partial \xi}{\partial x}\right)\right] - E2\frac{\partial}{\partial \xi}\left(J\frac{\partial \xi}{\partial x}\right) + \frac{\partial}{\partial \eta}\left[E2\left(J\frac{\partial \eta}{\partial x}\right)\right] - E2\frac{\partial}{\partial \eta}\left(J\frac{\partial \eta}{\partial x}\right) + \frac{\partial}{\partial \xi}\left[F2\left(J\frac{\partial \xi}{\partial y}\right)\right]$$
$$- F2\frac{\partial}{\partial \xi}\left(J\frac{\partial \xi}{\partial y}\right) + \frac{\partial}{\partial \eta}\left[F2\left(J\frac{\partial \eta}{\partial y}\right)\right] - F2\frac{\partial}{\partial \eta}\left(J\frac{\partial \eta}{\partial x}\right) = JS2$$

$$=> J\frac{\partial U2}{\partial t} + J\frac{\partial}{\partial \xi}\left[E2\left(\frac{\partial \xi}{\partial x}\right) + F2\left(\frac{\partial \xi}{\partial y}\right)\right] + J\frac{\partial}{\partial \eta}\left[E2\left(\frac{\partial \eta}{\partial x}\right) + F2\left(\frac{\partial \eta}{\partial y}\right)\right] = JS2 \qquad \text{(Others are zero)}$$

$$=> \frac{\partial L}{\partial t} + \frac{\partial M}{\partial \xi} + \frac{\partial N}{\partial \eta} = K \qquad (3.31)$$

Where,

$$L = JU2, M = J\left[E2\left(\frac{\partial \xi}{\partial x}\right) + F2\left(\frac{\partial \xi}{\partial y}\right)\right], N = J\left[E2\left(\frac{\partial \eta}{\partial x}\right) + F2\left(\frac{\partial \eta}{\partial y}\right)\right], K = JS2$$

The continuity equation then can be written as,

$$\frac{\partial}{\partial t}[Jh] + \frac{\partial}{\partial \xi}\left[J\left\{\frac{\partial \xi}{\partial x}(hu) + \frac{\partial \xi}{\partial y}(hv)\right\}\right] + \frac{\partial}{\partial \eta}\left[J\left\{\frac{\partial \eta}{\partial x}(hu) + \frac{\partial \eta}{\partial y}(hv)\right\}\right] = 0$$

$$=> \frac{\partial}{\partial t}[Jh] + \frac{\partial}{\partial \xi}\left[Jh\left\{\frac{\partial \xi}{\partial x}(u) + \frac{\partial \xi}{\partial y}(v)\right\}\right] + \frac{\partial}{\partial \eta}\left[Jh\left\{\frac{\partial \eta}{\partial x}(u) + \frac{\partial \eta}{\partial y}(v)\right\}\right] = 0$$

$$=> \frac{\partial}{\partial t}[Jh] + \frac{\partial}{\partial \xi}[JhU] + \frac{\partial}{\partial \eta}[JhV] = 0 \qquad (3.32)$$

Where,

$$U = \frac{\partial \xi}{\partial x}(u) + \frac{\partial \xi}{\partial y}(v), V = \frac{\partial \eta}{\partial x}(u) + \frac{\partial \eta}{\partial y}(v)$$

U and V are the velocity components in computational directions ξ and η respectively.

Momentum equation in ξ direction can be written as,

$$\frac{\partial}{\partial t}[Jhu] + \frac{\partial}{\partial \xi}\left[J\left\{\frac{\partial \xi}{\partial x}\left(hu^2 + g\frac{h^2}{2}\right) + \frac{\partial \xi}{\partial y}(huv)\right\}\right] + \frac{\partial}{\partial \eta}\left[J\left\{\frac{\partial \eta}{\partial x}\left(hu^2 + g\frac{h^2}{2}\right) + \frac{\partial \eta}{\partial y}(huv)\right\}\right]$$
$$= -Jgh\left(S_{ox} - \frac{n^2 u\sqrt{u^2 + v^2}}{h^{\frac{4}{3}}}\right)$$

$$=> \frac{\partial}{\partial t}[Jhu] + \frac{\partial}{\partial \xi}\left[J\left\{hu\left(\frac{\partial \xi}{\partial x}u + \frac{\partial \xi}{\partial y}v\right) + \frac{\partial \xi}{\partial x}\left(g\frac{h^2}{2}\right)\right\}\right] + \frac{\partial}{\partial \eta}\left[J\left\{hu\left(\frac{\partial \eta}{\partial x}u + \frac{\partial \eta}{\partial y}v\right) + \frac{\partial \eta}{\partial x}\left(g\frac{h^2}{2}\right)\right\}\right]$$
$$= -Jgh\left(S_{ox} - \frac{n^2 u\sqrt{u^2+v^2}}{h^{\frac{4}{3}}}\right)$$

$$=> \frac{\partial}{\partial t}[Jhu] + \frac{\partial}{\partial \xi}\left[J\left\{hUu + \frac{\partial \xi}{\partial x}\left(g\frac{h^2}{2}\right)\right\}\right] + \frac{\partial}{\partial \eta}\left[J\left\{hVu + \frac{\partial \eta}{\partial x}\left(g\frac{h^2}{2}\right)\right\}\right]$$
$$= -Jgh\left(S_{ox} - \frac{n^2 u\sqrt{u^2+v^2}}{h^{\frac{4}{3}}}\right) \quad (3.33)$$

Similarly, momentum equation in η direction can be written as,

$$=> \frac{\partial}{\partial t}[Jhv] + \frac{\partial}{\partial \xi}\left[J\left\{hUv + \frac{\partial \xi}{\partial y}\left(g\frac{h^2}{2}\right)\right\}\right] + \frac{\partial}{\partial \eta}\left[J\left\{hVv + \frac{\partial \eta}{\partial y}\left(g\frac{h^2}{2}\right)\right\}\right]$$
$$= -Jgh\left(S_{oy} - \frac{n^2 v\sqrt{u^2+v^2}}{h^{\frac{4}{3}}}\right) \quad (3.34)$$

Equations (3.32) to (3.34) can together be written in matrix form as,

$$\frac{\partial L}{\partial t} + \frac{\partial M}{\partial \xi} + \frac{\partial N}{\partial \eta} = K \quad (3.35)$$

Where,

$$L = J\begin{bmatrix} h \\ hu \\ hv \end{bmatrix}, M = J\begin{bmatrix} hU \\ hUu + \frac{\partial \xi}{\partial x}\left(g\frac{h^2}{2}\right) \\ hUv + \frac{\partial \xi}{\partial y}\left(g\frac{h^2}{2}\right) \end{bmatrix}, N = J\begin{bmatrix} hV \\ hVu + \frac{\partial \eta}{\partial x}\left(g\frac{h^2}{2}\right) \\ hVv + \frac{\partial \eta}{\partial y}\left(g\frac{h^2}{2}\right) \end{bmatrix},$$

$$K = J\begin{bmatrix} 0 \\ gh\left(S_{ox} - \frac{n^2 u\sqrt{u^2+v^2}}{h^{\frac{4}{3}}}\right) \\ gh\left(S_{oy} - \frac{n^2 v\sqrt{u^2+v^2}}{h^{\frac{4}{3}}}\right) \end{bmatrix}$$

In equation (3.35) the terms, J, $\frac{\partial \xi}{\partial x}, \frac{\partial \xi}{\partial y}, \frac{\partial \eta}{\partial x}, \frac{\partial \eta}{\partial y}$ are results of grid transformation and are generally calculated using central finite difference approximations.

3.6 Conclusions

The following conclusions are obtained from this chapter.

1. Different forms of governing equations are presented. Effort of better representation of physical processes and computational domain has let to continuous development of the governing equations from a relatively simpler form to a more complex form. Increase in complexities increases requirement of more computational time and capacity.
2. Depending upon the situation to be simulated, appropriate version should be used.

CHAPTER 4

NUMERICAL SOLUTION OF GOVERNING EQUATIONS

4.1 Introduction

The governing equations of unsteady free surface flow are a set of nonlinear first-order, hyperbolic partial differential equations for which closed-form solutions are not available, except for very simplified one-dimensional cases. Therefore, these equations are solved numerically. The solution techniques for some of the numerical methods and the results obtained from all of them are presented and discussed in this chapter.

4.2 Finite difference method

The finite difference techniques are developed based on the approximations that permit replacing differential equations by difference equations. These finite difference approximations are algebraic in form, and the solutions are derived at grid points. Thus, a finite difference solution basically involves three steps:

i. Dividing the solution domain into grids of nodes.
ii. Approximating the given differential equation by finite difference equivalence that relates the solutions to grid points.
iii. Solving the difference equations subject to the prescribed boundary conditions and/or initial conditions.

When a direct computation of the dependent variables can be made in terms of known quantities, the computation is said to be explicit. When the dependent variables are defined by coupled sets of equations, and either a matrix or iterative technique is needed to obtain the solution, the numerical method is said to be implicit. Four different finite difference schemes namely Lax diffusive scheme, MacCormack predictor corrector scheme, Modified predictor corrector scheme and Beam and Warming scheme have been used in this study to solve the governing equations of unsteady free surface flow both in one dimensional (1D) and two dimensional (2D) formulation and their relative merits and limitations have been compared with an objective to select the best among them for river modeling.

4.2.1 Lax diffusive scheme

Lax diffusive scheme is an explicit finite difference scheme which is first order accurate in time and second order accurate in space. The major advantages associated with this scheme are that it is single step requiring less computational time and no artificial viscosity is needed as there is no numerical oscillation. Sharp and Moore (1976) first gave the step by step procedure for using this scheme for solution of the governing equations in 1D (Saint Venant's equations) form. Since then a many researchers (Miller and Chaudhry 1989; Navarro and Villanueva 1999; Macchione and Morelli 2003; Saikia and Sarma 2006; Akbari and Firoozi 2010; Soleymani and Delphi 2012) have been applying this scheme for solution of unsteady free surface flow equations. The formulation of this scheme for 1D and 2D unsteady free surface flow equations are presented in the subsequent section.

4.2.1.1 Formulation for 1D governing equations

The finite difference formulation of equation (3.3) using the Lax diffusive scheme can be written as (Chaudhry 2008),

$$U1_i^{k+1} = \frac{1}{2}\left(U1_{i+1}^k - U1_{i-1}^k\right) - \frac{1}{2}\frac{\Delta t}{\Delta x}\left(E1_{i+1}^k - E1_{i-1}^k\right) - \Delta t S1_i^* \qquad (4.1)$$

Where, Δx is the grid spacing in flow direction designated by the subscript i, Δt is the grid spacing in the time axis (time step) designated by the superscript k. Value of $S1_i$* is calculated as given below,

$$S1_i^* = \frac{1}{2}\left(S1_{i+1}^k + S1_{i-1}^k\right)$$

4.2.1.2 Formulation for 2D governing equations

Using the Lax diffusive scheme, the finite difference formulation of 2D unsteady free surface flow equation (equation 3.35) can be written as,

$$L_{i,j}^{k+1} = \frac{1}{4}\left(L_{i,j+1}^k + L_{i,j-1}^k + L_{i+1,j}^k + L_{i-1,j}^k\right) - \frac{1}{2}\frac{\Delta t}{\Delta \xi}\left(M_{i,j+1}^k - M_{i,j-1}^k\right) - \frac{1}{2}\frac{\Delta t}{\Delta \eta}\left(N_{i+1,j}^k - N_{i-1,j}^k\right) - \Delta t K_{i,j}^* \qquad (4.2)$$

Where, $\Delta\xi$ is the grid spacing in flow direction designated by the subscript i, $\Delta\eta$ is the grid spacing in transverse direction designated by the subscript j, Δt is the grid spacing in the time axis (time step) designated by the superscript k. Value of $K_{i,j}$* is calculated as given below,

$$K^{*}_{i,j} = \frac{1}{4}\left(K^{k}_{i,j+1} + K^{k}_{i,j-1} + K^{k}_{i+1,j} + K^{k}_{i-1,j}\right)$$

4.2.2 MacCormack predictor corrector scheme

MacCormack predictor corrector is an explicit finite difference scheme, second order acuurate both in space and time. The scheme is composed of two steps called predictor step and corrector step. In the predictor step, using forward differnce a solution is obtained which is further corrected in the corrector step using backward difference leading to second order accurcy. One of the major advantages of this scheme is that it can handle the mixed subcritical superitical flow. This scheme has a very good ability to simulate the bores or shocks. It has been used by numerous investigators (Fennema and Chaudhry 1986, 1990; Bellos et al. 1991; Bhallamudi and Chaudhry 1992; Navarro et al. 1992; Fiedler and Ramirez 2000; Liang et al. 2006, 2007; Tsakiris and Bellos 2014) in the past for solution of the unsteady flow equations in diverse situations and yield satisfactory results.

4.2.2.1 Formulation for 1D governing equations

The predictor step can be formulated for equation (3.3) as (Chaudhry 2008),

$$U1^{p}_{i} = U1^{k}_{i} - \frac{\Delta t}{\Delta x}\left(E1^{k}_{i} - E1^{k}_{i-1}\right) - \Delta t S1^{k}_{i} \tag{4.3}$$

The predicted values are then used in the corrector step as,

$$U1^{c}_{i} = U1^{k}_{i} - \frac{\Delta t}{\Delta x}\left(E1^{p}_{i+1} - E1^{p}_{i}\right) - \Delta t S1^{p}_{i} \tag{4.4}$$

Where, superscripts k and c correspond to predicted and corrected values respectively. Final values of the flow variables in the next time step are then calculated form the following formula,

$$U1^{k+1}_{i} = \frac{1}{2}\left(U1^{p}_{i} + U1^{c}_{i}\right) \tag{4.5}$$

4.2.2.2 Formulation for 2D governing equations

In 2D formulation the predictor step for the governing equations is as given below (Chaudhry 2008),

$$L_{i,j}^{p} = L_{i,j}^{k} - \frac{\Delta t}{\Delta \xi}\left(M_{i,j}^{k} - M_{i,j-1}^{k}\right) - \frac{\Delta t}{\Delta \eta}\left(N_{i,j}^{k} - N_{i-1,j}^{k}\right) - \Delta t K_{i,j}^{k} \quad (4.6)$$

The predicted values are then used in the corrector step as,

$$L_{i,j}^{c} = L_{i,j}^{k} - \frac{\Delta t}{\Delta \xi}\left(M_{i,j+1}^{k} - M_{i,j}^{k}\right) - \frac{\Delta t}{\Delta \eta}\left(N_{i+1,j}^{k} - N_{i,j}^{k}\right) - \Delta t K_{i,j}^{p} \quad (4.7)$$

Final values of the flow variables in the next time step are then calculated form the following formula,

$$L_{i,j}^{k+1} = \frac{1}{2}\left(L_{i,j}^{p} + L_{i,j}^{c}\right) \quad (4.8)$$

4.2.3 Modified predictor corrector scheme

The well-known MacCormack scheme in a slightly modified (Sarma 1999) form has been used here. The set of governing equations used for modeling purpose has an inherent property of signal propagation i.e., in case of subcritical flow the information comes both from upstream and downstream, while the information comes only from upstream if the flow is supercritical.

Hence, in the subcritical region backward finite difference approximation is used for predictor step and forward finite difference approximation is used in the corrector step. In the supercritical region as the control is always on the upstream side, use of forward finite difference approximation in the corrector step is omitted to eliminate erroneous influence of downstream flux on the computed values. This simple technique has made application of the scheme possible in the mixed flow regions also. Later, Saikia (2007) applied this technique for dam break flow in actual river terrain and obtained good results.

4.2.3.1 Formulation for 1D governing equations

Using modified predictor corrector scheme, the predictor step can be formulated for equation (3.3) as,

$$U1_i^p = U1_i^k - \frac{\Delta t}{\Delta x}\left(E1_i^k - E1_{i-1}^k\right) - \Delta t S1_i^k \quad (4.9)$$

The predicted values are then used in the modified corrector step as,

(a) If $u < \sqrt{(gh)}$, subcritical flow

$$U1_i^c = U1_i^k - \frac{\Delta t}{\Delta x}\left(E1_{i+1}^p - E1_i^p\right) - \Delta t S1_i^p \quad (4.10)$$

(b) If $u > \sqrt{(gh)}$, supercritical flow

$$U1_i^c = U1_i^p \quad (4.11)$$

Final values of the flow variables in the next time step are then calculated form the following formula,

$$U1_i^{k+1} = \frac{1}{2}\left(U1_i^p + U1_i^c\right) \quad (4.12)$$

4.2.3.2 Formulation for 2D governing equations

The predictor step for the 2D shallow water equations can be written as,

$$L_{i,j}^p = L_{i,j}^k - \frac{\Delta t}{\Delta \xi}\left(M_{i,j+1}^k - M_{i,j}^k\right) - \frac{\Delta t}{\Delta \eta}\left(N_{i+1,j}^k - N_{i,j}^k\right) - \Delta t K_{i,j}^k \quad (4.13)$$

The predicted values are then used in the corrector step as,

(a) If $\sqrt{(u^2 + v^2)} < \sqrt{(gh)}$, subcritical flow

$$L_{i,j}^c = L_{i,j}^k - \frac{\Delta t}{\Delta \xi}\left(M_{i,j+1}^k - M_{i,j}^k\right) - \frac{\Delta t}{\Delta \eta}\left(N_{i+1,j}^k - N_{i,j}^k\right) - \Delta t K_{i,j}^p \quad (4.14)$$

(b) If $\sqrt{(u^2 + v^2)} > \sqrt{(gh)}$, supercritical flow

$$L_{i,j}^c = L_{i,j}^p \quad (4.15)$$

Final values of the flow variables in the next time step are then calculated form the following formula,

$$L_{i,j}^{k+1} = \frac{1}{2}\left(L_{i,j}^{p} + L_{i,j}^{c}\right) \tag{4.16}$$

4.2.4 Beam and Warming implicit scheme

Beam and Warming (1976) introduced this scheme for solution of the two dimensional Euler equations. Fennema and Chaudhry (1987) first used this scheme for solution of the 1D governing equations of unsteady free surface flow for simulation of dam break induced flow. The major advantages of Beam and Warming scheme are that it is non-iterative, converges quickly and larger time step than that of explicit scheme can be applied. Later many researchers have applied this scheme for various problems (Fennema and Chaudhry 1989; Molls et al. 1995; Kassem and Chaudhry 1998; Molls and Zhao 2000; Kassem and Chaudhry 2005; Rahimpour and Tavakoli 2011) and obtained very good results.

4.2.4.1 Formulation for 1D governing equations

In 1D case the final solution is obtained by solving a block tridiagonal system. For the efficient solution of the block tridiagonal system, Thomas algorithm (Niyogi 2009) is used. The equation solved in x-direction is as follows (Chaudhry 2008),

$$\left[I1 + \Delta t \frac{\theta}{1+\gamma}\left(\frac{\partial A1}{\partial x} + B1\right)\right] U1^{*} = -\Delta t \frac{1}{1+\gamma}\left(\frac{\partial E1}{\partial x} + S1\right)^{k} \tag{4.17}$$

Final value of U1 in the next time is calculated from the formula given below,

$$U1_{i}^{k+1} = U1_{i}^{k} + U1_{i}^{*} \tag{4.18}$$

Where, I1 is the identity matrix of size 2 by 2, A1 and B1 are the jacobians of matrices E1 and S1 respectively given by,

$$A1 = \begin{bmatrix} 0 & 1 \\ gh - u^2 & 2u \end{bmatrix}, \qquad B1 = \begin{bmatrix} 0 & 0 \\ -gS_0 - \frac{7}{3}gn^2u^2h^{-\frac{4}{3}} & 2gn^2uh^{-\frac{4}{3}} \end{bmatrix}$$

In equation (4.17), θ and γ are factors, values of which lead to different formulations of Beam and Warning scheme. Different values of these parameters are given in Chaudhry (2008). In this work θ=1 and γ=0.5 (three point backward formulation) are used.

4.2.3.2 Formulation for 2D governing equations

For the 2D case, the solution is advanced in a two-step (double sweep) sequence, where each step involves the solution of a block tridiagonal system. For the efficient solution of the block tridiagonal system, Thomas algorithm (Niyogi 2009) is used. In the first sweep (ξ-direction), an intermediate solution L^{*} is obtained. This intermediate value is then used in the second sweep (η-direction) to obtain the solution L^{**}. The equations solved in ξ-direction and η-directions are as follows (Chaudhry 2008),

$$\left[I2 + \Delta t \frac{\theta}{1+\gamma}\frac{\partial}{\partial \xi} A2^{k}\right] L^{*} = -\Delta t \frac{1}{1+\gamma}\left(\frac{\partial M}{\partial \xi} + \frac{\partial N}{\partial \eta} + K\right)^{k} + \frac{\gamma}{1+\gamma}\Delta_t L^{k} \tag{4.19}$$

$$\left[I2 + \Delta t \frac{\theta}{1+\gamma}\left(\frac{\partial}{\partial \eta} B2 + Q2\right)^{k}\right] L^{**} = L^{*} \tag{4.20}$$

Final value of L in the next time step is then calculated as,

$$L_{i,j}^{k+1} = L_{i,j}^{k} + L_{i,j}^{**}$$

Where, I2 is the identity matrix of size 3 by 3, A2, B2 and Q2 are the jacobians of matrices M, N and K respectively.

The expressions for A2, B2 and Q2 are given below,

$$A2 = \begin{bmatrix} 0 & \frac{\partial \xi}{\partial x} & \frac{\partial \xi}{\partial y} \\ gh\frac{\partial \xi}{\partial x} - Uu & U + u\frac{\partial \xi}{\partial x} & u\frac{\partial \xi}{\partial y} \\ gh\frac{\partial \xi}{\partial y} - Uv & v\frac{\partial \xi}{\partial x} & U + v\frac{\partial \xi}{\partial y} \end{bmatrix}, \qquad B2 = \begin{bmatrix} 0 & \frac{\partial \eta}{\partial x} & \frac{\partial \eta}{\partial y} \\ gh\frac{\partial \eta}{\partial x} - Vu & V + u\frac{\partial \eta}{\partial x} & u\frac{\partial \eta}{\partial y} \\ gh\frac{\partial \eta}{\partial y} - Vv & v\frac{\partial \eta}{\partial x} & V + v\frac{\partial \eta}{\partial y} \end{bmatrix}$$

$$Q2 = \begin{bmatrix} 0 & 0 & 0 \\ -gS_{ox} - \frac{\frac{7}{3}gn^2u\sqrt{(u^2+v^2)}}{h^{\frac{4}{3}}} & \frac{2gn^2u^2 + gn^2v^2}{h^{\frac{4}{3}}\sqrt{(u^2+v^2)}} & \frac{gn^2uv}{h^{\frac{4}{3}}\sqrt{(u^2+v^2)}} \\ -gS_{oy} - \frac{\frac{7}{3}gn^2v\sqrt{(u^2+v^2)}}{h^{\frac{4}{3}}} & \frac{gn^2uv}{h^{\frac{4}{3}}\sqrt{(u^2+v^2)}} & \frac{gn^2u^2 + 2gn^2v^2}{h^{\frac{4}{3}}\sqrt{(u^2+v^2)}} \end{bmatrix}$$

For the 2D case also, the three point backward formulation is used (θ=1, γ=0.5).

4.2.5 Initial and Boundary condition

For solution of the finite difference equations presented above, initial and boundary conditions are necessary. For initial condition, the water depths over the whole channel were first computed assuming uniform flow from the known discharge value. The velocities were than calculated by dividing the discharge value by the known area of flow. Different types of boundary conditions required for both 1D and 2D cases for steady and unsteady flows are presented in the subsequent paragraphs.

4.2.5.1 1D case

For supercritical flow, values of two variables are needed to be applied on the upstream boundary. No boundary conditions are required at downstream, as no characteristics enter into the domain from downstream. However, for subcritical flow one variable is needed to be applied both at upstream and downstream boundary.

For hydrograph routing, hydrograph is needed to be applied on the upstream boundary. For the downstream boundary, solution of characteristics equation along with Manning's equation or extrapolation technique gives the value of the unknown variables.

4.2.5.1.1 Characteristic equation

The Saint Venant's equations neglecting the lateral inflow (Chaudhry 2008) are as follows,
The continuity equation,

$$\bar{V}\frac{\partial A}{\partial x} + A\frac{\partial \bar{V}}{\partial x} + b\frac{\partial h}{\partial t} = 0 \qquad (4.21)$$

And the momentum equation,

$$g\frac{\partial h}{\partial x} + \bar{V}\frac{\partial \bar{V}}{\partial x} + \frac{\partial \bar{V}}{\partial t} = g(S_o - S_f) \qquad (4.22)$$

Where, A = the cross-sectional area of the section, h = depth of flow at the section, $\bar{V}$ = mean velocity at the section, b = width of the top of the section, x = position of the section measured from the upstream end, t = time, g = acceleration due to gravity, S_0 = bed slope, and S_f = friction slope.

Now, the expression of celerity,

$$c = \sqrt{gh} \qquad => c^2 = gh \qquad => \frac{2c}{g}dc = dh \tag{4.23}$$

Using the expressions of h and dh in equation (4.21) leads to,

$$\overline{V}b\frac{2c}{g}\frac{\partial c}{\partial x} + b\frac{c^2}{g}\frac{\partial \overline{V}}{\partial x} + b\frac{2c}{g}\frac{\partial c}{\partial t} = 0 \tag{4.24}$$

$$2\overline{V}\frac{\partial c}{\partial x} + c\frac{\partial \overline{V}}{\partial x} + 2\frac{\partial c}{\partial t} = 0 \tag{4.25}$$

For the momentum equation (4.22) leads to,

$$2c\frac{\partial c}{\partial x} + \overline{V}\frac{\partial \overline{V}}{\partial x} + \frac{\partial \overline{V}}{\partial t} = g(S_o - S_f) \tag{4.26}$$

Adding equations (4.25) and (4.26),

$$\frac{\partial \overline{V}}{\partial t} + (\overline{V} + c)\frac{\partial \overline{V}}{\partial x} + 2\frac{\partial c}{\partial t} + 2(\overline{V} + c)\frac{\partial c}{\partial x} = g(S_o - S_f) \tag{4.27}$$

Subtracting equation (4.25) from (4.26),

$$\frac{\partial \overline{V}}{\partial t} + (\overline{V} - c)\frac{\partial \overline{V}}{\partial x} - 2\frac{\partial c}{\partial t} - 2(\overline{V} - c)\frac{\partial c}{\partial x} = g(S_o - S_f) \tag{4.28}$$

Equations (4.27) and (4.28) can be rearranged as,

$$(\overline{V} + c)\frac{\partial(\overline{V} + 2c)}{\partial x} + \frac{\partial(\overline{V} + 2c)}{\partial t} = g(S_0 - S_f) \tag{4.29}$$

$$(\overline{V} - c)\frac{\partial(\overline{V} - 2c)}{\partial x} + \frac{\partial(\overline{V} - 2c)}{\partial t} = g(S_0 - S_f) \tag{4.30}$$

Now, if € = ($\overline{V}$+2c) be any function then,

$$\frac{d(\overline{V} + 2c)}{dt} = \frac{\partial(\overline{V} + 2c)}{\partial x}\frac{\partial x}{\partial t} + \frac{\partial(\overline{V} + 2c)}{\partial t} \tag{4.31}$$

Now the RHS of equation (4.31) and LHS of equation (4.29) are identical provided,

$$\frac{\partial x}{\partial t} = (\bar{V} + c)$$

And hence it can be established that,

$$\frac{d(\bar{V} + 2c)}{dt} = g(S_o - S_f) = \text{const.} \qquad \text{if } \frac{\partial x}{\partial t} = (\bar{V} + c)$$

$$\frac{d(\bar{V} - 2c)}{dt} = g(S_o - S_f) = \text{const.} \qquad \text{if } \frac{\partial x}{\partial t} = (\bar{V} - c)$$

Where,

$$\frac{d(\bar{V} + 2c)}{dt} = g(S_o - S_f) = \text{const.}$$

Is the positive characteristic equation and the slope of the line is,

$$\frac{\partial x}{\partial t} = (\bar{V} + c)$$

And,

$$\frac{d(\bar{V} - 2c)}{dt} = g(S_o - S_f) = \text{const.}$$

Is the negative characteristic equation and the slope of the line is,

$$\frac{\partial x}{\partial t} = (\bar{V} - c)$$

Now, for supercritical flow,

Fr>1, Where, Fr is the Froude number given by,

$$Fr = \frac{\bar{V}}{\sqrt{gh}} = \frac{\bar{V}}{c}$$

In this case,

$$Fr > 1 \qquad \Rightarrow \frac{\bar{V}}{c} > 1 \qquad \Rightarrow \bar{V} > c$$

And hence,

$$\frac{\partial x}{\partial t} = (\bar{V} + c) \text{ and } \frac{\partial x}{\partial t} = (\bar{V} - c), \text{both are positive.}$$

The shapes of these lines are shown in figure 4.1.

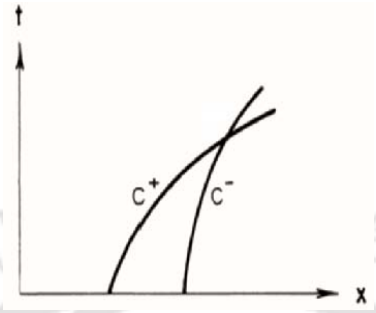

Figure 4.1 Characteristics direction for supercritical flow

Similarly for subcritical and critical flows, the shapes of the characteristic lines are as shown in figures 4.2 and 4.3 respectively,

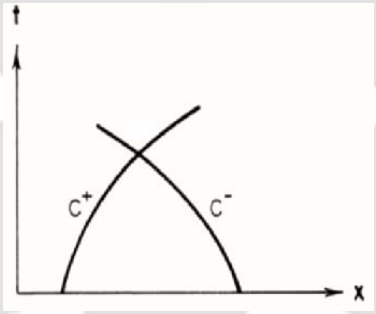

Figure 4.2 Characteristics direction for subcritical flow

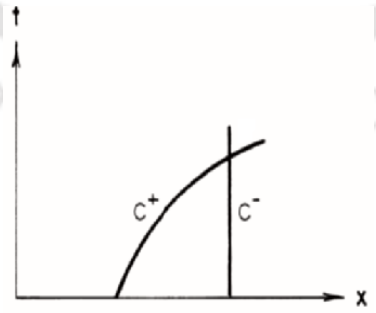

Figure 4.3 Characteristics direction for critical flow

Now, from figures 4.1, 4.2 and 4.3, it can be observed that for any types of flow the +ve characteristics equations are sloping downwards. Again if at downstream boundary, the flow is assumed to be uniform, Manning's equation can be applied at downstream. In this way combination of Manning's equation and +ve characteristics equations can be solved simultaneously to obtain the unknown variables at the downstream boundary for the next time level.

4.2.5.1.2 Extrapolation technique

The unknown flow variables at the downstream boundary can also be evaluated by extrapolation from the interior domain (Anderson et. al 1984). The extrapolation may be considered as first order or second order as given below,

For first order extrapolation, value of any variable (f) at 'n' node will be,

$$f(n) = f(n-1) \tag{4.32}$$

Similarly, using second order extrapolation,

$$f(n) = 2f(n-1) - f(n-2) \tag{4.33}$$

4.2.5.2 2D case

For 2D case, two different types of boundary exist. One is open boundary, through which flow enters or leaves the domain. Another is the solid boundary or the river bank, through which no flow takes place. For supercritical case, at upstream all the three variables are needed to be specified. Whereas at downstream no conditions are required, as no characteristics enter into the domain. At downstream these variables are extrapolated from interior domain. However for subcritical case two boundary conditions are required at upstream and one is needed at downstream.

For routing of hydrograph, at upstream boundary flow hydrograph is needed to be specified. At downstream boundary, extrapolation technique or solution of characteristics equation can give the required boundary condition.

The solid banks are simulated as free slip boundaries (Klonidis and Soulis 2001). The values of h and u are extrapolated from interior domain. For enabling no cross flow through the boundaries,

v value is set to zero. The groynes are simulated using reflection procedure given by Chaudhry (2008). Reflective boundary condition is applied, when flow impinges upon a fixed surface. Reflective boundary condition is implemented by creating dummy cell at the end of the surface as shown in figure 4.4. The direction of normal velocity component is altered here to have zero resultant velocity at the solid wall.

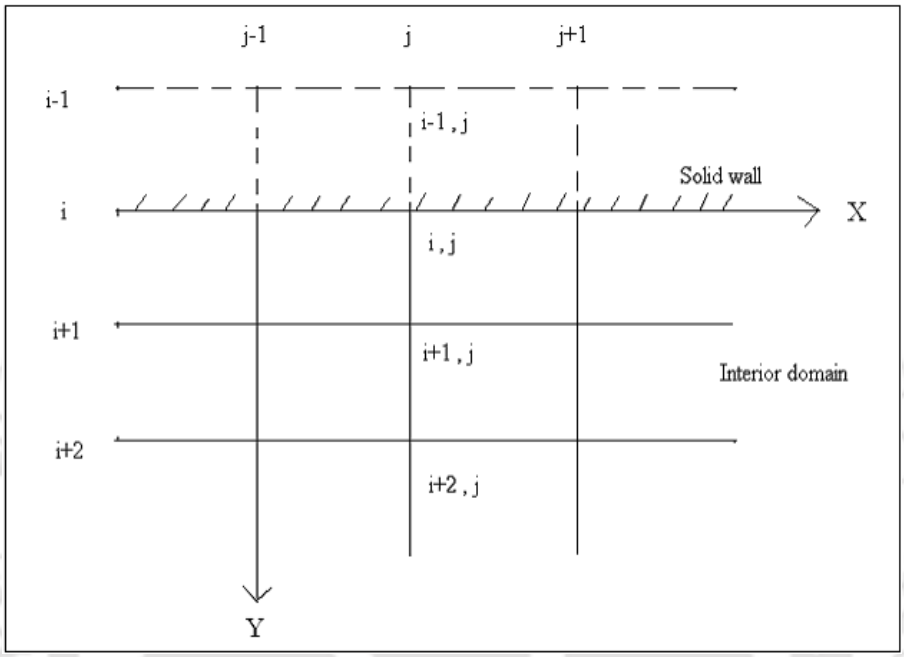

Figure 4.4 Reflection boundary stencil

The value of the flow variable at dummy cell is given by,

$$h(i-1, j, k) = h(i+1, j, k)$$
$$u(i-1, j, k) = u(i+1, j, k)$$
$$v(i-1, j, k) = -v(i+1, j, k) \quad (4.34)$$

The sand bars are simulated using the technique of no flow boundary (Molls and Chaudhry 1995). In this technique, both the velocity components are set zero for the grid points falling under sand bar.

4.2.6 Stability of the hydrodynamic model

All the four numerical schemes presented above are based on time marching technique. For numerical stability of the models, the value of Δt must be specified to satisfy the COURANT-FRIEDRICHS-LEWY (CFL) condition. For 1D case, the CFL condition is (Chaudhry 2008),

$$\Delta t = CN \times \min\left\{\frac{\Delta x}{\left(u + \sqrt{gh}\right)}\right\} \tag{4.35}$$

For 2D case, the CFL condition can be written as (Molls and Chaudhry 1995),

$$\Delta t = CN \times \min\left[\left|\frac{U}{\Delta\xi}\right| + \left|\frac{V}{\Delta\eta}\right| + \sqrt{gh}\left\{\left(\frac{\frac{\partial\xi}{\partial x}}{\Delta\xi} + \frac{\frac{\partial\eta}{\partial x}}{\Delta\eta}\right)^2 + \left(\frac{\frac{\partial\xi}{\partial y}}{\Delta\xi} + \frac{\frac{\partial\eta}{\partial y}}{\Delta\eta}\right)^2\right\}^{\frac{1}{2}}\right]^{-1} \tag{4.36}$$

Where, CN is the Courant number. Molls and Zhao (2000) while using Beam and Warming scheme for their case observed that a maximum value of 2.5 can be specified for CN for the solution to be stable. However for Lax diffusive, MacCormack predictor corrector and modified predictor corrector schemes, this value is limited to 1 only.

4.2.7 Artificial Viscosity

The Lax diffusive method presented above is a first order accurate method. While, the MacCormack predictor corrector, Modified predictor corrector and the Beam and Warming methods are second order accurate. The usual property of second order accurate methods is that they produce dispersive errors (Chaudhry 2008). The dispersive errors usually produce oscillations in the computed results in the vicinity of steep wave fronts. These oscillations are purely due to numerical errors and have nothing to do with the physical phenomenon being simulated. To smooth these oscillations, artificial viscosity or sometimes called artificial damping is added to the scheme. This procedure smoothes the oscillations where large gradients are present; however, it leaves the relatively smooth areas undisturbed. The artificial viscosity models used for the three second order schemes are presented below,

4.2.7.1 Artificial Viscosity for predictor corrector schemes

In this method, the final values of the primitive flow variables in equation (4.8) are modified as **(**Chaudhry 2008**)**,

$$L_{i,j}^{k+1} = L_{i,j}^{k+1} + D_x L_{i,j}^{k+1} + D_y L_{i,j}^{k+1} \tag{4.37}$$

Where,

$$D_x L_{i,j}^{k+1} = \left[\epsilon_{x_{j+\frac{1}{2}}}\left(L_{i,j+1}^{k+1} - L_{i,j}^{k+1}\right) - \epsilon_{x_{j-\frac{1}{2}}}\left(L_{i,j}^{k+1} - L_{i,j-1}^{k+1}\right)\right] \tag{4.38}$$

$$D_y L_{i,j}^{k+1} = \left[\epsilon_{y_{i+\frac{1}{2}}}\left(L_{i+1,j}^{k+1} - L_{i,j}^{k+1}\right) - \epsilon_{y_{i-\frac{1}{2}}}\left(L_{i,j}^{k+1} - L_{i-1,j}^{k+1}\right)\right] \tag{4.39}$$

$$\epsilon_{x_{j+\frac{1}{2}}} = CS\frac{\Delta x}{\Delta t}\max\left(\omega x_{i,j}^{k+1}, \omega x_{i,j+1}^{k+1}\right) \tag{4.40}$$

$$\epsilon_{x_{j-\frac{1}{2}}} = CS\frac{\Delta x}{\Delta t}\max\left(\omega x_{i,j-1}^{k+1}, \omega x_{i,j}^{k+1}\right) \tag{4.41}$$

$$\epsilon_{y_{i+\frac{1}{2}}} = CS\frac{\Delta y}{\Delta t}\max\left(\omega y_{i,j}^{k+1}, \omega y_{i+1,j}^{k+1}\right) \tag{4.42}$$

$$\epsilon_{y_{i-\frac{1}{2}}} = CS\frac{\Delta y}{\Delta t}\max\left(\omega y_{i-1,j}^{k+1}, \omega y_{i,j}^{k+1}\right) \tag{4.43}$$

$$\omega x_{i,j}^{k+1} = \frac{\left|h_{i,j+1}^{k+1} - 2h_{i,j}^{k+1} + h_{i,j-1}^{k+1}\right|}{\left|h_{i,j+1}^{k+1}\right| + \left|2h_{i,j}^{k+1}\right| + \left|h_{i,j-1}^{k+1}\right|} \tag{4.44}$$

$$\omega y_{i,j}^{k+1} = \frac{\left|h_{i+1,j}^{k+1} - 2h_{i,j}^{k+1} + h_{i-1,j}^{k+1}\right|}{\left|h_{i+1,j}^{k+1}\right| + \left|2h_{i,j}^{k+1}\right| + \left|h_{i-1,j}^{k+1}\right|} \tag{4.45}$$

In equations (4.40) to (4.43) presented above, CS is a constant used to regulate the amount of dissipitation. A small value in the order of just as to remove the numerical oscillation should be used for CS (In the range of 0-0.4). Same artificial viscosity model is also used for modified predictor corrector method. For 1D formulation, the same artificial viscosity model is used provided that only D_x portion is required in this case.

4.2.7.2 Artificial Viscosity for Beam and Warming scheme

Artificial viscosity model is used in the Beam and Warming scheme by adding the following equation to the RHS of equation (4.19),

$$AV = CT\left[\left(L_{i,j+1}^{k+1} - 2L_{i,j}^{k+1} + L_{i,j-1}^{k+1}\right) + \left(L_{i+1,j}^{k+1} - 2L_{i,j}^{k+1} + L_{i-1,j}^{k+1}\right)\right] \quad (4.46)$$

In case of 1D formulation, the following term is added to the RHS of equation (4.17),

$$AV = CT\left(U1_{i+1}^{k+1} - 2U1_{i}^{k+1} + U1_{i-1}^{k+1}\right) \quad (4.47)$$

In this case, CT is the regulating coefficient in the order of (0-0.4)

4.3 Results and Discussion

All of the numerical schemes and the boundary conditions presented above are tested for various test problems to select the best one interms of robustness and accuracy. The results obtained are presented in the subsequent sections.

4.3.1 Comparison of different downstream boundary conditions

For river modeling, generally the upstream boundary is known in the form of constant inflow discharge or flow hydrograph. So far downstream Boundary condition is concerned; selecting one from several options becomes a critical decision. To study the effect of different downstream boundary conditions on computed profile, a hydrograph is routed through a hypothetical channel by employing the two downstream boundary conditions considered in this study and results obtained are compared.

The hypothetical channel considered is a rectangular channel of length 32000 m having a constant width of 900 m. Slope of the channel considered is 1:1000; while the manning's roughness value for the channel is 0.031. The total channel is discretized into 161 grids resulting a Δx of value 200 m. The value of Δt used is 20 second, leading to a CN of 0.8. The hydrograph applied at the upstream boundary is shown in figure 4.5. In this case, the governing equations in 1D are solved using Lax diffusive scheme. Water surface elevations along the channel at two different times obtained using both the downstream boundary conditions are plotted to have a comparison between the results.

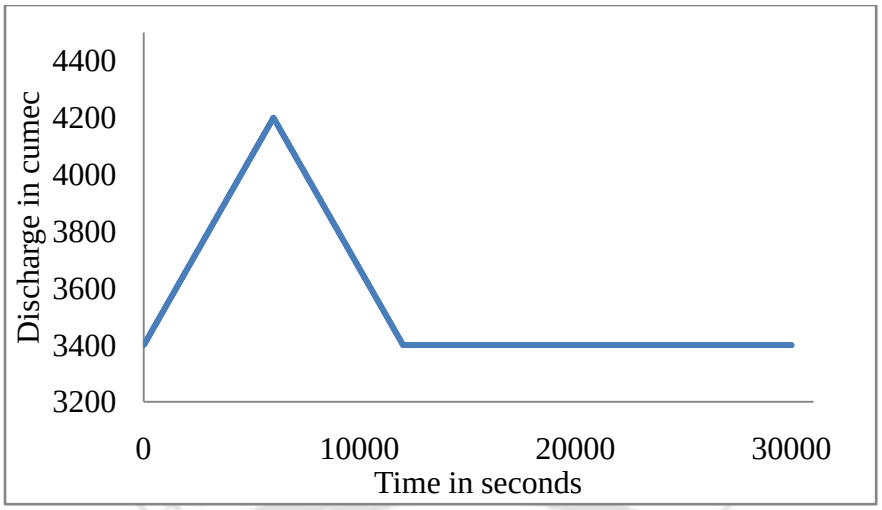

Figure 4.5 Upstream hydrograph for downstream boundary condition comparison

Figures 4.6 and 4.7 show the water surface elevation along the channel after 6000 seconds and 12000 seconds respectively. From the figures it is observed that, characteristic equation solution technique and extrapolation techniques applied at downstream boundary produces same results.

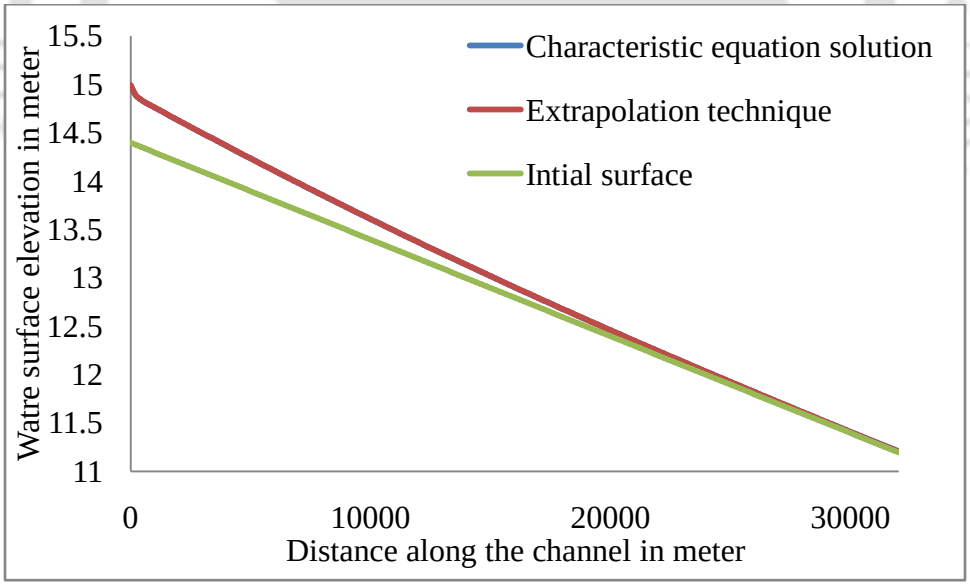

Figure 4.6 Water surface elevation along the channel after 6000 seconds

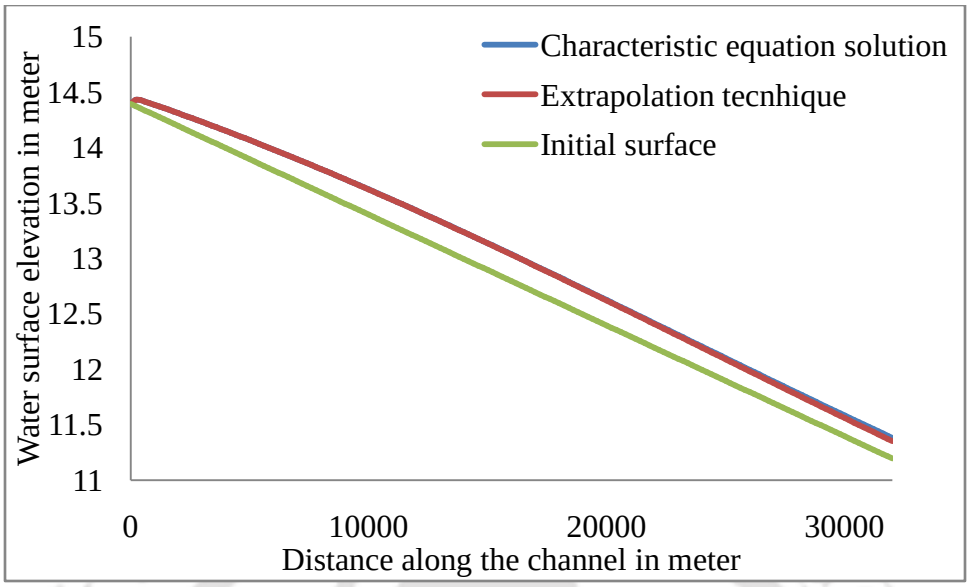

Figure 4.7 Water surface elevation along the channel after 12000 seconds

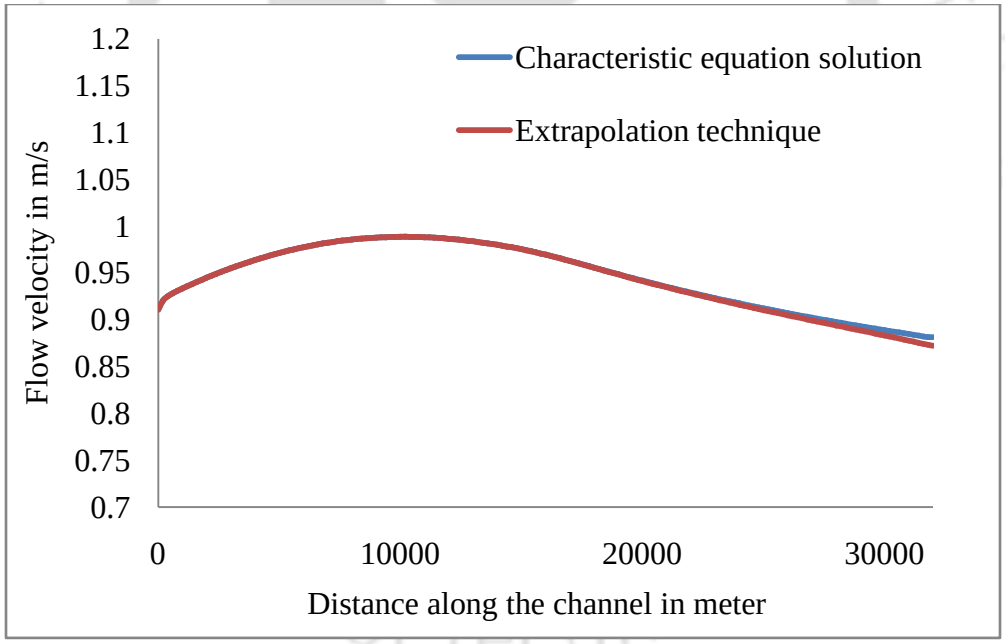

Figure 4.8 Water flow velocity along the channel after 8000 seconds

In the comparison of velocity along the channel for both the downstream boundary conditions (figure 4.8), it is further observed that results are very similar. From the comparisons of water depths and velocities, it may be concluded that same amount of accuracy can be achieved by utilizing extrapolation technique at less computational effort, as compared to characteristic

equation solution technique. Considering this, extrapolation technique has been used for calculating the unknown variables at downstream boundary.

4.3.2 Flow hydrograph routing using 1D approximation of governing equations

To compare the computational efficiency and stability of all the four numerical schemes presented in this study, an example from a previous study (Akbari and Firoozi 2010) is taken. In this example, a flow hydrograph is routed through a 29000 m long rectangular channel of constant top width of 120 m. The flow hydrograph is shown in figure 4.9. The slope of the channel considered is 1:1640. Manning's n for the channel is considered as 0.023. The whole length of the channel is discretized into 29 finite difference grids of size 1000 m. A temporal step of 150 second is considered for diffusive scheme, predictor corrector scheme and modified predictor corrector scheme. However, due to implicit nature of Beam and Warming scheme, a larger time step of 400 second is considered for this scheme.

The routed hydrograph at a distance of 16000 m from upstream boundary is shown in figure 4.10. From the figure it can be observed that, for all the schemes, the peak is occurring at 7 hrs from the beginning of hydrograph. The peak discharge at that time for that cross section is observed as approximately 2.45 cumec/m. Figure 4.11 shows the observed hydrograph at the downstream using all the scheme. For this position also, similar results are obtained by all the schemes. However, for this position time to peak is 9 hrs with a peak value of 2.4 cumec/m.

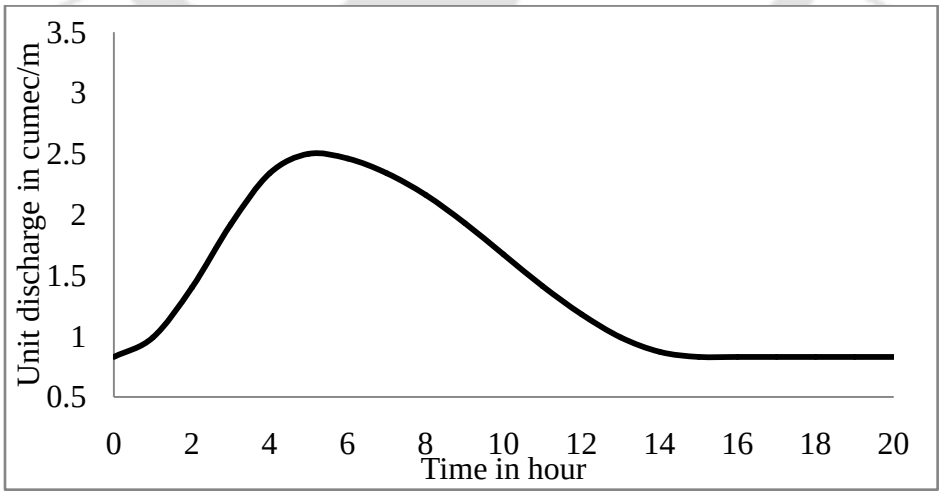

Figure 4.9 Upstream hydrograph for routing by 1D approximation

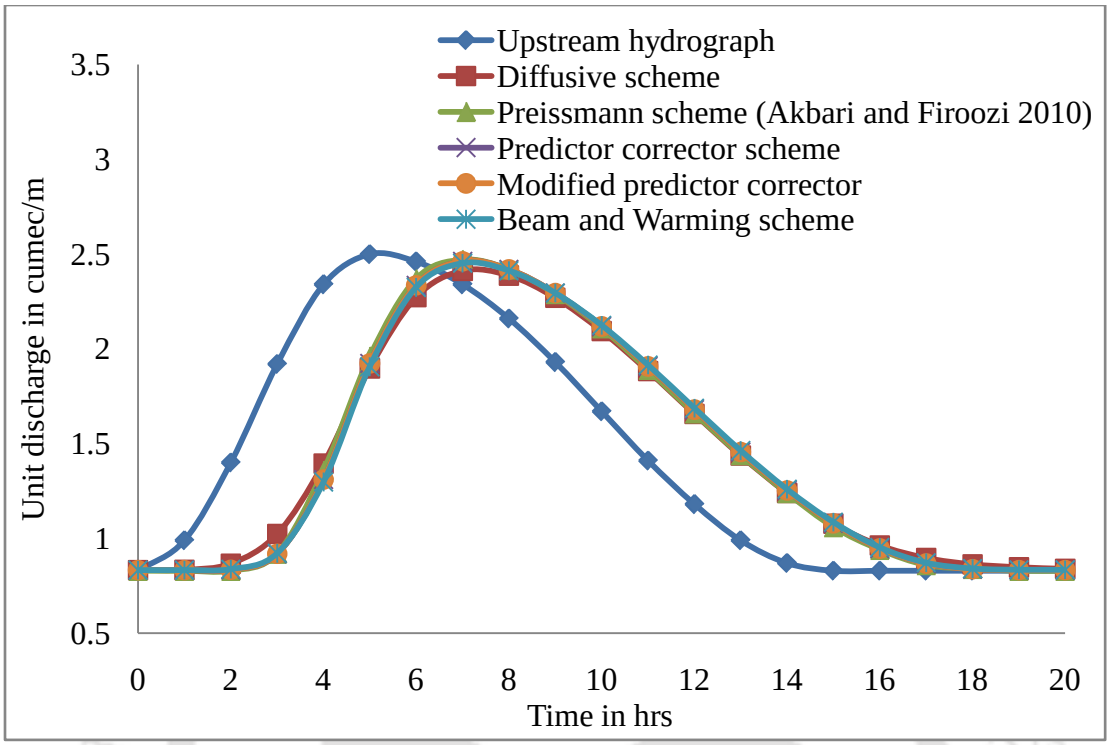

Figure 4.10 Hydrographs at 16000 m downstream evaluated using 1D approximation

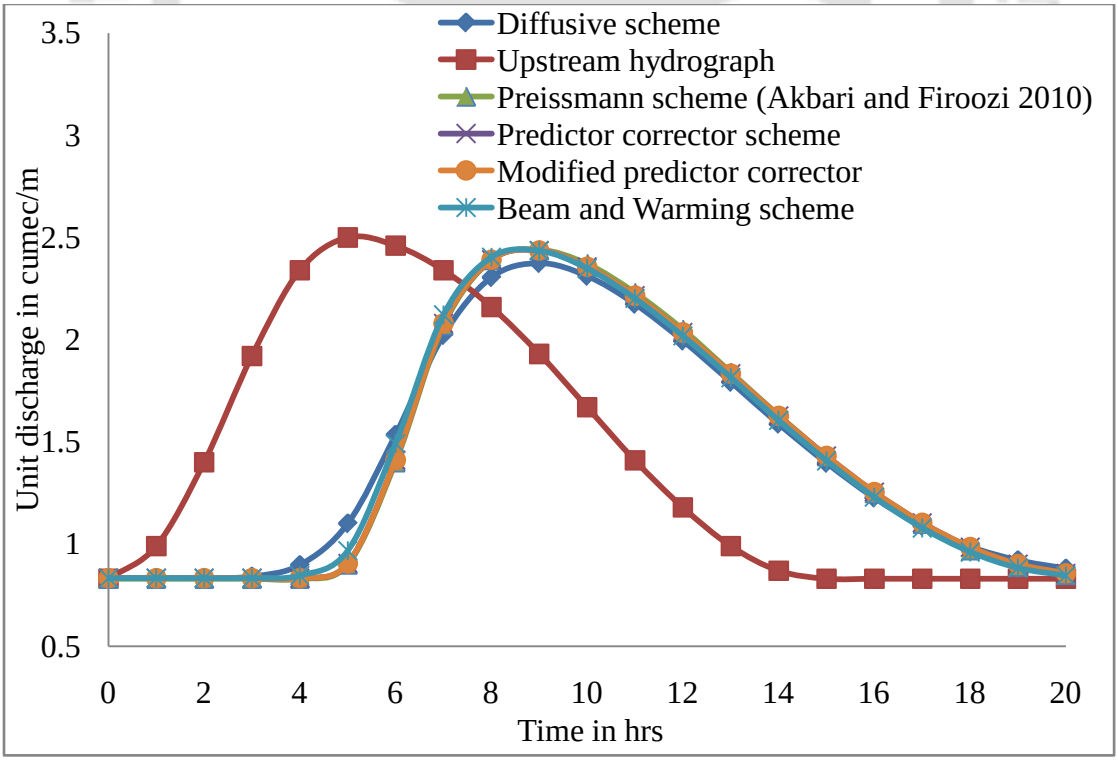

Figure 4.11 Hydrographs at downstream evaluated using 1D approximation

Table 4.1 presents a comparison of all these numerical schemes in respect of stability (represented by value of courant number and artificial viscosity) and total computational time. Several trials are made to confirm the maximum value of courant number for each of these schemes for which the scheme remains stable. To eliminate effect of computer capacity, all the programs are run on a Windows 7 based computer with Pentium dual core processor with 2.1 GHz.

Table 4.1 Comparison of schemes in 1D approximation

Numerical scheme	Δx (meter)	Δt (second)	Courant number (CN)	Artificial viscosity	Computational time required (second)
Lax diffusive	1000	150	0.83	-	0.091
Predictor corrector	1000	150	0.83	CS=0.01	0.44
Modified predictor corrector	1000	150	0.83	CS=0.01	0.44
Beam and Warming	1000	400	2.22	CT=0.02	2.34

From table 4.1 it may be noted that, Lax diffusive scheme takes lowest computational time followed by MacCormack predictor corrector scheme, modified predictor corrector scheme and Beam and warming scheme. The program of the diffusive scheme is very simple and hence takes less time than the other programs. However, a larger value of CN can be used in case of Beam and warming scheme due to implicit nature. Moreover, artificial viscosities are taken in predictor corrector, modified predictor corrector and Beam and warming schemes as they are second order accurate scheme.

4.3.3 Flow hydrograph routing using 2D approximation of governing equations

For hydraulic routing using 2D approximation of governing equations, a hypothetical river of length 30000 m is considered having a width of 600 m. A slope of 1:5000 and a manning's roughness value of 0.013 are considered for the river. The whole river is discretized into finite difference grid of size 61 by 7. This discretization leads to a value of 500 m for Δx and a value of 100 m for Δy. For the diffusive scheme, predictor corrector scheme and modified predictor

corrector scheme, a temporal step of 40 second is used. However, for the Beam and warming scheme this value is 120 second.

Figure 4.12 shows the upstream flow hydrograph. Figure 4.13 shows the routed hydrographs at a section 15000 m downstream using all the schemes. Similarly, figure 4.14 shows the routed hydrographs at downstream. From these figures it can be observed that all the four schemes are giving exactly same results.

Table 4.2 shows a detail comparison of all the schemes. It may be noted from the table that, Beam and warming scheme remains stable for CN more than 1 though it takes larger computational time.

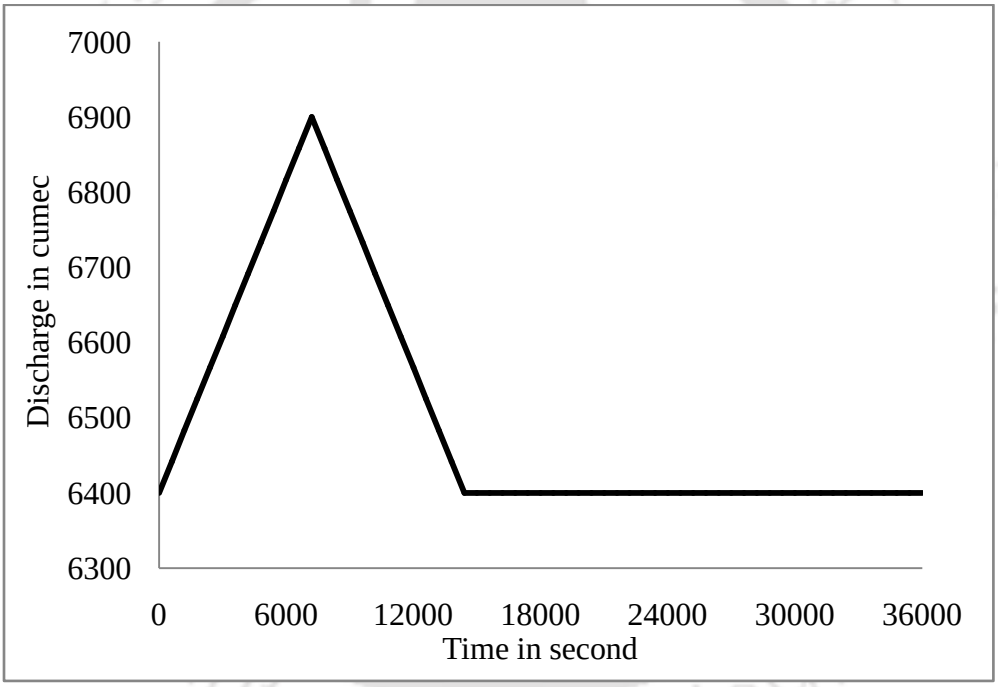

Figure 4.12 Upstream hydrograph for routing by 2D approximation

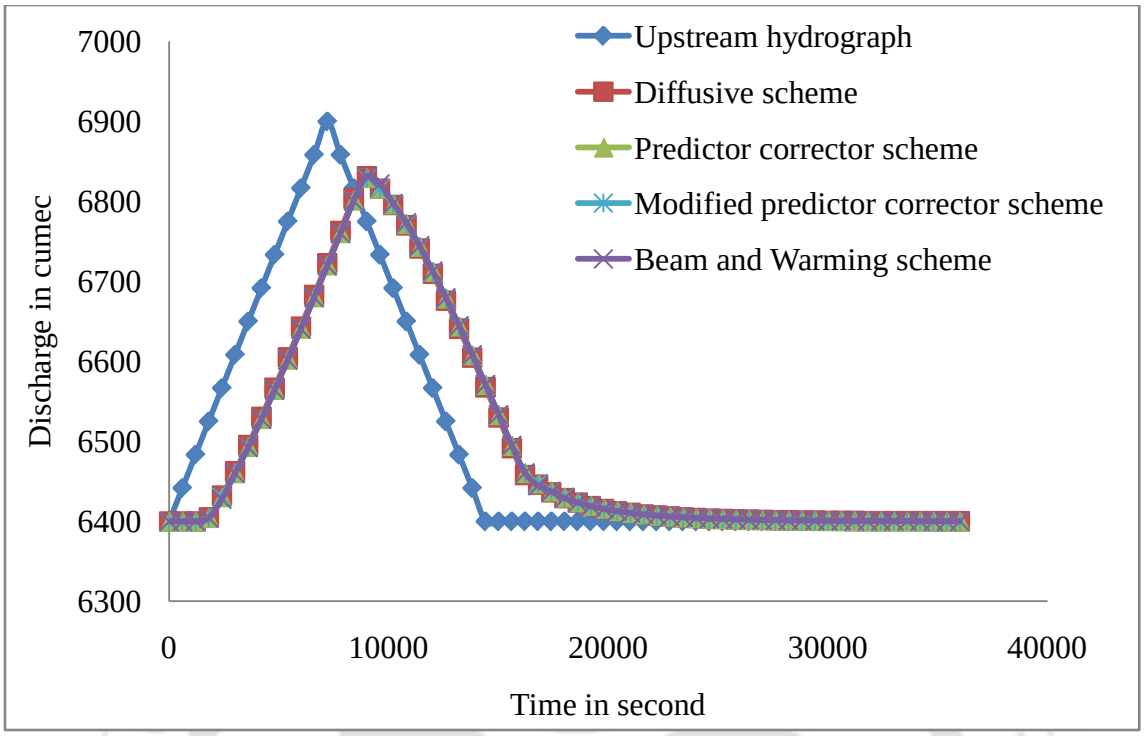

Figure 4.13 Hydrographs at 15000 m downstream evaluated using 2D approximation

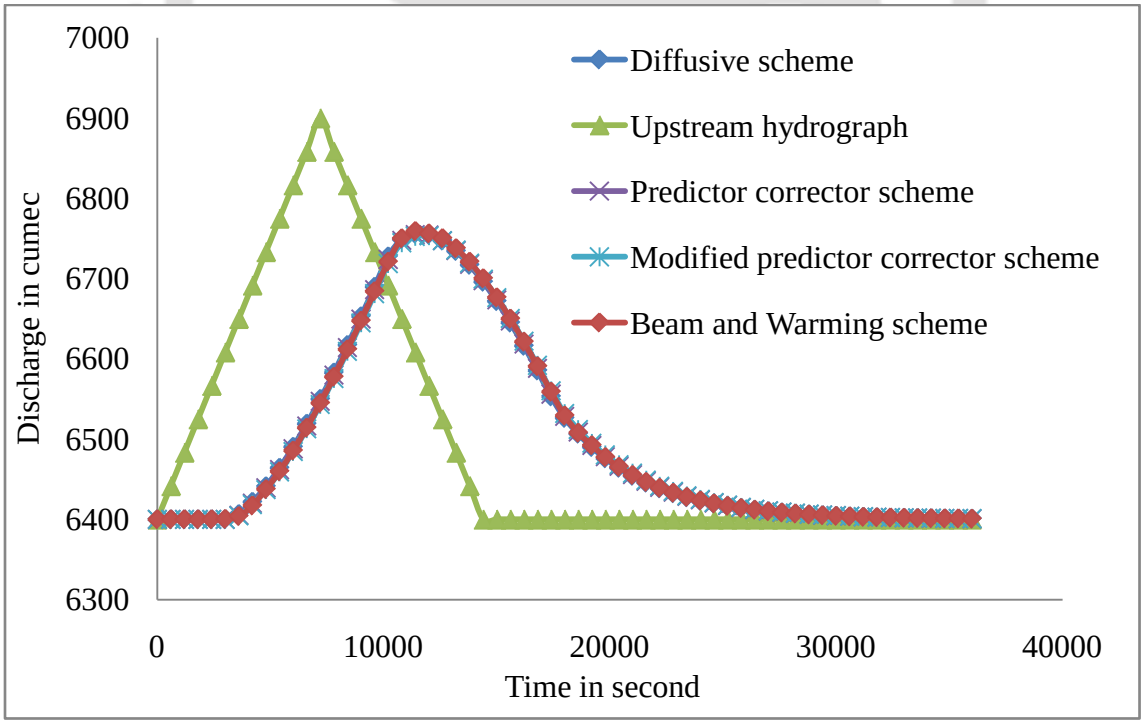

Figure 4.14 Hydrographs at downstream evaluated using 2D approximation

Table 4.2 Comparison of schemes in 2D approximation

Numerical scheme	Δx (meter)	Δy (meter)	Δt (second)	Courant number (CN)	Artificial viscosity	Computational time required (second)
Diffusive	500	100	40	0.73	-	8.8
Predictor corrector	500	100	40	0.73	0.4	35.34
Modified Predictor corrector	500	100	40	0.73	0.4	35.34
Beam and Warming	500	100	120	2.2	0.2	59.2

4.3.4 Simulation of flow processes around groyne

Groyne or spur dike is one of the commonly used river training structures, which is constructed from the bank extending towards the main flow for various objectives. Some of such objectives are, reduction of erosion, deflecting/repelling the flow away from the bank for its safety, increasing flow depth to facilitate navigation, to create recreational reach and achieving vibrant but stable near-bank channel for river front development. Due to the various features of groyne, groyne simulation study has become very essential study for hydraulic engineers.

To appraise the performances of all the numerical schemes considered in this study in case of flow simulation around groynes, the experimental data obtained by Rajaratnam and Nwachukwu (1983) is used. The experimental studies were done on a straight rectangular flume of 37 m long and 0.914 m wide. The groyne considered was an aluminum plate, of length 0.15 m. The extent of the area that has been simulated mathematically is from 1.8 m upstream of the groyne to 3.6 m downstream of the groyne. The study area is discretized to finite difference grid of size 97 × 45. Manning's n value is taken equal to 0.01 for the smooth channel. At the upstream boundary, u velocity is 0.253 m/s and v velocity is 0 m/s. The value of h is extrapolated from interior domain. However at downstream, the values of u and v are extrapolated from interior domain and h is fixed to a value of 0.189 m. A CN value of 0.83 is considered for Lax diffusive, predictor corrector and modified predictor corrector scheme, and a value of 2.2 is considered for the Beam

and warming scheme. The value of CS for the original and modified predictor corrector schemes is taken as 0.08. Similarly, for Beam and warming scheme CT value is considered as 0.01.

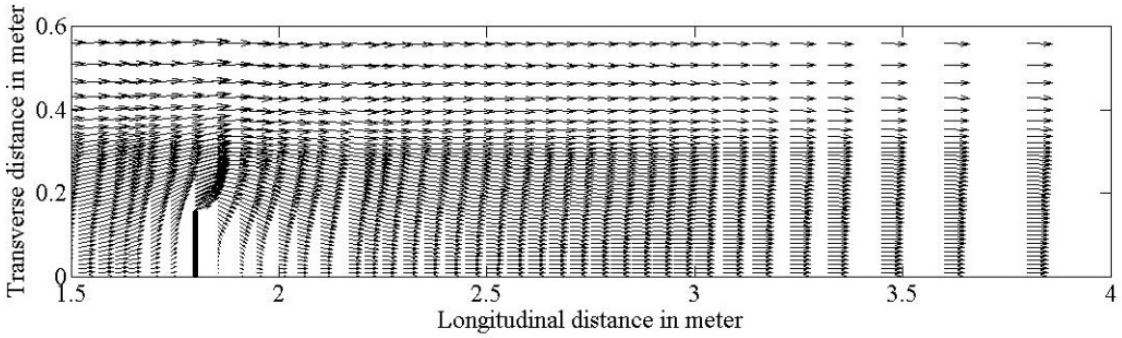

Figure 4.15 Velocity vector plot for Rajaratnam and Nwachukwu (1983) channel using Lax diffusive scheme

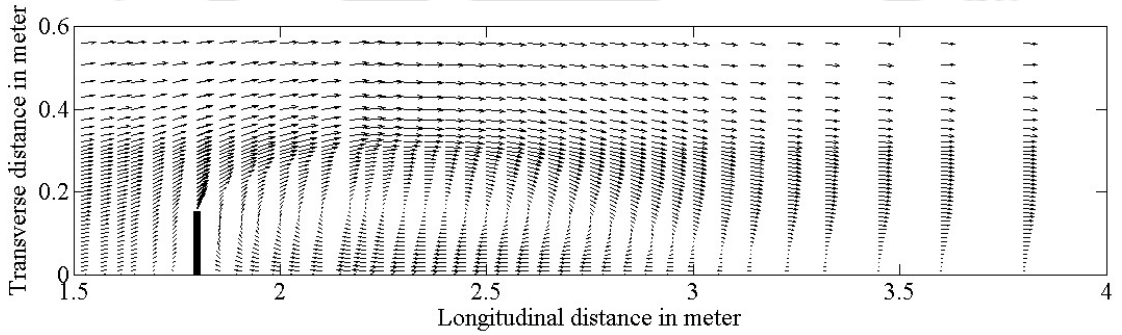

Figure 4.16 Velocity vector plot for Rajaratnam and Nwachukwu (1983) channel using Predictor corrector scheme

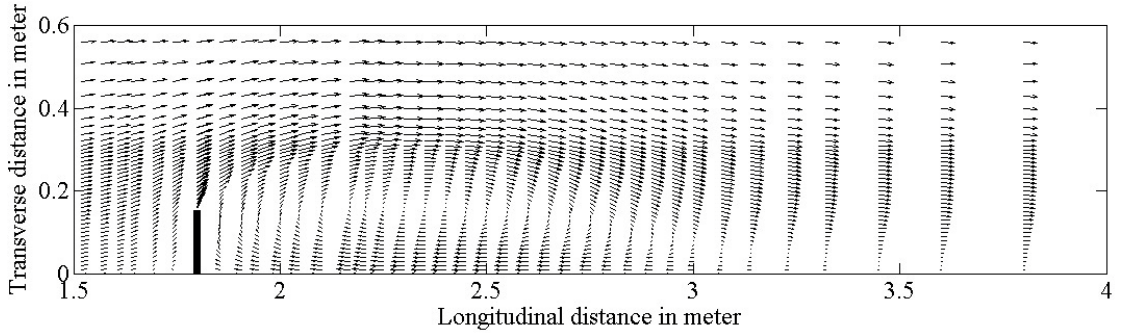

Figure 4.17 Velocity vector plot for Rajaratnam and Nwachukwu (1983) channel using modified predictor corrector scheme

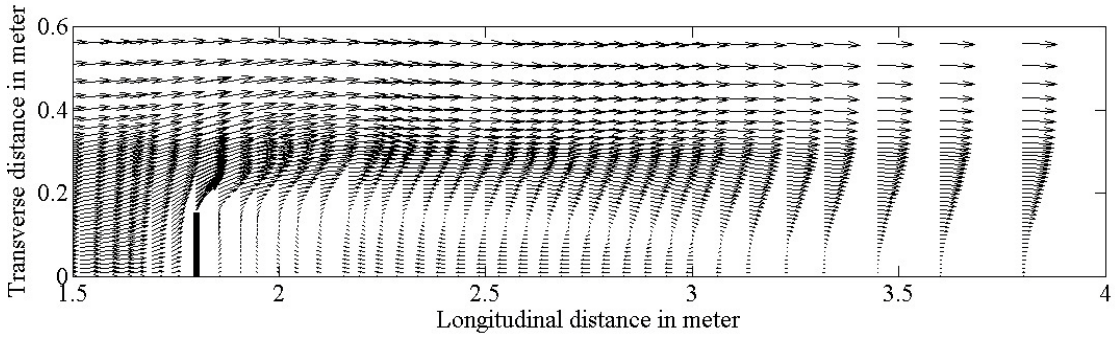

Figure 4.18 Velocity vector plot for Rajaratnam and Nwachukwu (1983) channel using Beam and warming scheme

Figures 4.15, 4.16, 4.17 and 4.18 shows the velocity vector plot for diffusive, predictor corrector, modified predictor corrector and Beam and warming schemes respectively. In the diffusive scheme, a very small recirculation zone is developed downstream of the groyne. It may be due to the excessive dissipation error associated with this scheme. However, a prominent recirculation zone is developed at downstream of the groyne which ends at 3.48 m for the remaining three schemes. In the experimental case, the recirculation zone ended at 3.6 m.

The resultant velocity (W) is non-dimensionalized with respect to free stream velocity of 0.253 m/s. Figures 4.19, 4.20, 4.21 and 4.22 shows the comparison of simulated and experimental velocities at four different distances of 0.15 m, 0.225 m, 0.4 m and 0.6 m respectively from the lower bank. From these figures it can be easily noted that, Beam and warming scheme has the good potential to imitate the actual flow scenario around groynes out of the numerical schemes tested in this project. As flow simulation around groyne is the main base work in the present work, Beam and warming scheme is going to be used for the rest of the work.

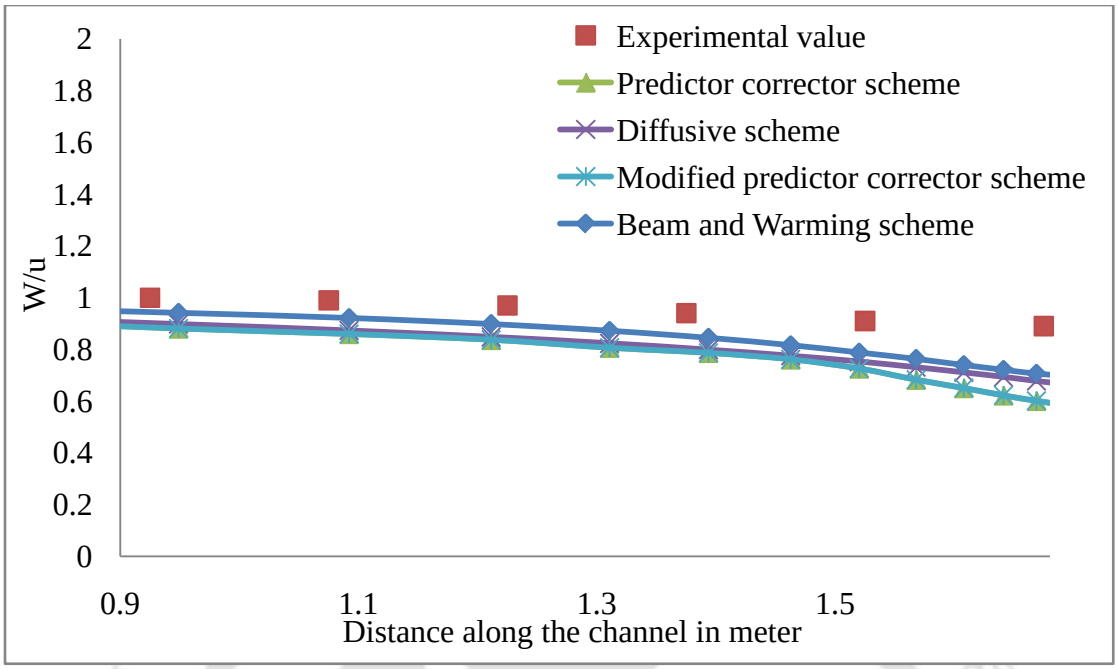

Figure 4.19 Experimental Vs computed velocity (distance=0.15 m) for Rajaratnam and Nwachukwu (1983) channel

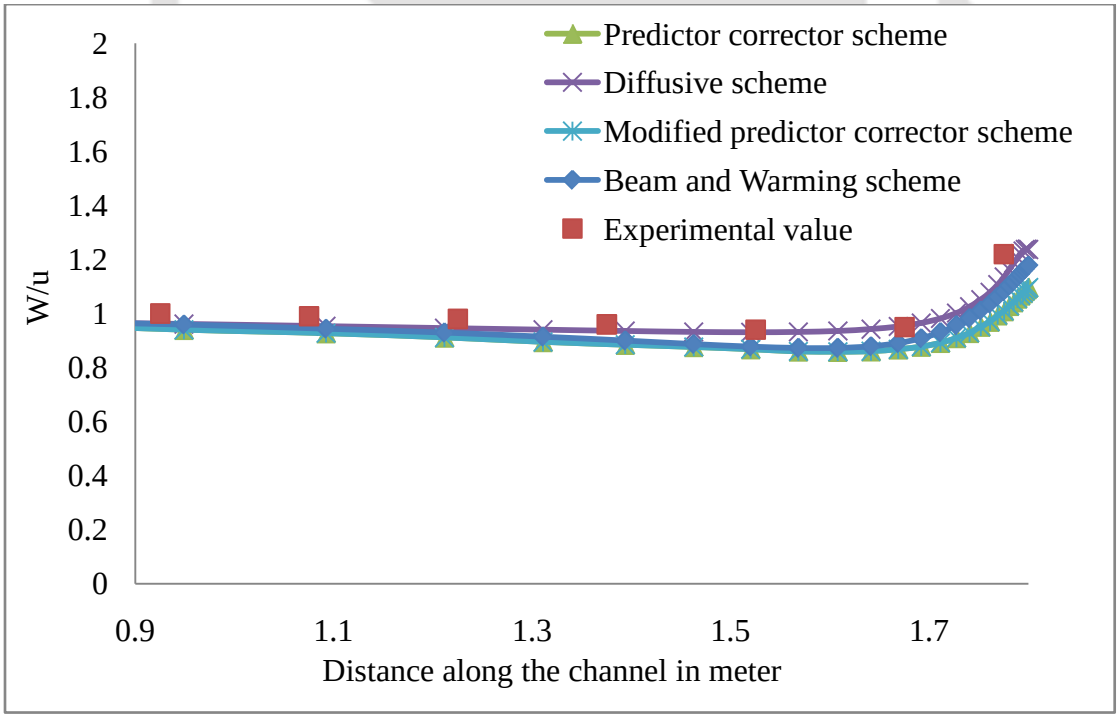

Figure 4.20 Experimental Vs computed velocity (distance =0.225 m) for Rajaratnam and Nwachukwu (1983) channel

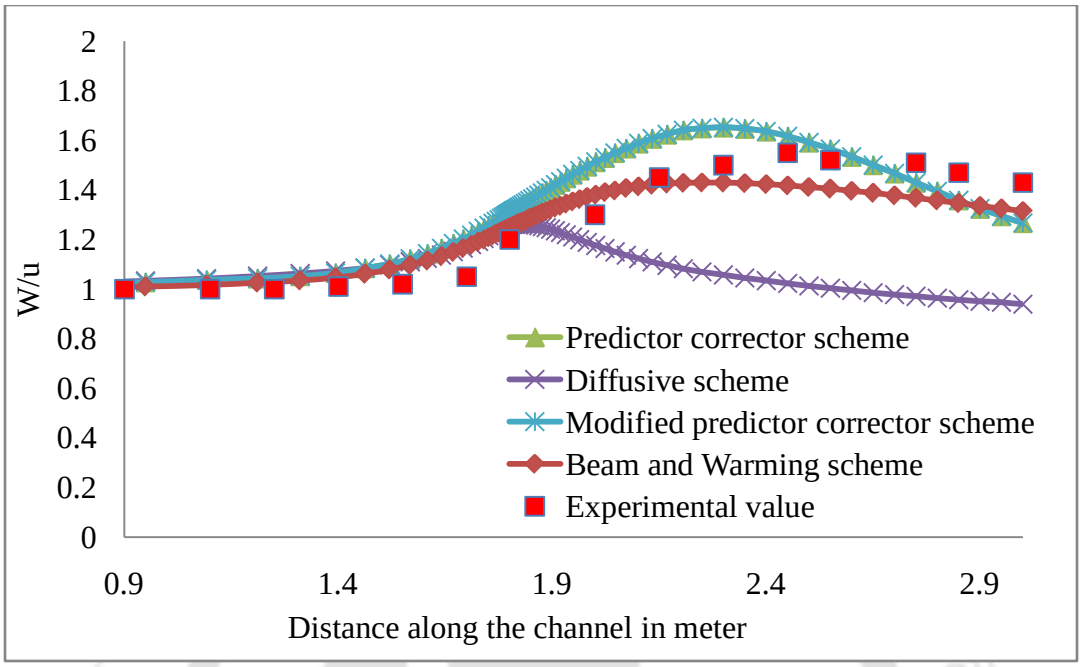

Figure 4.21 Experimental Vs computed velocity (distance =0.4 m) for Rajaratnam and Nwachukwu (1983) channel

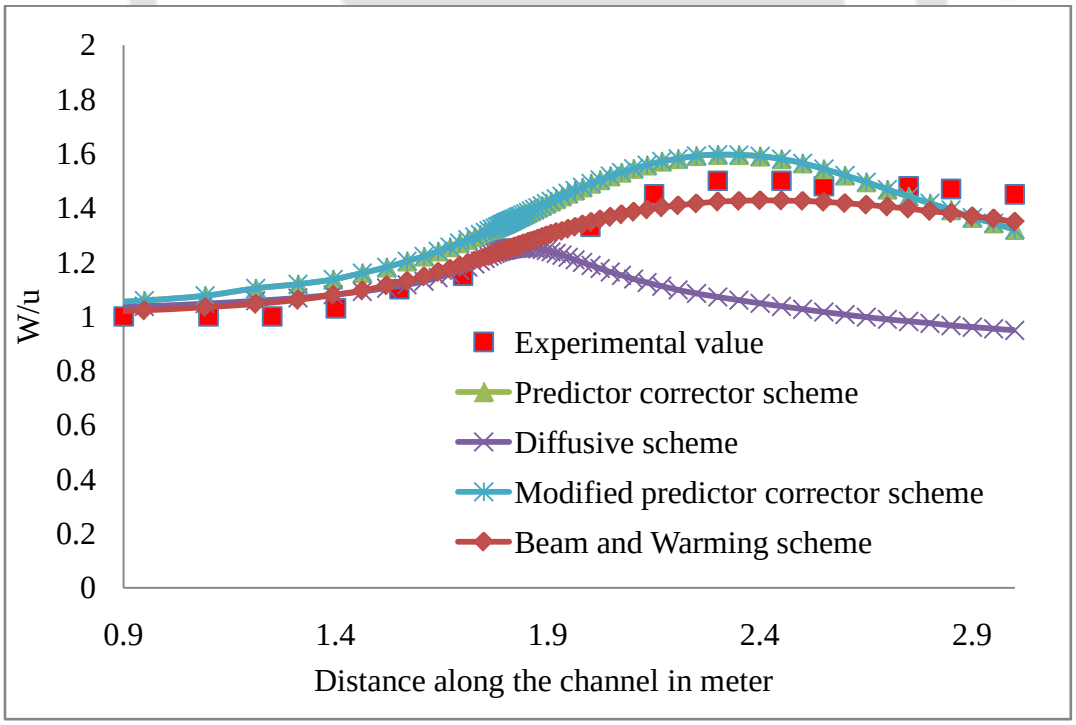

Figure 4.22 Experimental Vs computed velocity (distance =0.6 m) for Rajaratnam and Nwachukwu (1983) channel

4.3.5 Subcritical flow simulation in a U-bend

To assess the applicability of the present model in case of subcritical flow in non regular flow domain, the computed results are compared with experimental results obtained by Rozovskii (1957) and reported by Molls and Chaudhry (1995). The test channel is composed of one 180^0 curve connected by two straight channels of length 0.5 m each. The channel width is 0.8 m and the internal radius is 0.4 m. The entire channel is set on a horizontal bed. A (29×21) grid is generated for representing the flow domain. Figure 4.23 shows the study area along with the generated grid for the Rozovskii channel.

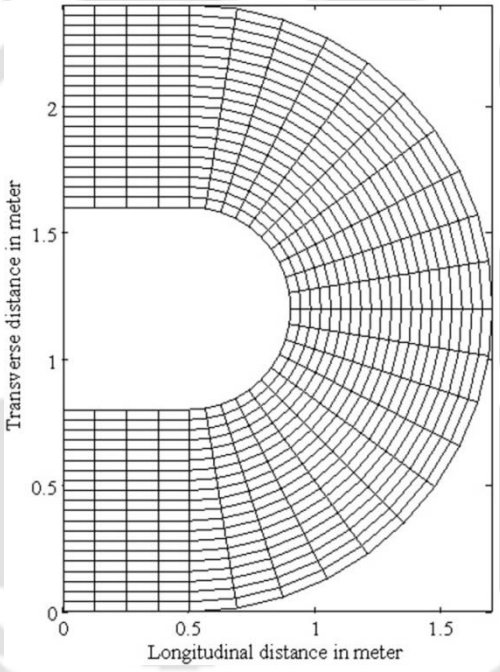

Figure 4.23 Study area along with the generated grid for the Rozovskii channel

No information was provided by Rozovskii about the value of manning's roughness n. A value of n equal to 0.01 is taken in the present model as the channel is said as smooth. The model is run for a CN of 1.3 and value of CT is 0.1. The discharge in the channel is 0.0123cumec. At the upstream boundary, the u velocity is specified as 0.265 m/s, and the v velocity is set to zero, and the depth is extrapolated from interior points. At the downstream boundary, the depth is taken from experimental water surface contours obtained by Rozovskii (1957). The downstream u and v velocities are extrapolated from interior points. Figure 4.24 shows the computed velocity vector and water depth contour line calculated by the present model.

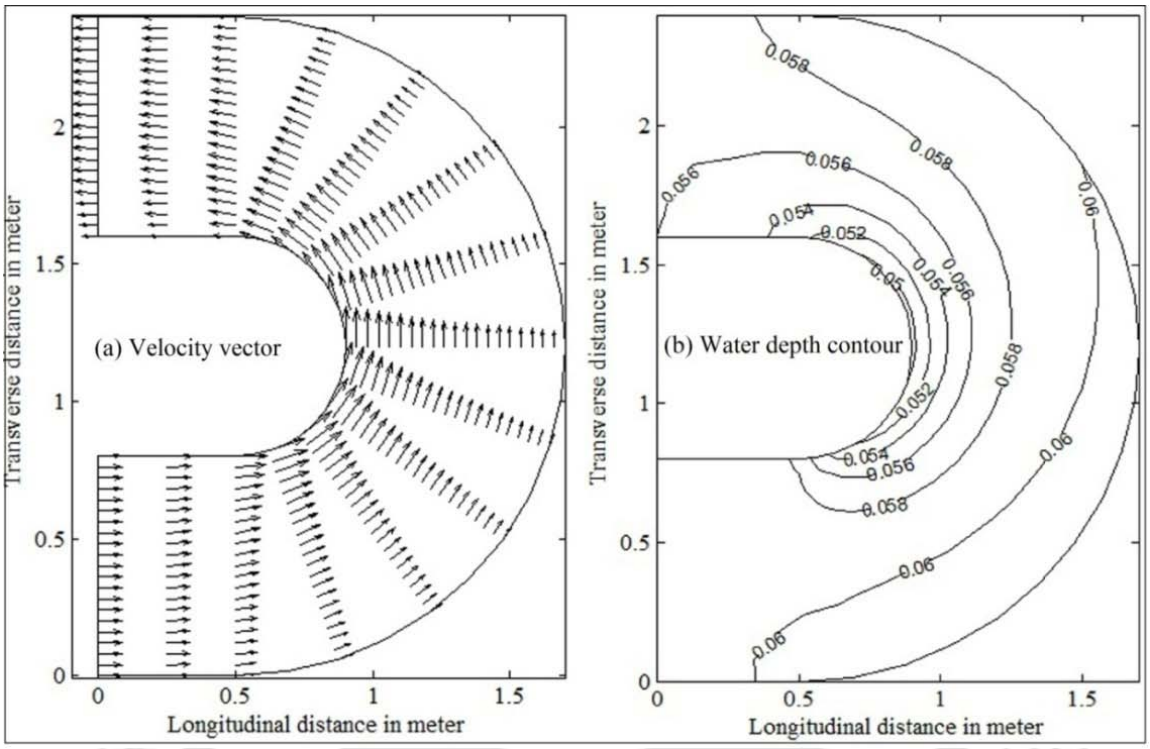

Figure 4.24 Results obtained by present model for the Rozovskii channel

The water depths along the banks obtained by the present model are compared with the experimental results. The channel length is non-dimensionalized as s/b. Where s is the distance along the center line of the channel and b is the channel width. Figure 4.25 shows the comparisons where a good agreement has been observed.

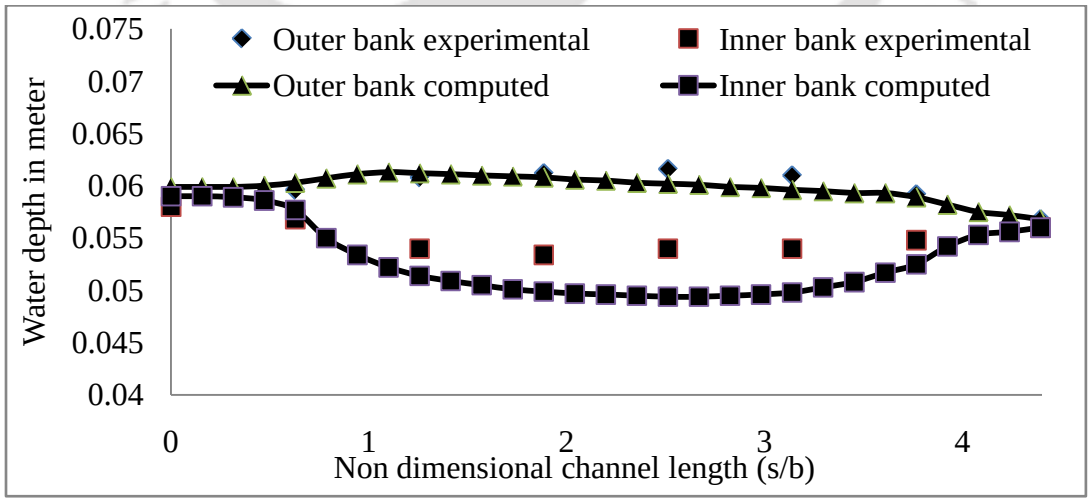

Figure 4.25 Comparison of water depth along the banks for Rozovskii channel

4.3.6 Supercritical flow simulation in a diverging channel

For validation of the present model in case of supercritical flow, the results obtained from experimental study done by Rouse et al. (1951) and reported by Farsirotou et al. (2002) are used. The inlet width of the channel is 10 m which gradually increases to a value of 28.37 m in 60 m. The channel area is discretized into finite difference grid of size (61×13) and is shown in figure 4.26.

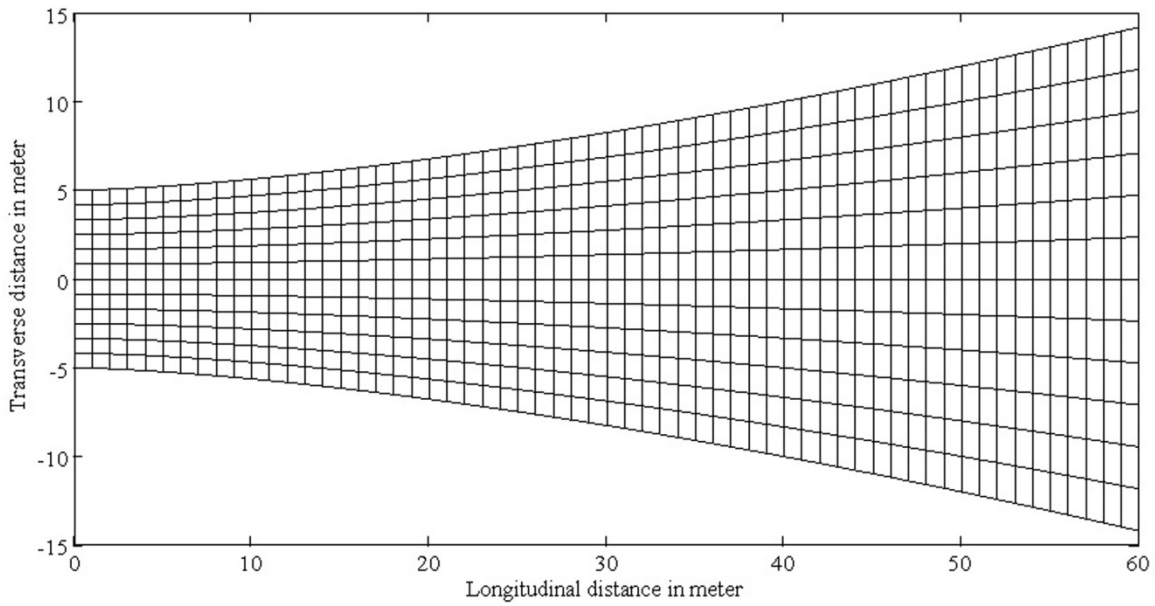

Figure 4.26 Study area along with the generated grid for the Rouse channel

For comparison with experimental results, the present model is run with same inputs as that of the experimental channel. The channel is horizontal and manning's roughness coefficient is given as 0.012. The values of inlet flow variables h, u and v are 1 m, 12.5264 m/s and 0 m/s respectively. At downstream boundary all of these variables are extrapolated from interior domain as the flow is supercritical. The model is run for a CN of 1.8 while the CT value is taken as 0.12. Figures 4.27 and 4.28 show the computed velocity vector and water depth contour respectively.

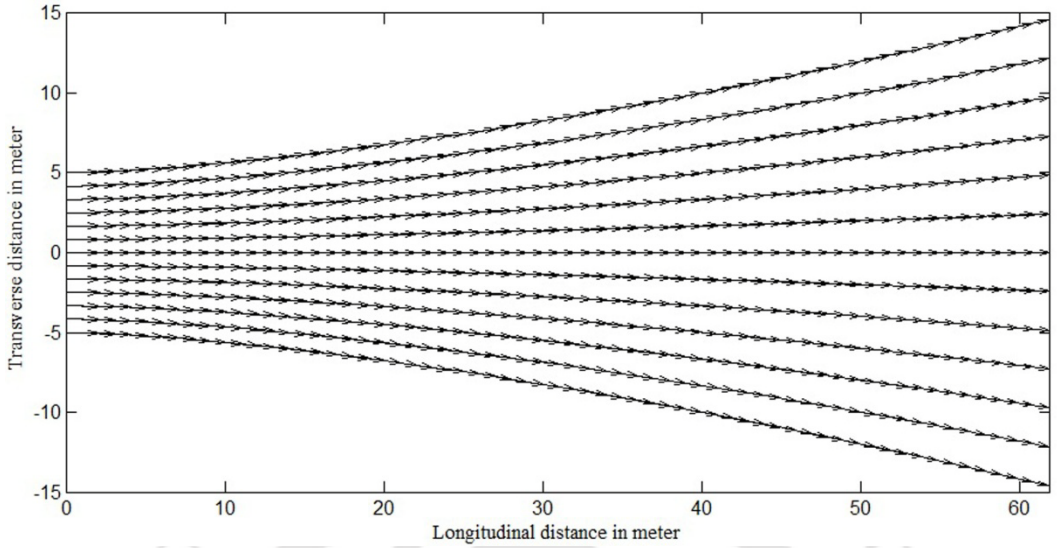

Figure 4.27 Computed velocity vector for the Rouse channel

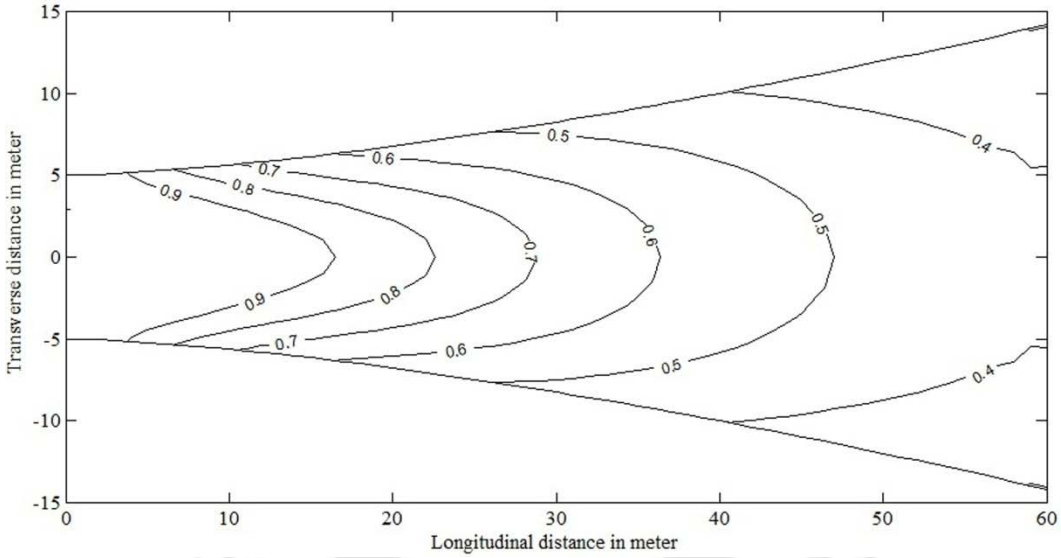

Figure 4.28 Computed water depth contour for the Rouse channel

The non dimensionalized water depth (h/h1) along three lines are compared between the experimental results and computed results to check the performance of the present model. The value of h1 is the upstream water depth which is equal to 1 m. The three lines considered are the axis of symmetry, the curved side and the middle line between these two lines. Figure 4.29 shows this comparison, where a good resemblance between experimental and computed results is observed.

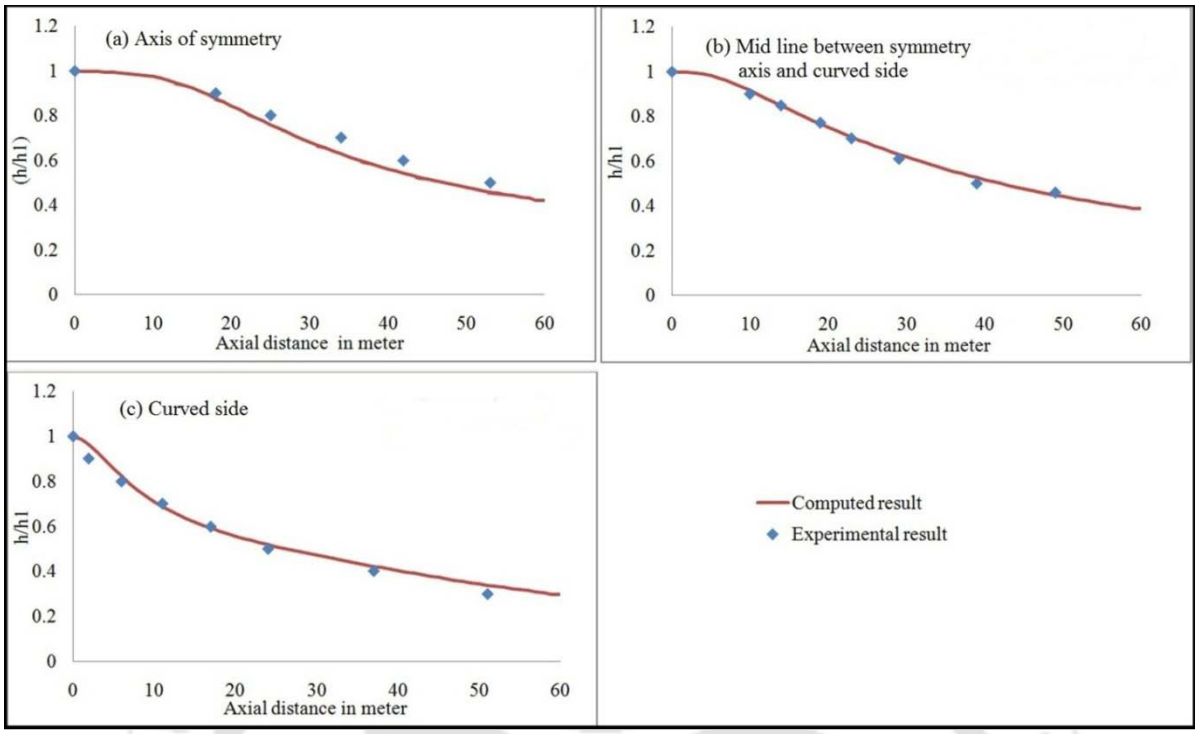

Figure 4.29 Comparison of experimental and computed water depths for Rouse channel

4.3.7 Mixed flow simulation in a converging channel

Sometimes subcritical and supercritical flows can occur concurrently in a channel flow. This type of flow is called mixed flow. To appraise the applicability of the present model in case of mixed flow condition, the computed results are compared with experimental results obtained by Coles and Shintaku (1943) and reported by Klonidis and Soulis (2001). The test channel is composed of two straight channels connected by a 1.49 m long straight walled contraction. The inlet and outlet widths are 0.629 m and 0.314 m respectively. There are no slopes along the channel or across the channel. A (21×37) grid is generated for the flow domain. Figure 4.30 shows the study area along with the finite difference grid.

The channel is said to be a smooth one. So a value of 0.01 is taken for manning's roughness value. A value of 2.2 is used for the CN, while the CT value is taken as 0.08. The flow is subcritical upstream of the contraction and slightly supercritical at the downstream boundary. The upstream and downstream depths are specified as 0.1762 m and 0.1132 m respectively. The upstream and downstream u velocities are extrapolated from interior points. The upstream v value is set to zero and the downstream v value is extrapolated from interior points. Figures 4.31

and 4.32 show the computed velocity vector and water depth contour line respectively calculated by the present model.

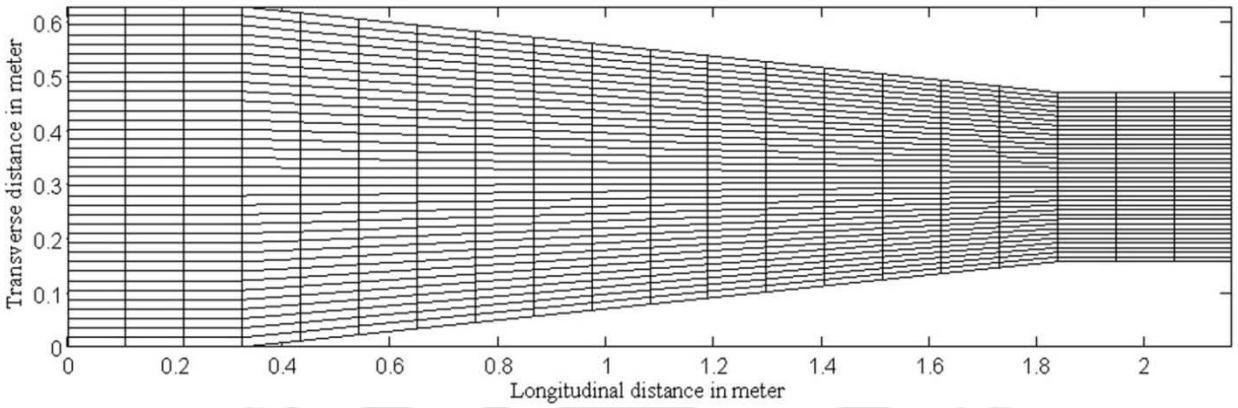

Figure 4.30 Study area along with the generated grid for the Coles and Shintaku channel

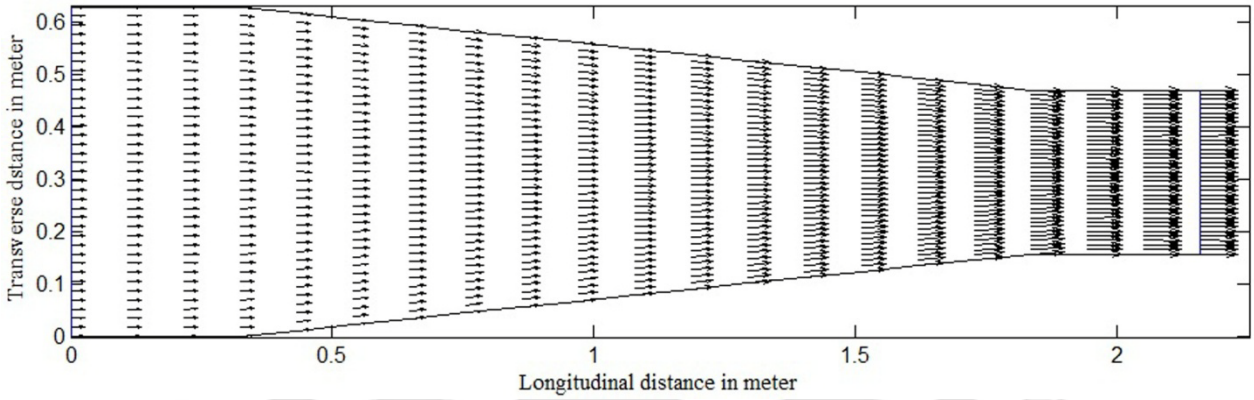

Figure 4.31 Computed velocity vector for the Coles and Shintaku channel

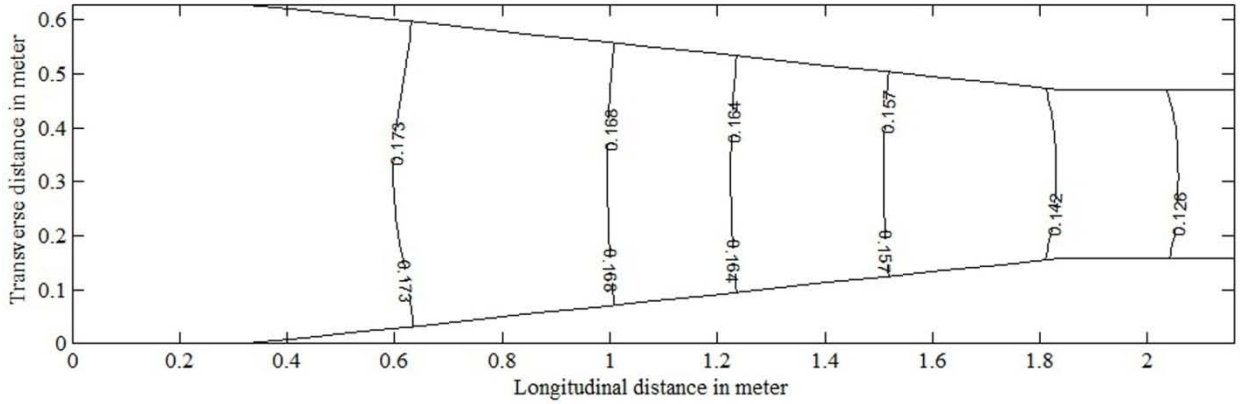

Figure 4.32 Computed water depth contour for the Coles and Shintaku channel

The water depths along the center line obtained by the present model are compared with the experimental results and the comparison is shown in figure 4.33. The figure shows a very good agreement between them and establishes the potentiality of the present model in case of mixed flow also.

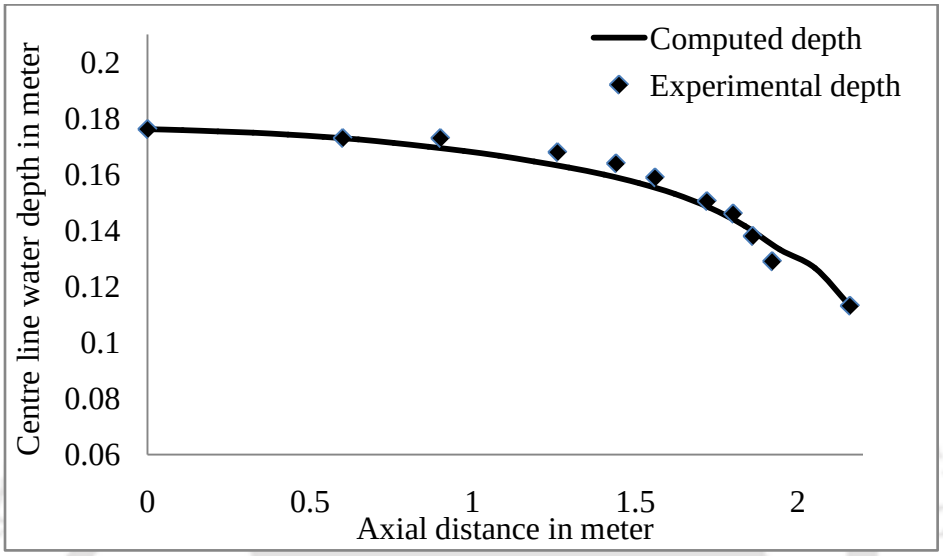

Figure 4.33 Comparison of experimental and computed depth for Coles and Shintaku channel

4.4 Conclusions

Folowing conclusions are obtained from this chapter.

1. First order accurate explicit Lax diffusive scheme, sceond order accurate explicit MacCormack predictor corrector and modified predictor corrector scheme and second order accurate implicit Beam and Warming schemes have been applied to solve the governing equations of unsteady free surface flows both in 1D and 2D approximations. It has been observed that for hydrograph routing in prismatic channel all the schemes have good accuracy.
2. Comparison of results obtained utilizing two different downstream boundary conditions such as, solution of characteristics equation and extrapolation technique reveals that using extrapolation technique can also lead to same quality results as that of charateristic equation solution technique at less computational effort.
3. From the comparion of simulation time required by all the four schemes for routing a flow hydrograph, it has been observed that, diffuxive scheme takes lowest time for

simulation. However, predictor corrctor and modified predictor corrector scheme takes equal computational time which is more than that of diffusive scheme. Moreover, Beam and Warming schemes takes the highest computational time among the compared schemes.

4. In case of flow simulation around groyne, it is observed that Beam and Warming has the highest accuracy in representing the flow scenario around the groyne.
5. Using the Beam and Warming scheme for the governing equations in a boundary fitted coordinate system, accurately simulated the flow scenarios for different flow regimes such as subcritical flow, supercritical flow and mixed flow.
6. Beam and Warming scheme is therefore chosen for simulating flow around river training work in this study.

CHAPTER 5

LINKED SIMULATION-OPTIMIZATION MODEL

5.1 Introduction

An important aspect of designing groyne system for any vulnerable river reach is the determination of number, position and length of each groyne. As these structures are very expensive, an optimization model is needed to determine the optimal combination of groynes leading to minimum construction cost of the groyne system. In this chapter, an optimization model is developed to find the cost effective combination of groyne system. The optimization model is solved using binary coded Genetic Algorithm (GA). To appraise the performance of the present model, it is applied for three different cases, which includes one hypothetical straight channel, one hypothetical meandering channel, and one hypothetical braided channel. Details of the optimization model developed for the affirmed purpose and results obtained by the model for all the three channels are presented in this chapter.

5.2 Development of optimization model

Groyne is a commonly used river training structure, which is constructed on the bank of a river extending towards the main channel. Groynes are constructed for various purposes; one of which is the reduction of water flow speed to a value for promoting sedimentation and which eventually prevents bank erosion. The cost of construction of a groyne is very expensive, as it requires huge quantity of high quality materials as well as sophisticated machineries for carrying out the construction. Therefore, an optimal combination of groynes in terms of their number, position and length should be taken up so as to minimize the total construction cost of the project. This necessitates a model study so that optimal combination of the groynes can be determined. Mathematical modeling is preferred over the physical model as there is limited scope in case of physical model for testing of large alternatives due to time and cost constraints. Generally, for selecting the optimal combination of groynes, some pre-decided combinations are chosen and are tested using flow simulation model to determine the best one from the chosen alternatives. This trial and error approach does not guarantee a true optimal combination, as the best one is chosen out of the combinations given by the user. Therefore, an optimization model is needed which can

obtain the global optimal combination of groynes leading to minimum construction cost. In order to obtain the optimal combination, the flow simulation model has to be incorporated with the optimization model. The flow simulation model can be incorporated using linked simulation-optimization model. The main objective of the linked simulation-optimization model is to minimize the total construction cost of groyne system while reducing the flow speed to a desired value. Based on the practical requirements, three different optimization formulations have been proposed which are described below.

5.2.1 Optimization Formulation I

For rivers facing bank erosion problem, groynes are generally constructed on the vulnerable areas to reduce the flow speed. For this case, the optimization model should have the capacity to determine the optimal combination of the groyne system such that any target flow speed can be achieved at desirable places within the river. Thus the main outcome of formulation I is to determine the number, position and length of the groynes that are to be placed on the banks of a river to achieve a predefined target speed on a predefined area within the river. The objective of this formulation is to minimize the total construction cost of the groyne system. The number of groynes having non-zero length is the required number of groynes. The optimization model can be formulated as given below.

Minimize

$$C(Lrg, Llg) = \sum_{Ng=1}^{N} (Lrg + Llg) \times C1 \tag{5.1}$$

Subject to,

$$UU \leq \Omega \tag{5.2}$$

$$Llg_{min} \leq Llg \leq Llg_{max} \tag{5.3}$$

$$Plg_{min} \leq Plg \leq Plg_{max} \tag{5.4}$$

$$Lrg_{min} \leq Lrg \leq Lrg_{max} \tag{5.5}$$

$$Prg_{min} \leq Prg \leq Prg_{max} \tag{5.6}$$

Where C is the total construction cost of groynes in ₹, C1 is the per meter construction cost of a groyne and is taken equal to ₹ 100000, Ng is the total number of groynes, Llg is the length of groyne on the left bank in terms of grid number, Lrg is the length of groyne on the right bank in terms of grid number, Plg is the position of groynes on the left bank in terms of grid number from upstream boundary, Prg is the position of groynes on the right bank in terms of grid number from upstream boundary, Llg_{max} is the maximum allowable length of groyne on left bank in terms of grid number, Lrg_{max} is the maximum allowable length of groyne on right bank in terms of grid number, Llg_{min} is the minimum allowable length of groyne on left bank in terms of grid number, Lrg_{min} is the minimum allowable length of groyne on right bank in terms of grid number, Plg_{min} to Plg_{max} is the extreme limit on the left bank in terms of grid number within which the groynes are to be placed, Prg_{min} to Prg_{max} is the extreme limit on the right bank in terms of grid number within which the groynes are to be placed, UU is the maximum speed on the specified areas in m/s and is obtained at every iteration of optimization model by simulating the hydrodynamic process, Ω is the target speed value in m/s.

5.2.2 Optimization Formulation II

In formulation I, it is observed that the position of groynes may be anywhere within the position limits. However, in practical situation sometimes it may not be possible to place groyne everywhere within the position limit. Thus it is necessary to fix the position of the groynes. In formulation II, it is considered that the positions of the groynes are already fixed on the banks. As such, the model will obtain the length and number of the groynes for achieving a predefined target speed on a predefined area within the channel which will yield minimum construction cost. The groynes having non-zero length is the required number of groynes. The mathematical formulation can be written as,

Minimize

$$C(Lrg, Llg) = \sum_{Ng=1}^{N} (Lrg + Llg) \times C1 \qquad (5.7)$$

Subject to,

$$UU \leq \Omega \qquad (5.8)$$

$$Llg_{min} \leq Llg \leq Llg_{max} \quad (5.9)$$

$$Lrg_{min} \leq Lrg \leq Lrg_{max} \quad (5.10)$$

Where, the parameters C, C1, Lrg, Llg, Llg_{min}, Llg_{max}, Lrg_{min}, Lrg_{max}, Ng, UU and Ω defines the same as that of formulation I.

5.2.3 Optimization Formulation III

In formulations I and II, number of groynes may be any number within the allowable limits. In some situation sufficient funds may not be available to construct the required numbers of groynes as obtained by formulation I and II. In such situation, the designer may be asked by the authority to implement only the fixed number of groynes that is possible with the available fund. Therefore, in the formulation III, a modified formulation has been presented to account this situation. The objective of this formulation is therefore to find out the location of the available groynes of known length which will provide minimum speed of water on a predefined area. The optimization model can be formulated as given below,

Minimize UU (5.11)

Subject to,

$$Plg_{min} \leq Plg \leq Plg_{max} \quad (5.12)$$

$$Prg_{min} \leq Prg \leq Prg_{max} \quad (5.13)$$

Where, the parameters UU, Plg_{min}, Plg_{max}, Prg_{min}, Prg_{max}, Plg and Prg define the same as that of formulation I.

5.3 Optimization algorithm

An optimization technique is required to solve the linked simulation-optimization models formulated above. It has been observed that the classical gradient based methods are not suitable for solving the non-convex nonlinear problems. Moreover, the classical methods are also not suitable for solving integer problem or mixed-integer problem. On the other hands, global search methods, such as GAs are suitable for solving the non-linear non-convex problems as they have the mechanism to overcome the local optimal solutions. As stated earlier, the variables in this

optimization problem are number, length and position of groynes. The number of groyne is always an integer number. However, position and length of groynes are here in terms of finite difference grids, which is again integer number. Since value of all these variables are integer, the present optimization model is solved using binary coded genetic algorithms with string length leading to an accuracy of one. This will result the values of the variables as integer.

5.3.1 Genetic Algorithm

Genetic Algorithm (GA) is an iterative based robust search technique which is based on the evolution process of natural species. GA has the following main advantages,

- Genetic algorithm is a method which is very easy to understand and it practically does not demand the knowledge of mathematics.
- Since GA works with a population of points instead of single point, simultaneous processing takes place on more than one string leading to a global solution many a time.
- GA is suitable for solving the non-linear non-convex problems as they are based on stochastic rules.

GA is generally consist of the following steps,

i. Select an initial population of strings.
ii. Evaluate the fitness of each string.
iii. Select strings from the current population to mate.
iv. Perform crossover (mating) for the selected strings.
v. Perform mutation for selected string elements.
vi. Repeat steps 2-5 for the required number of generations.

5.3.2 Encoding of variable

The first step for solving a problem using GA is the encoding of the variables in some string structures, called chromosomes. Most common method of encoding is binary coded, where strings are coded with some 1 and 0 s. Real coding of variables is also possible however, for handling integer variables binary coding with accuracy 1 is much suitable. The length of string is generally determined according to the desired accuracy.

5.3.3 Fitness function

As GA is based on the survival of the fittest principle of nature to make a search process, it is naturally suitable for solving maximization problems. Minimization problems are usually transformed into maximization problems by some suitable transformation. For minimization problems, the fitness function is an equivalent maximization problem chosen such that the optimum point remains unchanged.

For a maximization problem, the fitness function can be considered as same as that of the objective function and can be represented as,

$$F(x) = f(x) \tag{5.14}$$

Where, F(x) is the fitness function and f(x) is the objective function.

For a minimization problem the following fitness function is often used,

$$F(x) = \frac{1}{\{1 + f(x)\}} \tag{5.15}$$

This transformation does not alter the optimum point, but converts the minimization problem to an equivalent maximization problem.

5.3.4 GA operators

The following four operators are there in GA,

i. Selection/Reproduction
ii. Crossover
iii. Mutation
iv. Elitism

5.3.5 Selection

Selection is the process to select the good populations out of the initial populations taken to participate in crossover. It is achieved by creating multiple copies of good population and at the same time eliminating the bad solutions to keep the total population same. Some methods that are generally used for selection purpose are,

i. Tournament selection
ii. Roulette wheel selection
iii. Rank selection, etc.

In tournament selection several tournaments are played among a few individuals taken randomly from the initial population and the winner of each tournament is selected. Finally, in the new population multiple copies of the good solution are placed by eliminating the bad solutions to create the mating pool.

In Roulette wheel selection, each member of the population is allocated one slot on the wheel according as their proportionate fitness value. The wheel is then run for number of times equal to the population size and for each run one population is selected. Since the population with larger fitness value has larger area on the wheel, multiple copies of good populations are selected by this technique to participate in crossover process.

In Roulette wheel selection if there is high variation in fitness values among the individuals, then there is very low chance of selection of population of low fitness value. It is because; in the wheel most area is covered by good individuals. This problem can be avoided by using ranking selection procedure. In this procedure, some ranks are given to the individuals according as their fitness value and the wheel is filled up with percentage of the ranks.

Deb (1999) showed that, out of the above selection processes tournament selection has better convergence and computational time.

5.3.6 Crossover

In selection process, new populations are not created but multiple copies of populations with high fitness values are created. However, crossover operator is used to create new solutions from the existing solutions available in the mating pool after applying selection. In crossover process, any two solution strings are randomly taken from the mating pool with some probability and some portion of the strings is exchanged between the strings to create new strings. Some of the crossover processes mostly used are, single point crossover, double point crossover and uniform crossover.

In single point crossover (figure 5.1), a crossover section is chosen beyond which all data are swapped between the parent strings.

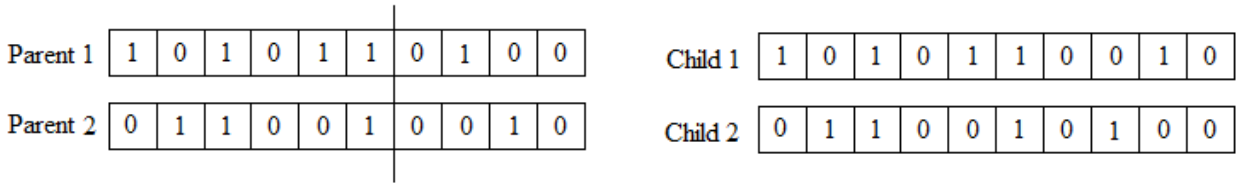

Figure 5.1 Single point crossover approach

In double point crossover (figure 5.2), two crossover sections are chosen between which all data are swapped between the parent strings.

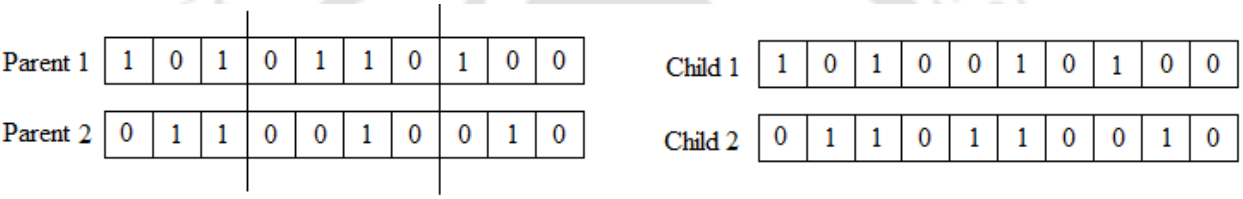

Figure 5.2 Double point crossover approach

In uniform crossover (figure 5.3), a fixed mixing ratio between two parents is chosen such that with respect to that ratio data are swapped between the parents although crossover point may be anywhere. If a mixing ratio of 0.5 is taken then half data from each of the parents will be swapped with any crossover point.

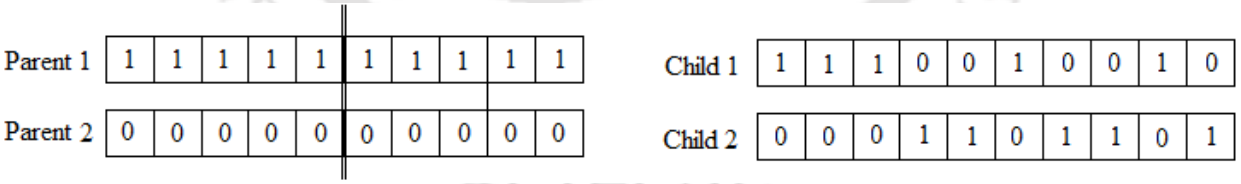

Figure 5.3 Uniform crossover approach

5.3.7 Mutation

In the mutation process some new populations are created by flipping 1 and 0 with some mutation probability to maintain diversity in the population. The mutation process is introduced

to prevent premature convergence to local optima by randomly inserting new points in the search space. Figure 5.4 shows the mutation process.

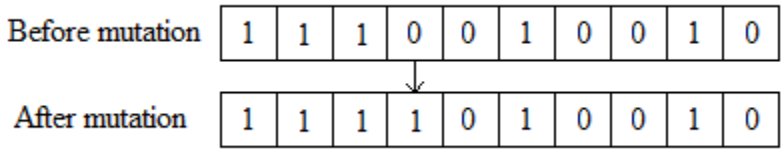

Figure 5.4 Mutation approach

5.3.8 Elitism

Elitism is another process employed by GA which preserves some good solution and directly sends them to next generation without passing through any crossover and mutation processes. It is usually done to prevent the damaging of good solution by the above two processes.

5.4 Solution of linked simulation-optimization model with GA

The simulation-optimization model is solved using binary coded genetic algorithms. The selection operator is carried out using the tournament selection method with a tourney size of two. A value of the probability of crossover of 0.9, a value for mutation probability of 0.003 and a value for elitism fraction of 0.1 are employed in all the formulations. All the formulations are run for 100 generations. Figure 5.5 shows the schematic representation of the GA based linked simulation-optimization model. The initial population is created randomly between specified lower and upper bounds, which are actually some strings (chromosome) representing the location and length of the groynes. For each chromosome, the model finds the fitness and constraint function values of the problem. The fitness value is calculated using the transformation function mentioned in equation 5.15. The hydrodynamic model needs to run with the combination as specified in the chromosome for calculating the constraint function (equations 5.2 and 5.8). The constraint optimization problem has been converted to an unconstrained problem using penalty parameter approach. Thus, the augmented objective function value is calculated using the output from the hydrodynamic model, the cost function value and the value of other constraints. The population is then checked for termination criteria. If it is satisfied, the iteration will be

terminated. If not, the population will pass through the genetic operators, i.e. selection, crossover, mutation and elitism.

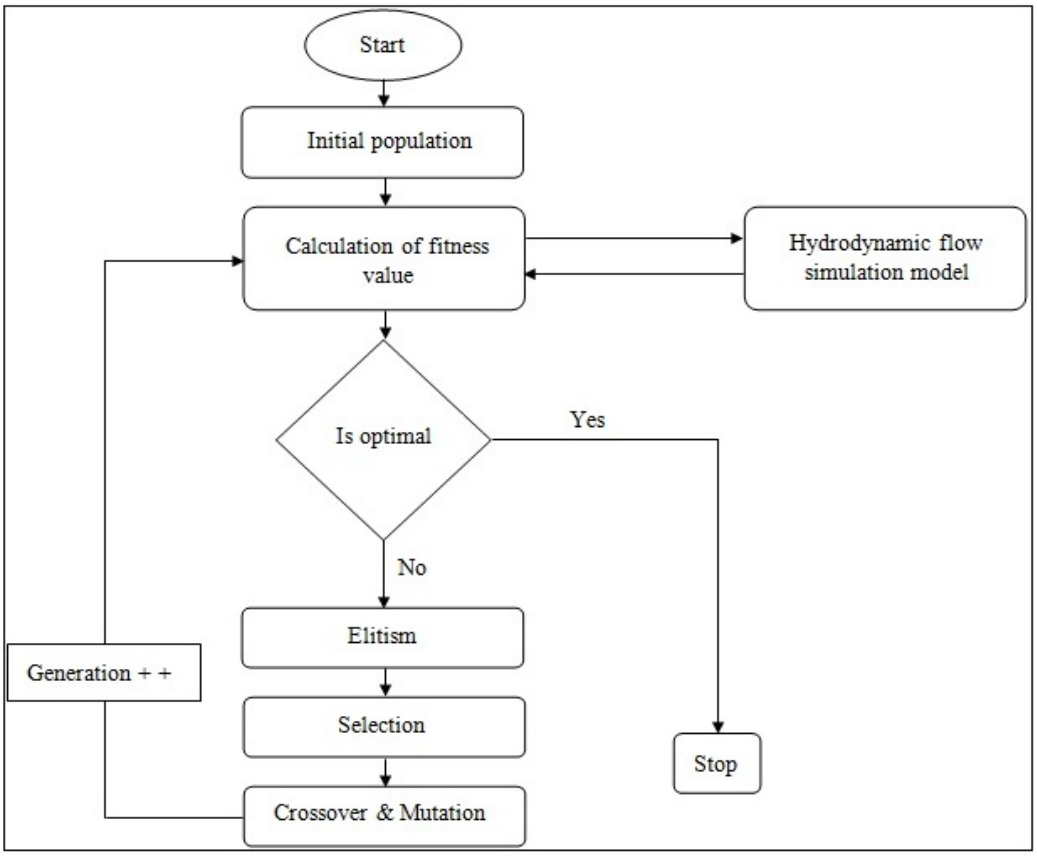

Figure 5.5 Schematic representation of the proposed linked simulation-optimization model

5.5 Application of the proposed methodology

The proposed model is tested for three different cases. In the first case, the model is applied on a hypothetical straight channel. In the second case, it is applied on a hypothetical bend channel for showing its applicability in case of meandering flow domain. For showing the applicability of the proposed model in case of braided channel, it is also applied for a hypothetical braided channel.

5.5.1 Hypothetical straight channel

The performance of the proposed methodology is first evaluated by applying it on a straight rectangular shaped hypothetical channel of length 800 m and width 180 m. The computational

domain is divided into finite difference grids of 81 by 19 points, which results an individual mesh size of 10 m by 10 m. It is proposed to create a low speed zone of 20 m width near the right bank extending from chainage 300 m to 500 m. The study area with the generated finite difference grid along with the proposed low speed zone is shown in figure 5.6.

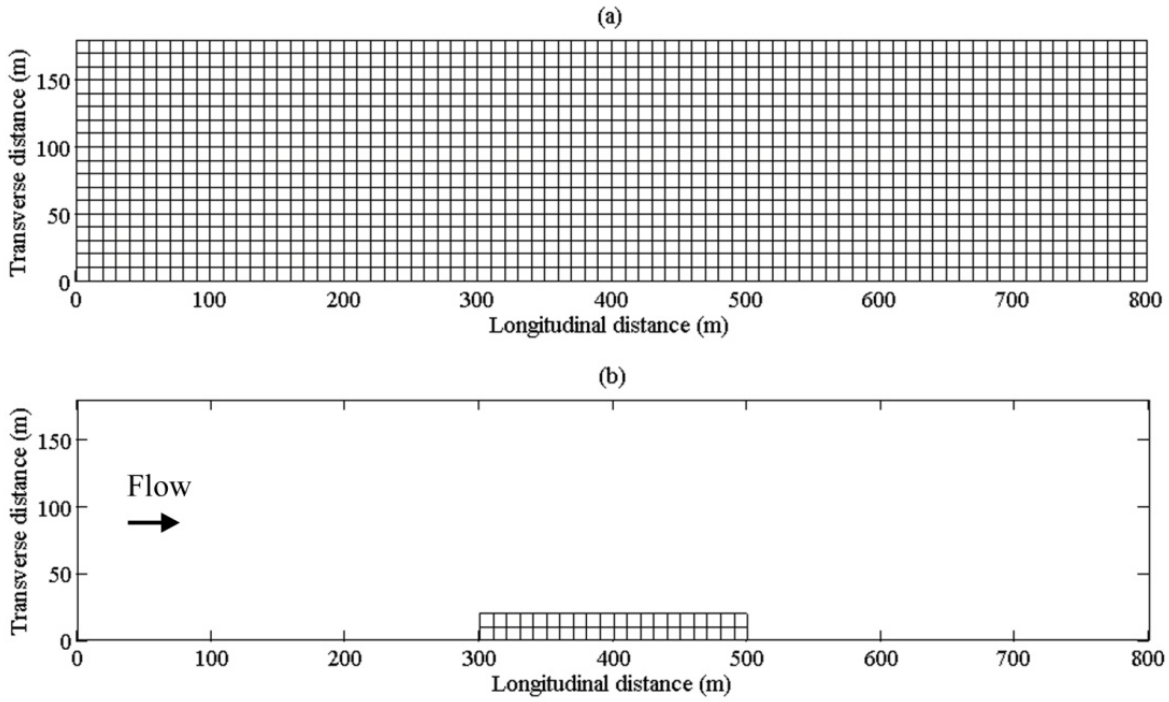

Figure 5.6 Study area along with low speed zone for the hypothetical straight channel: (a) study area with computational grid; (b) position of proposed low speed zone near the right bank

The hydrodynamic model is run with a discharge of1000cumec. A value of 3.2 is taken for CN in the hydrodynamic model. The artificial viscosity coefficient CT is set equal to 0.22. At the downstream boundary, h is fixed at a value of 5.1784 m which is obtained by using uniform flow for the discharge of 1000cumec. Manning's n value is taken as 0.031 and the slope of the channel is taken as 1:10000.

In this channel, since the low speed zone is situated on the right bank, groynes are placed on the right bank only. Binary coded string of length 3 is used for coding the decision variable length of groynes (Lrg) for the formulations I and II. For the formulation III, these values are fixed. The decision variables, position of groyne (Prg) for the formulations I and III, are coded using binary string of length 7. However for the formulation II, these values are fixed.

5.5.2 Hypothetical meandering channel

To study the performance of the proposed model in case of non regular flow domain, it is also applied on a hypothetical bend channel composed of two 90^0 curves connected by a short tangent. The inner radius of the bend channels are 350 m each and the width of the channel is 240 m. The lengths of the approach channel, middle channel and the exit channel are 246 m, 123 m and 246 m respectively. A finite difference grid of size 86×17 is generated for the study area. It is proposed to create two low speed zones near the outer banks of both the curves as these are the most vulnerable areas for bank erosion. Figure 5.7 shows the finite difference grid along with proposed low speed zones for this channel.

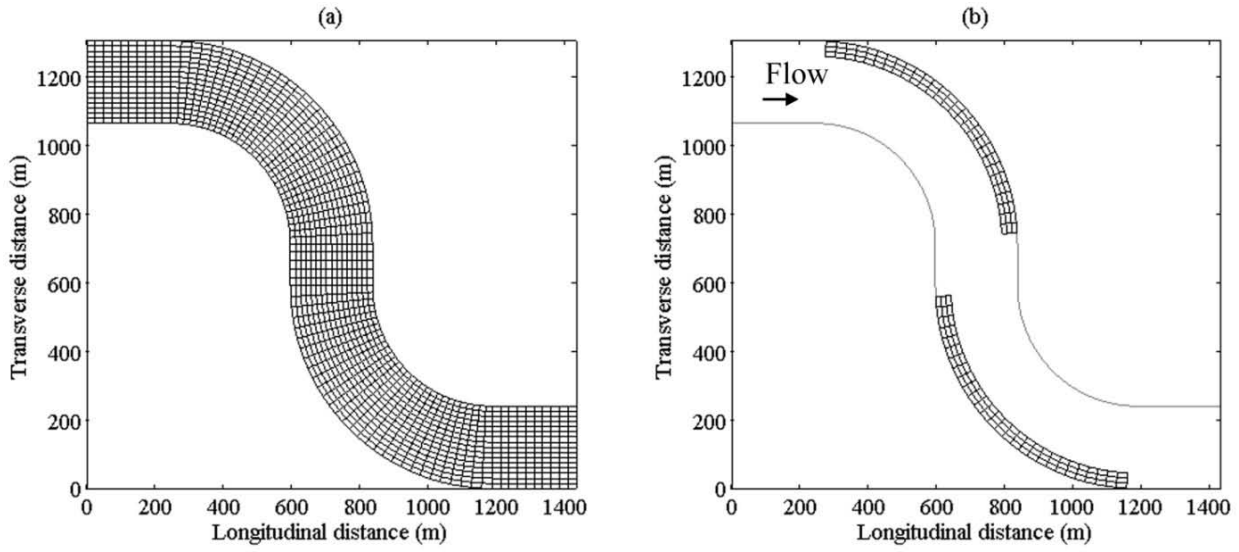

Figure 5.7 Study area along with low speed zone for the hypothetical meandering channel: (a) study area with computational grid; (b) position of proposed low speed zones near both the banks

The hydrodynamic model is run with a discharge of 1200 cumec. The value of the CN is considered as 1.2 and the optimum artificial viscosity coefficient CT is taken as 0.24. Manning's roughness value n is taken as 0.031. There is no lateral slope in the channel however longitudinal slope is taken as 1:10000.

Binary coded string of length 3 is used for coding the decision variable 'length of groyne' (Llg and Lrg). However, position of groyne (Plg and Prg) is coded using binary string of length 5.

5.5.3 Hypothetical braided channel

For apprising performance of the present model in case of braided channels, a hypothetical braided channel is considered. The channel length considered is about 1600 m and width varies from 500 m to 600 m. Figure 5.8 shows the hypothetical braided channel with three sand bars located arbitrarily.

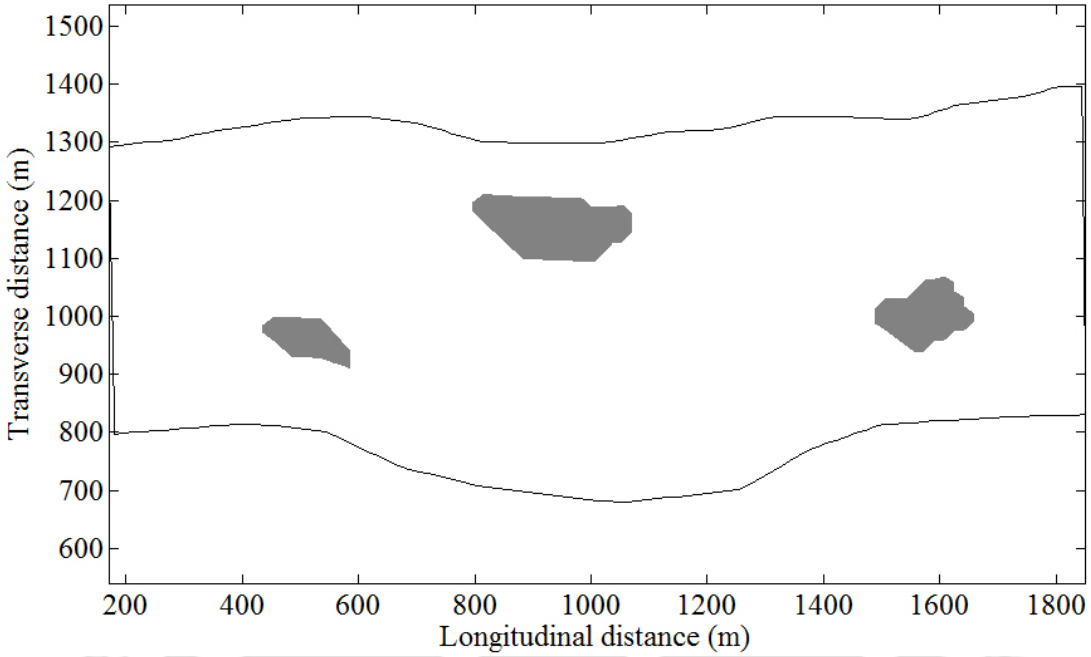

Figure 5.8 Hypothetical braided channel considered

A finite difference grid of size 100×40 is generated for the study area. Figure 5.9 shows the finite difference grid along with proposed low speed zone for this channel.

The hydrodynamic model in this case is run with a discharge of 2000 cumec. The value of the CN is considered as 2 and the optimum artificial viscosity coefficient CT is taken as 0.2. Manning's roughness value n is taken as 0.025 and the slope is taken as 1:10000.

Binary coded string of length 3 is used for coding the decision variable 'length of groyne' (Lrg). However, position of groyne (Prg) is coded using binary string of length 5.

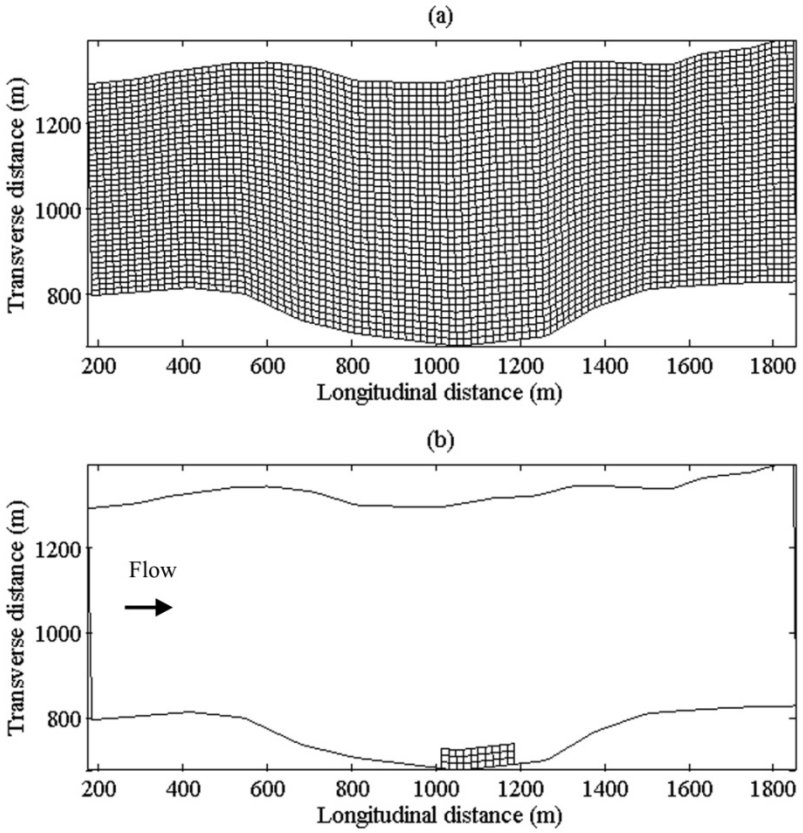

Figure 5.9 Study area along with low speed zone for the hypothetical braided channel: (a) study area with computational grid; (b) position of proposed low speed zone near the right bank

5.6 Results and discussion

The proposed genetic algorithms based linked simulation-optimization model is run for all the study channels with different formulations. The results obtained for different formulations and study channels are presented in the subsequent sections.

5.6.1 Hypothetical straight channel

The formulation I minimizes the total construction cost of the groyne system for attaining a target speed value of 0.3 m/s on the predefined area. In this formulation, the possible maximum number of groynes is taken as 5 within the position limits. For each of the groyne, the associated variables are position and length of groynes. As such, the number of variables is 10. The initial population is taken as 100. The values of Prg_{min} and Prg_{max} are considered as grid numbers 21 and 61 respectively from upstream boundary. Similarly, the values of Lrg_{min} and Lrg_{max} are considered as grid numbers 0 and 4 respectively from right bank. In this case, the present model

results in 2 number of groynes (Ng=2) having length of 20 m each for attaining the predefined target speed value. The corresponding positions obtained are 260 m and 430 m from upstream boundary. The actual length and position of groynes in meter are obtained by multiplying the value of the integer variable obtained from the optimization model with the grid spacing value. With this combination, the total construction cost is found to be ₹ 4×10^6. Figure 5.10 shows the velocity vector plot and speed contour map with the proposed combination of groynes for this scenario. It has been observed that in between the groynes, the length of the velocity vectors are very less representing very low speed on those areas (maximum speed of 0.30 m/s). This shows that the results are intuitively as expected.

Another experiment is also conducted to study the effect of target speed value on the optimal results. In this case the target speed value is considered as 0.2 m/s. For this limited speed value, the present model results in 2 number of groynes (Ng=2) with length 30 m each. The proposed positions of the groynes are 260 m and 440 m from the upstream boundary. Due to the increase in length of groynes, the total construction cost increases to ₹ 6×10^6. Figure 5.11 shows the velocity vector plot and speed contour map for the obtained optimal combination of groynes. It may be observed from the figure that the area under the low speed zone is larger in this case due to the longer groynes.

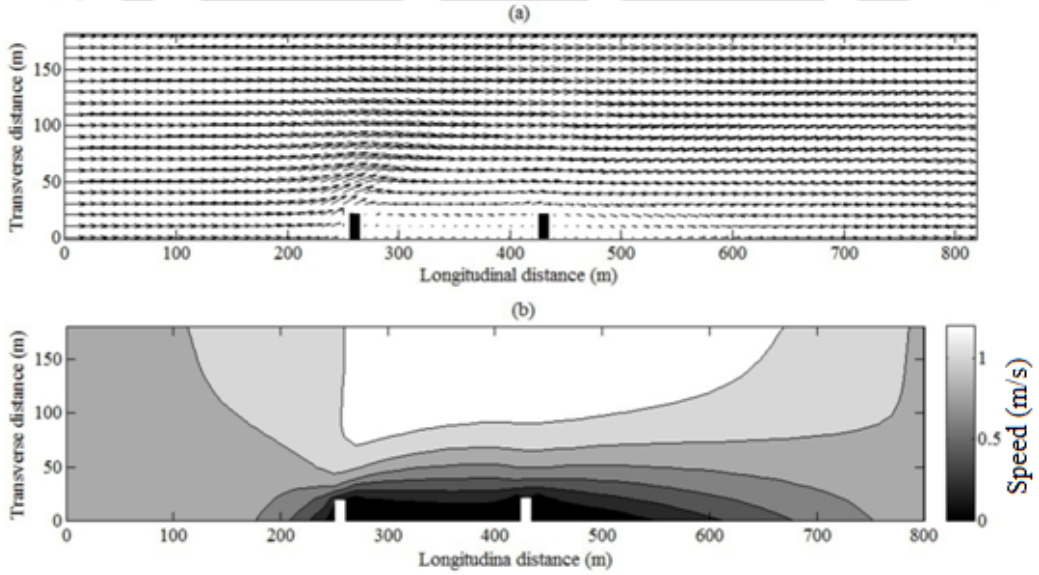

Figure 5.10 Optimal combination of groynes in hypothetical straight channel by formulation I with target speed value of 0.3 m/s: (a) velocity vector; (b) speed contour

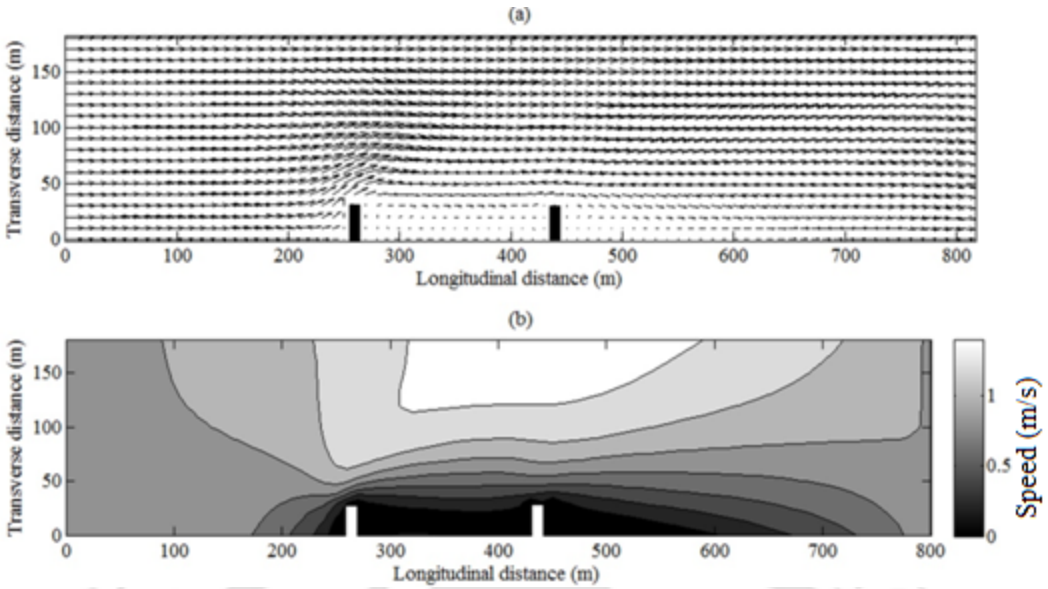

Figure 5.11 Optimal combination of groynes in hypothetical straight channel by formulation I with target speed value of 0.2 m/s: (a) velocity vector; (b) speed contour

In formulation II, the positions of groynes are fixed earlier. The groynes are placed uniformly at grid numbers of 21, 26, 31, 36, 41, 46, 51, 56 and 61 from the upstream boundary. For each of the groyne, the associated variable is only the length of groynes as the positions of the groynes are already fixed. Thus, the number of variables is 9. The initial population is taken as 90 and the value of Lrg_{min} and Lrg_{max} is taken as grid numbers 0 and 4 respectively. The model is run to find the required length of groynes on the positions mentioned above to obtain a target speed value of 0.3 m/s. In this case, the present model results in 3 number of groynes (Ng=3). The lengths of the groynes obtained are 20 m, 10 m and 10 m at positions of 340 m, 190 m and 490 m respectively from upstream boundary. The total construction cost is found as ₹ 4×10^6. Figure 5.12 shows the velocity vector plot and speed contour map for the optimal combination of groynes. The cost of the project is similar to the formulation I. However, the position and length of the groynes are different. This shows that the problem has alternate optimal solutions.

For a target speed value of 0.2 m/s, the model results in 2 numbers of groynes (Ng=2) of lengths 20 m and 40 m at positions of 290 m and 440 m respectively from upstream boundary. The total construction cost of the system is ₹ 6×10^6. Figure 5.13 shows the velocity vector plot and speed contour map for the proposed combination of groynes which will maintain a target speed of 0.2 m/s on the predefined area. It may be noted that the minimum cost achieved is same as that of

formulation I. However, the position and length of the groynes are different which shows that the problem has alternate optimal solutions.

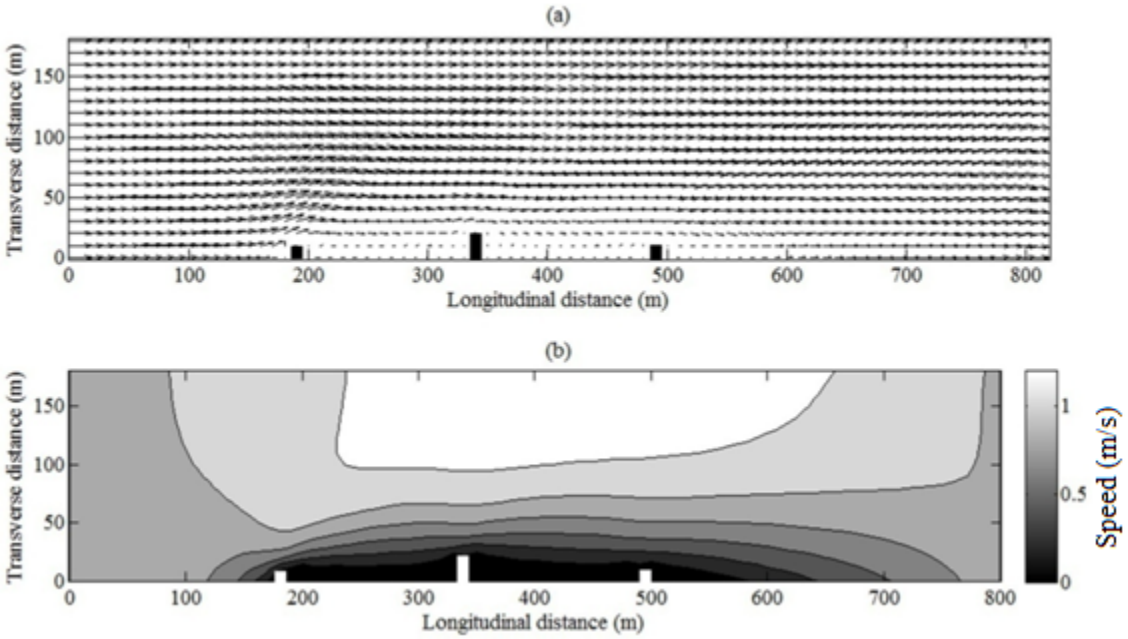

Figure 5.12 Optimal combination of groynes in hypothetical straight channel by formulation II with target speed value of 0.3 m/s: (a) velocity vector; (b) speed contour

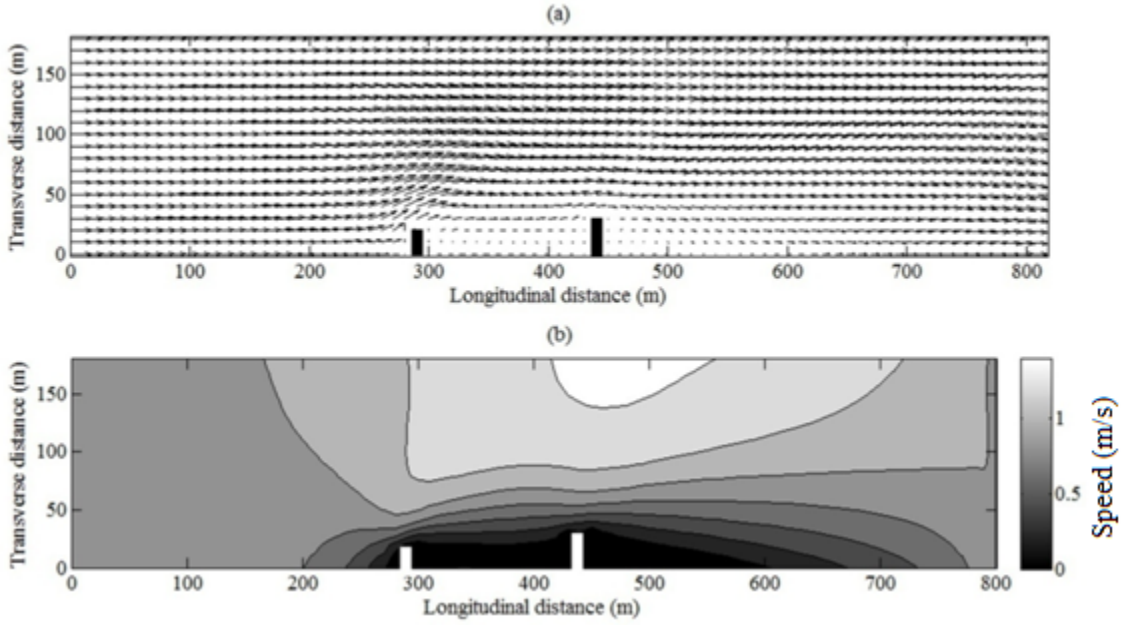

Figure 5.13 Optimal combination of groynes in hypothetical straight channel by formulation II with target speed value of 0.2 m/s: (a) velocity vector; (b) speed contour

In formulation III, it is assumed that 3 (Ng=3) number of groynes of length (Lrg) 40 m are available which can be constructed with the budget available with the department. In such a situation, the formulation III can be applied to find out the minimum speed that can be achieved using these three numbers of groynes. The variable in this formulation is only the position of groyne (Prg). Initial population of 30 is taken in this case. The value of Prg_{min} and Prg_{max} are taken as grid numbers 21 and 61. The optimal result shows that placing of these three groynes at 250 m, 340 m and 430 m from upstream boundary will give minimum speed at the predefined locations. The minimum speed achieved on the predefined area is 0.1283 m/s. Figure 5.14 shows the velocity vector plot and speed contour map with the proposed combination of groynes.

Another experiments is also conducted with 2 number of groynes (Ng=2) of length 40 m each. The population size considered is 20. The optimal result shows that the placement of groynes at 300 m and 400 m from upstream boundary achieved minimum speed of 0.2146 m/s at the predefined areas. It may be observed that as number of groynes considered here is two, the minimum speed achieved in this case is more than the previous case, where three groynes were used. The effect of reduction of speed can be visualized in figure 5.15. The figure shows the velocity vector plot and speed contour map for this scenario.

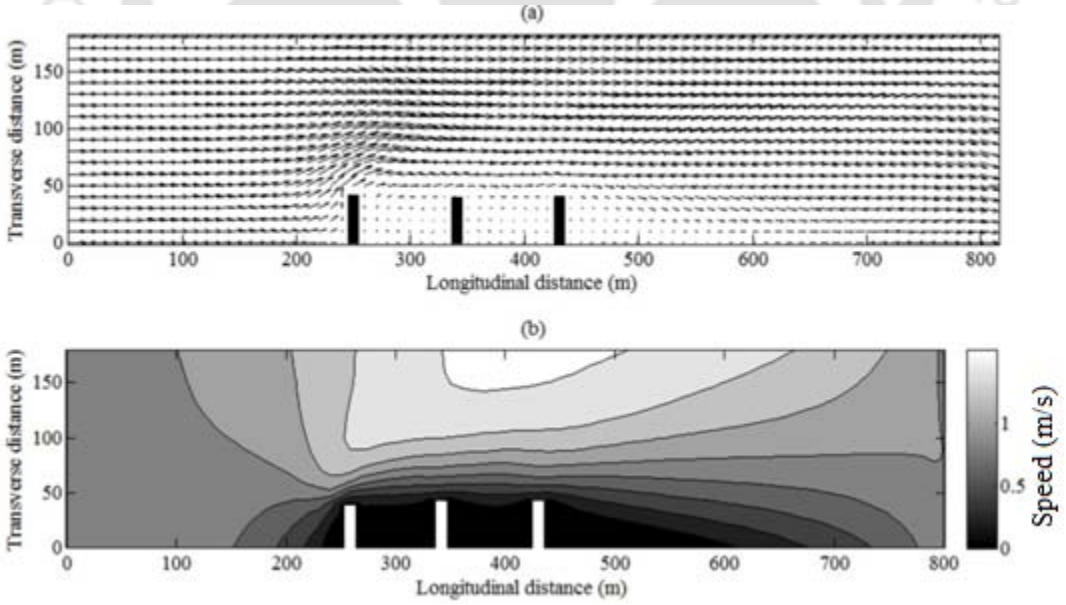

Figure 5.14 Optimal combination of groynes in hypothetical straight channel by formulation III with three groynes of length 40 m each: (a) velocity vector; (b) speed contour

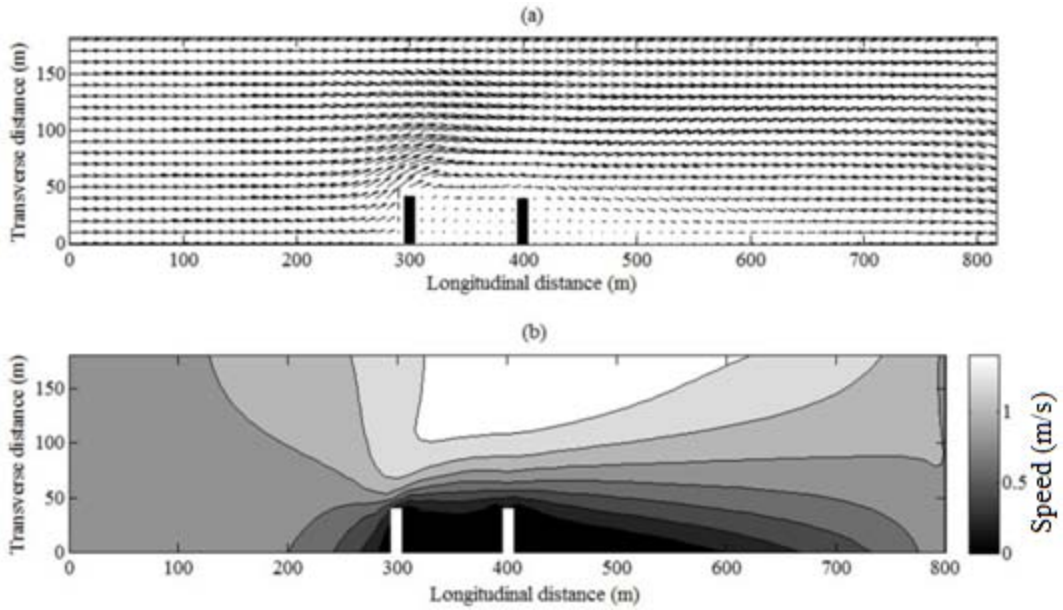

Figure 5.15 Optimal combination of groynes in hypothetical straight channel by formulation III with two groynes of length 40 m each: (a) velocity vector; (b) speed contour

5.6.2 Hypothetical meandering channel

All the optimization formulations are also applied to another hypothetical meandering channel. Formulation I minimizes the total construction cost of the groyne system for attaining a target speed value of 0.3 m/s on the predefined areas on both the banks. The value of Plg_{min} and Plg_{max} are taken as grid numbers 11 and 41 respectively. Similarly, at the right bank values of Prg_{min} and Prg_{max} are considered as 46 and 76 respectively. The value of Llg_{min} and Llg_{max} are taken as 0 and 4 respectively. For the right bank also, the value of Lrg_{min} and Lrg_{max} are taken as 0 and 4 respectively. Numbers of possible groynes on each of the banks are assumed as 6 within the position limits which leads to the total number of groynes of 12. The associated variables with all of these 12 groynes are the position of groyne and length of groyne. As such, the number of variables is 24. The population size considered is 240. The actual length of the groyne are calculated by multiplying the transverse grid spacing (15 m in this channel) with the integer of groyne length obtained from the optimization model. The present model results in 7 number (Ng=7) of groynes for attaining the predefined target speed value. Out of these 7 groynes, 4 groynes having length of 45 m, 30 m, 15m and 60 m are needed to be placed on the left bank at grid locations 13, 25, 28 and 41 respectively. The other 3 groynes of length 30 m, 15 m, and 15

m are to be placed on the right bank at locations 46, 60 and 75 respectively from the upstream. Figure 5.16 shows the velocity vector plot and speed contour map with the proposed combination of the groynes. The deflected pattern of the velocity vector towards the central portion of the channel due to the presence of the groynes can easily be seen in the figure. In between the groynes, the lengths of the velocity vectors are very less representing very low speed on those areas. For this combination, the total construction cost is found to be ₹ 2.10×10^7.

For achieving target speed value of 0.2 m/s on the predefined areas, there is a need of 7 numbers of groynes (Ng=7). Out of these 7 groynes, 4 groynes with length of 60 m, 45 m, 45 m and 45 m are needed to be placed on the left bank at the grid locations 11, 24, 29 and 41 respectively. On the right bank, optimal lengths of the groynes are 60 m, 15 m and 15 m and the positions are 46, 62 and 76 respectively. Figure 5.17 shows the velocity vector and speed contour map. As a result of increase in length of the groynes, the total construction cost is also raised to ₹ 2.85×10^7.

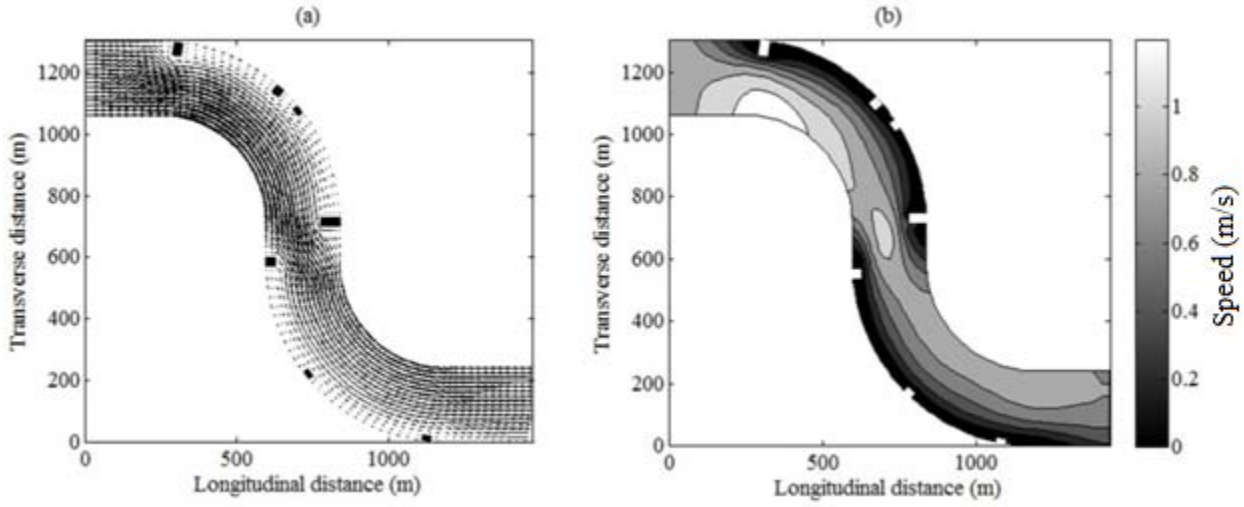

Figure 5.16 Optimal combination of groynes in hypothetical meandering channel by formulation I with target speed value of 0.3 m/s: (a) velocity vector; (b) speed contour

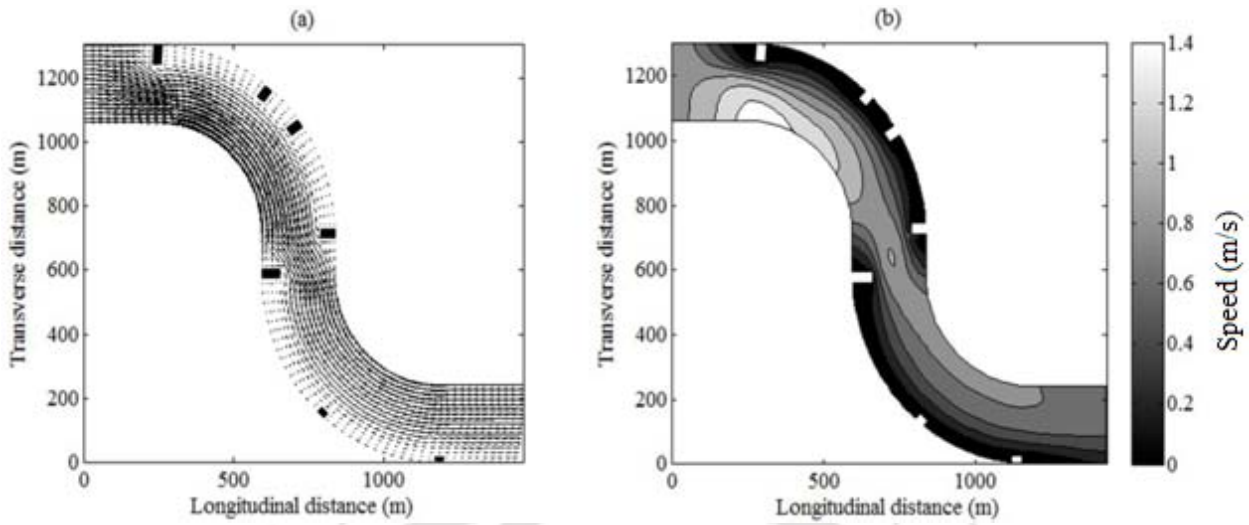

Figure 5.17 Optimal combination of groynes in hypothetical meandering channel by formulation I with target speed value of 0.2 m/s: (a) velocity vector; (b) speed contour

In case of formulation II, the positions of the groynes are already fixed on both the banks. On the left bank, the groynes are placed uniformly at grid number 11, 16, 21, 26, 31, 36 and 41. On the right bank, these positions are on grid number 46, 51, 56, 61, 66, 71 and 76. From these positions, it can be observed that the possible maximum number of groynes is 14. For each of the groyne, the associated variable is only length of groynes as positions of the groynes are already fixed. Thus, the number of variables is 14. The initial population is taken as 140 and the value of Llg_{min} and Llg_{max} are taken as 0 and 4 respectively. Similarly the value of Lrg_{min} and Lrg_{max} are considered as 0 and 4 respectively. The formulation II of the proposed model is run to find the required length of groynes on those specified 14 positions to achieve a target speed of 0.3 m/s on the predefined areas. The present model results in 7 number of groynes (Ng=7). Out of these, 4 groynes having lengths of 30 m, 15 m, 45 m and 60 m are to be placed on the left bank at the grid number 11, 16, 26 and 41 respectively. Similarly, the optimal positions of the groynes on the right bank are found as 46, 61 and 76 with optimal lengths of 30 m, 15 m and 15 m respectively. The total construction cost is found to be ₹ 2.10×10^7. It can be seen that the cost of construction is similar to formulation I which shows that the problem has alternate optimal solutions. Figure 5.18 shows the velocity vector plot and speed contour map for the optimal combination of groynes.

In order to reduce the target speed to 0.2 m/s, 7 number of groynes (Ng=7) is sufficient. However, position and length of the groynes are different than the previous case. Out of these 7 groynes, 4 groynes having length of 45 m each are to be placed on the left bank at position 11, 21, 31 and 41 respectively. The remaining 3 groynes are to be placed at the right bank at optimal position of 46, 61 and 76 having length of 45 m, 15 m and 45 m respectively. The total construction cost is ₹ 2.85×10^7. In this case also, the construction cost is similar to formulation I. Figure 5.19 shows the velocity vector plot and speed contour map with this proposed combination of groynes. It may be observed that the lengths of the groynes required are more when the speed reduction to be achieved is more. These results are intuitively as expected.

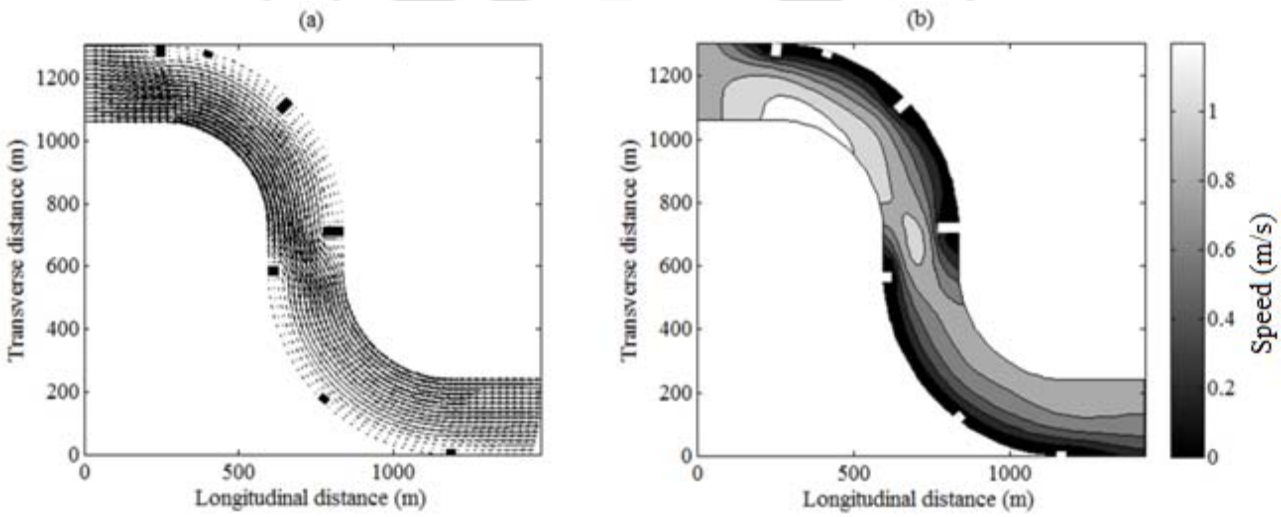

Figure 5.18 Optimal combination of groynes in hypothetical meandering channel by formulation II with target speed value of 0.3 m/s: (a) velocity vector; (b) speed contour

For formulation III, it is considered that 6 numbers of groynes of length 45 m are available or can be constructed with the available funds. It is also considered that 3 groynes will be placed at the left bank and another 3 will be placed at the right bank. The optimization model will find out the position of the groynes. Thus, the variable is only the position of the groynes. The initial population of 60 is taken in this case. The value of Plg_{min} and Plg_{max} are taken as grid numbers 11 and 41 respectively. Similarly the value of Prg_{min} and Prg_{max} are taken as 46 and 76 respectively. The resulting positions of the three groynes on the left bank given by the present model are at grid numbers 12, 26 and 39. Similarly, the resulting positions on right banks are grid numbers 47, 63 and 71. These optimal positions of these 6 groynes can minimize the flow

speed on the predefined areas up to 0.3213 m/s. Figure 5.20 shows the velocity vector plot and speed contour map for this combination of groynes. Another experiment with 4 numbers of groynes, 2 in each banks shows that flow speed at the predefined location can be reduced to 0.4897 m/sec. In this case, the initial population considered is 40. The resulting positions of groynes given by the model are 15 and 36 on the left bank and 47 and 69 at the right bank. Figure 5.21 shows the velocity vector plot and speed contour map with this combination.

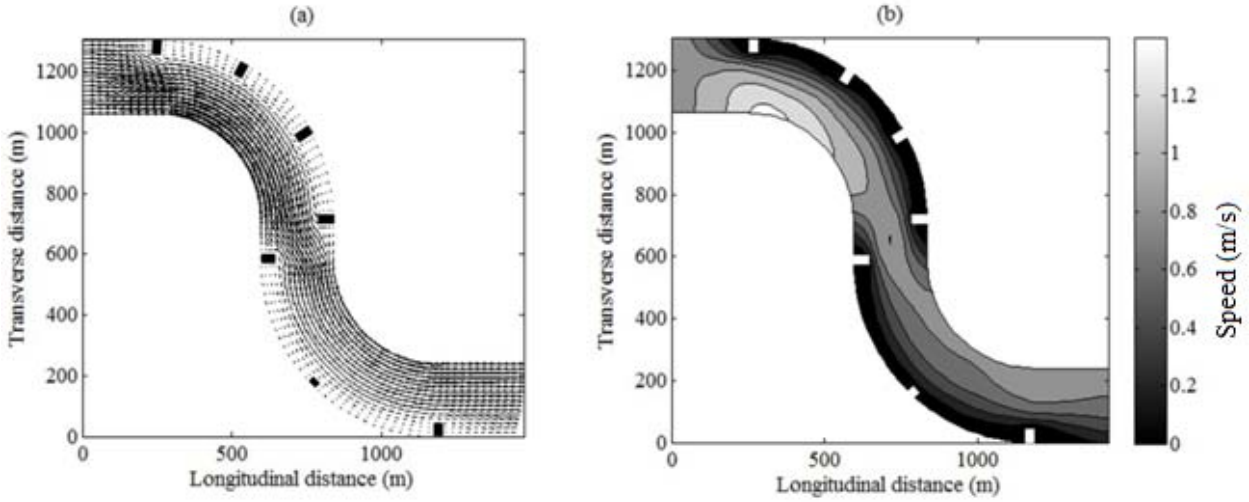

Figure 5.19 Optimal combination of groynes in hypothetical meandering channel by formulation II with target speed value of 0.2 m/s: (a) velocity vector; (b) speed contour

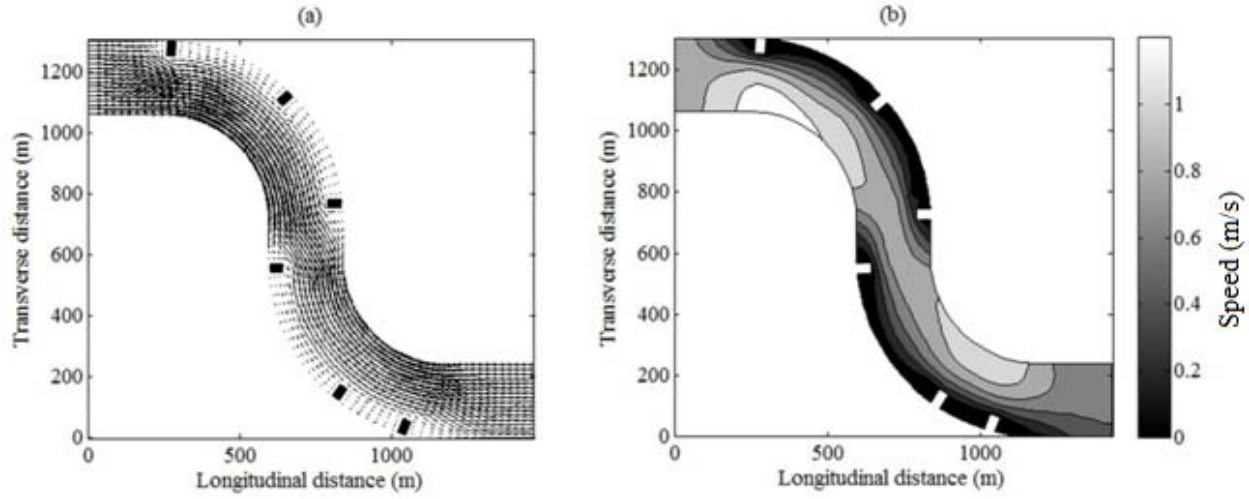

Figure 5.20 Optimal combination of groynes in hypothetical meandering channel by formulation III with six groynes of length 45 m each: (a) velocity vector; (b) speed contour

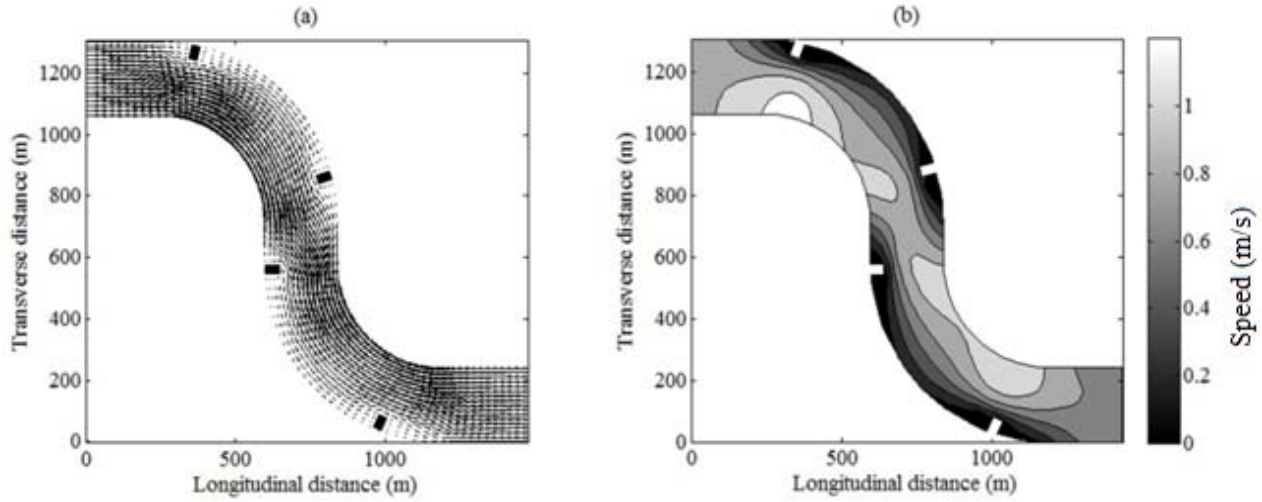

Figure 5.21 Optimal combination of groynes in hypothetical meandering channel by formulation III with four groynes of length 45 m each: (a) velocity vector; (b) speed contour

5.6.3 Hypothetical braided channel

The basic objective of conducting this numerical experimentation is to ensure applicability of the concept in braided channel. More details of its application in braided channel will be presented in the next chapter through its application in a vulnerable braided reach of river Brahmaputra. Therefore, formulation I is only run in this exercise and results are presented below.

For this channel, formulation I is used to minimize the total construction cost of the groyne system for attaining a target speed value of 0.15 m/s on the predefined area. In this formulation, the possible maximum number of groynes is taken as 3 within the position limits, leading to initial population of 60. The values of Prg_{min} and Prg_{max} are considered as grid numbers 40 and 70 respectively from upstream boundary. Similarly, the values of Lrg_{min} and Lrg_{max} are considered as grid numbers 0 and 5 respectively from right bank. In this case, the present model results in 2 number of groynes (Ng=2) having length of 65 m each for attaining the predefined target speed value. The corresponding positions obtained are grid numbers 50 and 59 from upstream boundary. The actual length and position of groynes in meter are obtained by multiplying the value of the integer variable obtained from the optimization model with the grid spacing value. With this combination, the total construction cost is found to be ₹ 1.35×10^7.

Figures 5.22 and 5.23 show the velocity vector plot and speed contour map respectively with the proposed combination of groynes for this scenario.

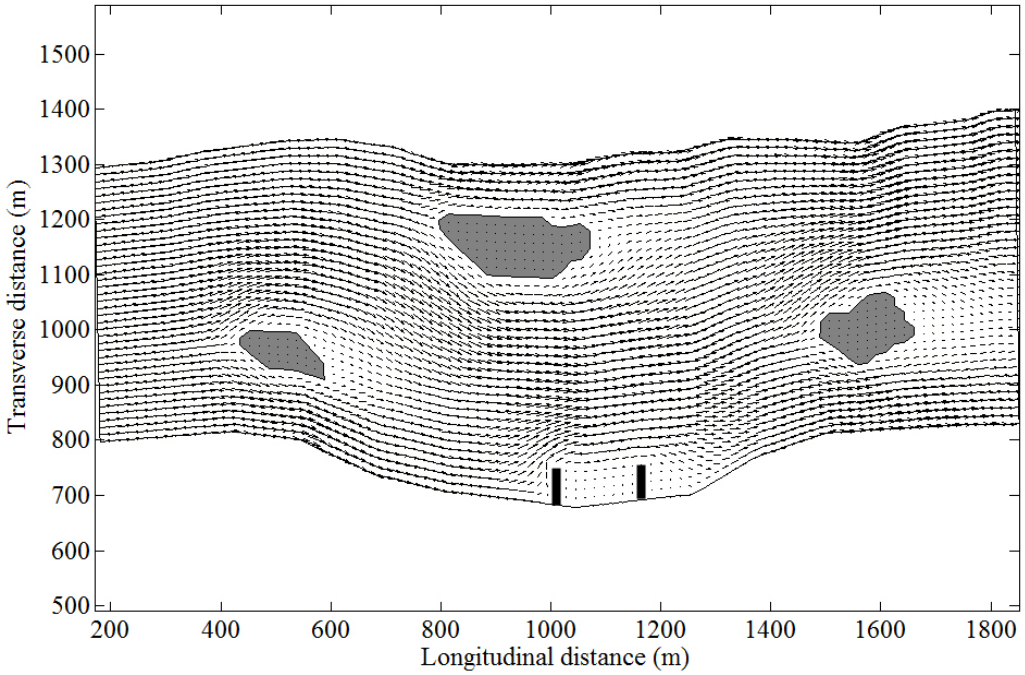

Figure 5.22 Velocity vector with optimal combination of groynes in hypothetical braided channel

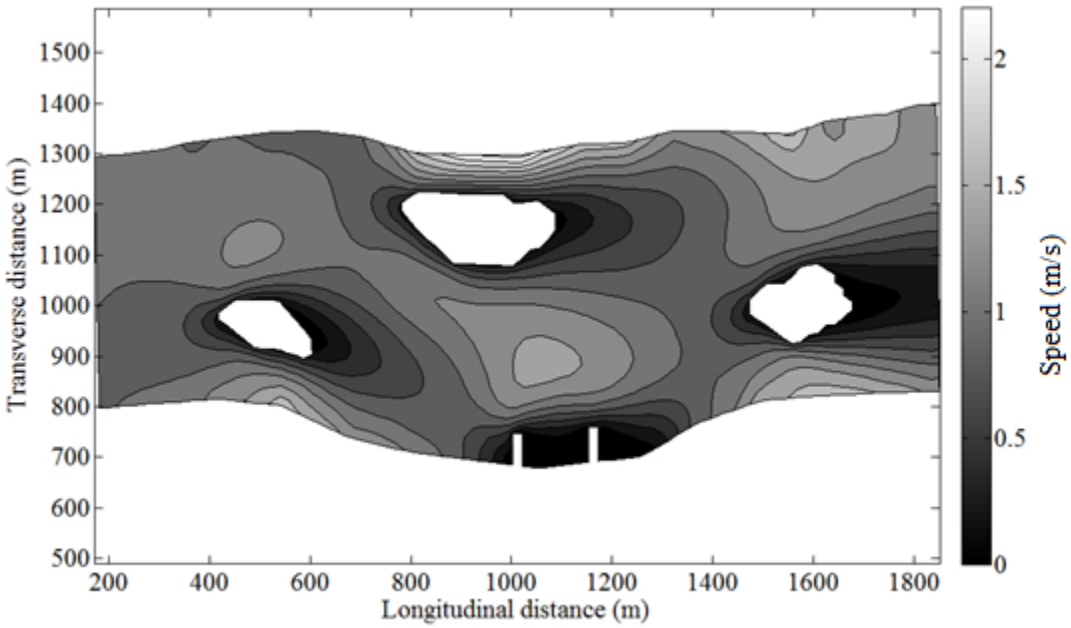

Figure 5.23 Speed contour with optimal combination of groynes in hypothetical braided channel

5.7 Computational efficiency of the proposed model

The proposed model for the above test examples are run on a Windows 7 based Intel Core 2 Quad CPU with 2.66 GHZ Processor computer. Matlab is used for running the linked GA based simulation-optimization model. For checking the computational efficiency of the present methodology, the computational time required for all the channels for different formulations are found out and are presented in table 5.1. From the table it is observed that, the computational time required for formulation I in all the channels are very high, i.e. 100 hr for the hypothetical straight channel, 180 hr for the hypothetical meandering channel and 50 hr for the hypothetical braided channel. Computational time required by formulation II is lesser than formulation I (85 hr and 105 hr for the straight and meandering channels respectively). However, for formulation III, this is further less (32 hr and 20 hr with different number of groynes for straight channel, 45 hr and 30 hr with different number of groynes for meandering channel). This shows that the time required by the proposed model is basically dependent upon the size of the problem being considered.

Table 5.1 Computational time required for all the cases

Channels and formulations	**Approximate computational time required (hr)**
Straight channel, formulation I (target speed 0.3 m/s)	100
Straight channel, formulation I (target speed 0.2 m/s)	100
Straight channel, formulation II (target speed 0.3 m/s)	85
Straight channel, formulation II (target speed 0.2 m/s)	85
Straight channel, formulation III (3 groynes)	32
Straight channel, formulation III (2 groynes)	20
Meandering channel, formulation I (target speed 0.3 m/s)	180
Meandering channel, formulation I (target speed 0.2 m/s)	180
Meandering channel, formulation II (target speed 0.3 m/s)	105
Meandering channel, formulation II (target speed 0.2 m/s)	105
Meandering channel, formulation III (6 groynes)	45
Meandering channel, formulation III (4 groynes)	30
Braided channel, formulation I (target speed 0.15 m/s)	200

5.8 Conclusions

A linked simulation-optimization model has been developed for determination of optimal combination of groynes leading to minimum construction cost. From the study, the following conclusions are drawn.

1. The proposed GA based linked simulation-optimization model has been applied for three different test problems including a hypothetical straight channel, a hypothetical bend channel and a hypothetical braided channel. It has been observed that, the model has capability to produce good results.
2. It has been observed that, when the value of target speed reduces, the total length of groynes required for achieving that target speed value also increases. This increase in groyne length ultimately increases the total construction cost of the project. Reversely, formulation on minimizing flow speed reveals that increase in number of groyne can reduce the flow speed on the predefined area further.
3. The computational time required by the present model is mainly dependent on the initial population considered in the genetic algorithms model. Population size equals to ten times the number of variable is sufficient to get better performance.
4. Though computational time required for such genetic algorithms based linked simulation-optimization model is high, this may not be considered as a limitation, as number of alternatives tested during the computational procedure is enormous. Test of such large alternatives would have otherwise taken much more time and effort as compared to the time required by the model.

CHAPTER 6

MODEL APPLICATON IN BRAHMAPUTRA RIVER

6.1 Introduction

The river Brahmaputra and its tributary constitute a major river system of Northeastern part of India. Extensive bank erosion, particularly during the flood period, has been observed in several reaches of river Brahmaputra. An area extending from Dhing to Hilloikhunda located on south bank of Brahmaputra River in the Nagaon and Marigao district of Assam in India is also suffering from the problem of extensive river bank erosion. There is also a growing public demand to have bank protection measures in this vulnerable reach. Therefore this reach is considered to evaluate the practical applicability of the proposed linked simulation-optimization model.

Required field data is collected with the support of Water Resources Department of Govt. of Assam. A field survey is also carried out with the help of Water Resources Department of Govt. of Assam. Bathymetry developed from the field survey is used for model development. To have a basis of comparison of different aspects of the proposed model, effort has been made to determine the best possible solution from some chosen alternatives using conventional iterative approach. Best solution thus obtained is then compared with the optimal solution given by the proposed linked simulation-optimization model. The details of the model results and their comparisons are presented in this chapter.

6.2 Study area

The size of the study area is approximately of 44km x 35km where the erosion affected areas are located on the south bank of Brahmaputra. The vulnerable area is extending from the hillock of Burha Mayang at Lat 26^0 16' 30"N & Long 92^0 01' 00"E up to the Lat 26^0 24' 16"N & Long 92^0 13' 00"E towards upstream. Figure 6.1 shows the satellite image of the study area.

6.3 Field survey

A GPS (Global Positioning System) survey is carried out for reconnaissance of the area and also to plan bathymetric survey. Figure 6.2 and 6.3 show the progressive bank failure indicating

severity of the bank erosion problem at that reach. Satellite data and toposheets are referred for understanding the history of failure. Local people are also consulted (figure 6.4) to verify some of the findings derived from satellite data. Figure 6.5 shows the digitized bank line of the study area at different times.

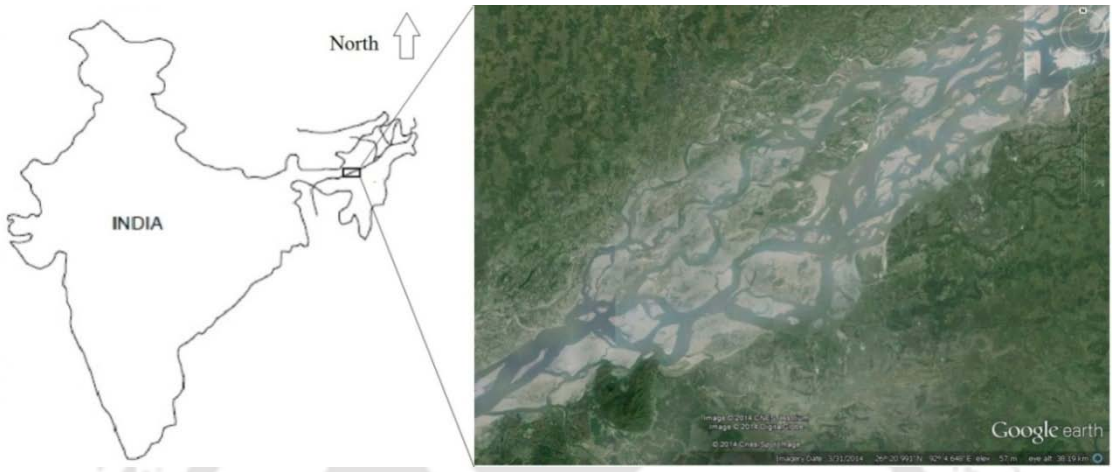

Figure 6.1 Location of study area with respect to India

Figure 6.2 Bank facing erosion

Figure 6.3 Bank on the verge of erosion

Figure 6.4 Authors discussion with local people

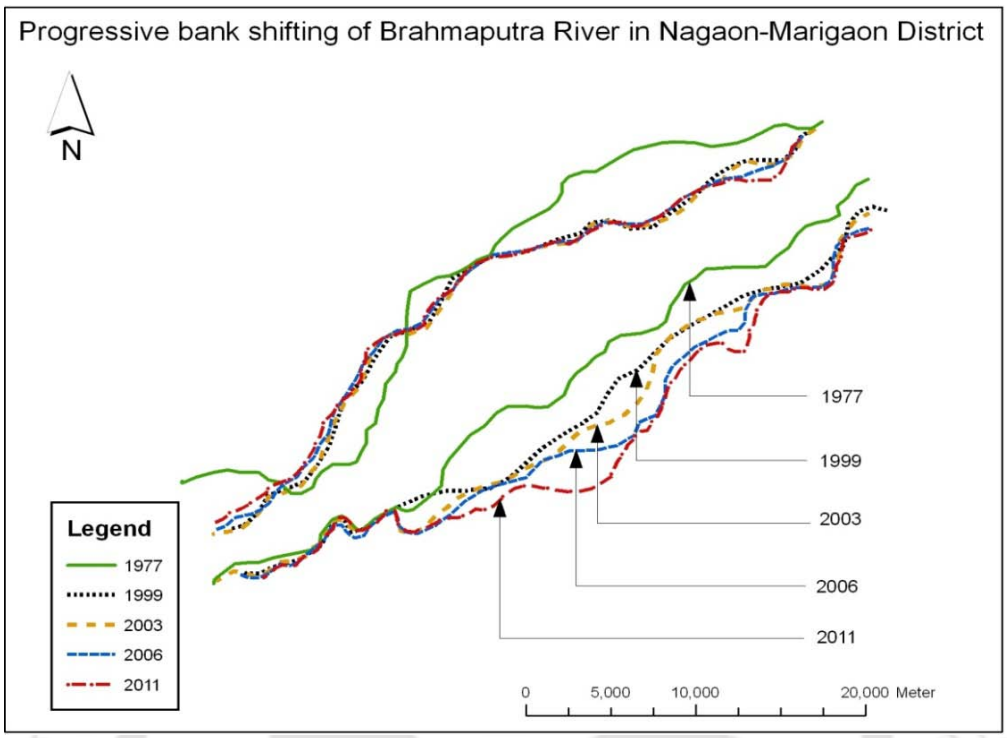

Figure 6.5 Bank line position at different years

6.4 Optimal combination of groynes by iterative approach

For determination of optimal combination of groynes by iterative procedure, the flow processes within the river is needed to be simulated with different alternate combination of groynes. For a fair comparison of the proposed model, it is decided to use a well established flow simulation software in the iterative approach. MIKE21C is one such software, developed by Danish Hydraulics Institute, in Denmark and provides a wide range of modeling facilities for diverse situation. Some of the studies done with MIKE21C for different aspects of river flow simulation are available in Hassan and Dibike (1999), Hye and Jahan (2000), Beck and Basson (2008), etc. Therefore MIKE21C is used for obtaining the best solution through iterative approach.

6.4.1 Mathematical background of MIKE21C

MIKE 21C is based on a curvilinear grid where hydrodynamics, sediment transport and river morphology can be simulated. The governing equations for the hydrodynamic simulation in MIKE21C are the fully dynamic and vertically integrated equations of continuity and conservation of momentum in two directions. The equations are given below,

$$\frac{\partial H}{\partial t}+\frac{\partial p}{\partial ss}+\frac{\partial q}{\partial nn}-\frac{q}{R_{ss}}+\frac{p}{R_{nn}}=0 \tag{6.1}$$

$$\frac{\partial p}{\partial t}+\frac{\partial}{\partial ss}\left(\frac{p^2}{h}\right)+\frac{\partial}{\partial nn}\left(\frac{pq}{h}\right)+2\frac{pq}{hR_{nn}}+\frac{p^2-q^2}{hR_{ss}}+gh\frac{\partial H}{\partial ss}+\frac{g}{Cz^2}\frac{p\sqrt{p^2+q^2}}{h^2}=RHS \tag{6.2}$$

$$\frac{\partial q}{\partial t}+\frac{\partial}{\partial ss}\left(\frac{pq}{h}\right)+\frac{\partial}{\partial nn}\left(\frac{q^2}{h}\right)+2\frac{pq}{hR_{ss}}+\frac{q^2-p^2}{hR_{nn}}+gh\frac{\partial H}{\partial nn}+\frac{g}{Cz^2}\frac{q\sqrt{p^2+q^2}}{h^2}=RHS \tag{6.3}$$

Where ss, nn are the coordinates in the curvilinear system, p, q are the mass fluxes in the ss and nn direction respectively, H is the water level, h is the water depth, g is gravitational acceleration, Cz is Chezy roughness coefficient, R_{ss}, R_{nn} are radius of curvature of ss and nn line, respectively, RHS is right hand side in the force balance contains Reynolds stresses, Coriolis force and Atmospheric pressure. In MIKE21C, the equations (6.1), (6.2) and (6.3) are solved using finite difference Alternate Direction Implicit (ADI) scheme.

6.4.2 Computational grid and bathymetry

To include the bathymetry in the model and to compute the different variables in terms of the velocity and water depth, a computational grid of size (199×149) is generated as shown in figure 6.6. Datum for bathymetry preparation is taken as Mean Sea Level (MSL) at Karachi. For preparation of the bathymetry, data obtained from cross section survey done in the mid of July 2010 is used. The prepared bathymetry in 3D is shown in figure 6.7.

6.4.3 Initial and Boundary condition

As initial condition water surface at a falling slope is applied on the whole area. Flow condition is analysed for two different steady state conditions. One for very high discharge (60000 cumec) representing extreme event and the other representing monsoon flow with moderately high discharge (40000 cumec). Constant water stages of 52 meter and 49 meter are applied at the downstream boundary for the discharge of 60000 cumec and 40000 cumec respectively, as per the stage discharge relationship provided by the Water Resources Department, Govt. of Assam.

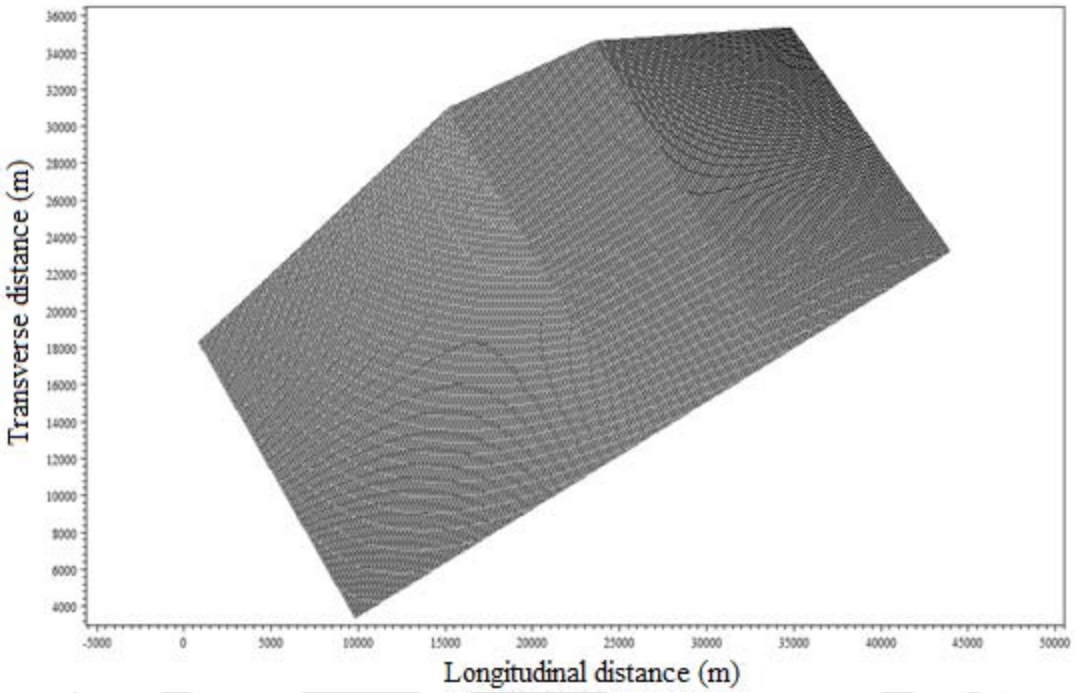

Figure 6.6 Computational grid generated for the study area

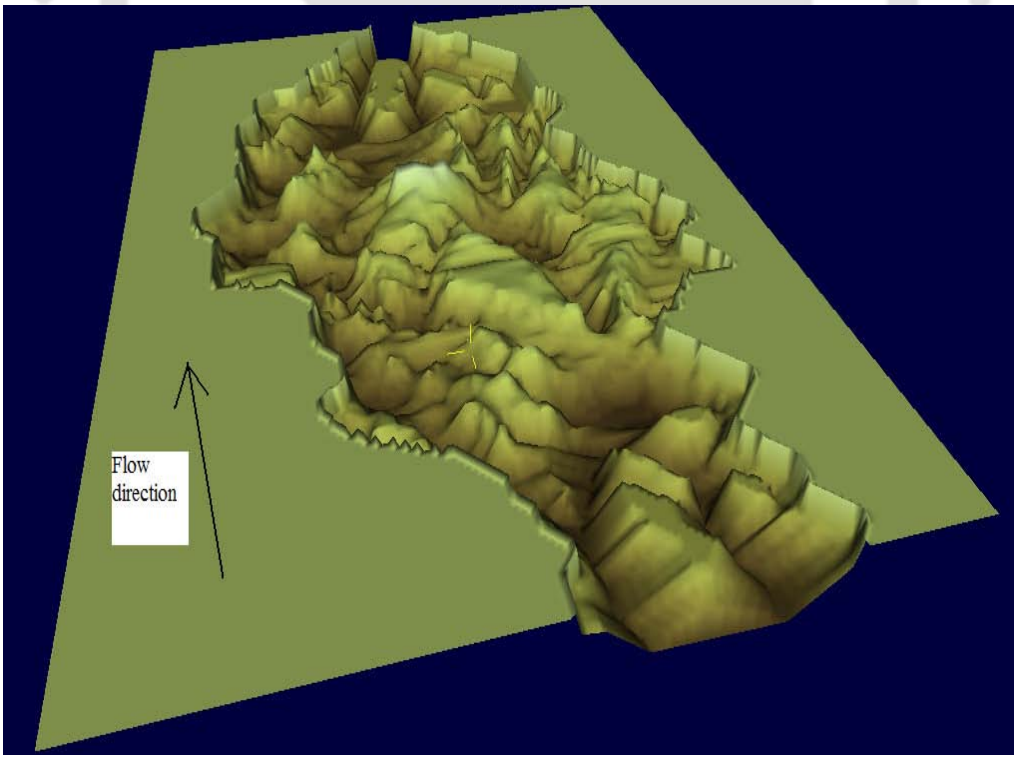

Figure 6.7 Bathymetry of the study area

6.4.4 Calibration of the model

Model set in MIKE21C is calibrated with the help of observed velocity in one of the sub channels. Model is run for the discharge, which is obtained for the date on which the velocities were recorded in the field. Flow velocity in a transverse cross section of that channel is compared with the simulated velocities to calibrate the model. Manning's roughness parameter for this kind of channel ranges from 0.025 to 0.035 (Chaudhry 2008; Saikia and Sarma 2007). The model is calibrated with the eddy viscosity and fine tuning of manning's roughness parameter is also done within the range mentioned above. Coefficient of eddy viscosity is calibrated for the model as 5.0 with value of Manning n as 0.031. Figure 6.8 shows the observed and computed velocity with these model parameters.

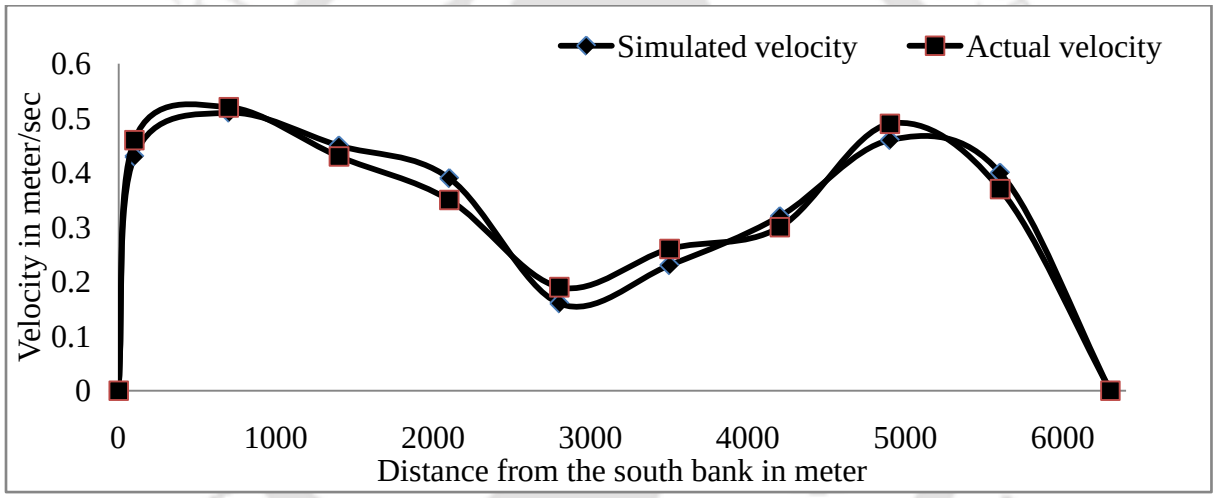

Figure 6.8 Comparison of simulated and actual velocity

6.4.5 Results and discussion for iterative approach

The calibrated model is used to test performance of different possible alternative measures in terms of their capability of diverting flow away from the bank and reducing flow speed near the vulnerable area to the desired level. Process of bank erosion is quite complex and several factors such as direction of attack, flow speed, seepage condition, property of bank material, river bank slope etc. influence bank erosion process. Water speed is one of the important factors, as reduction of speed can help preventing bank failure by reducing water energy and promoting deposition of sediment in the failing reach. Therefore, target speed and flow direction can be considered as an index for observing performance of alternative combinations of protection

measures. Based on the experience, a velocity of 0.5m/s is considered as safe velocity for this river reach.

6.4.5.1 With discharge of 60000 cumec (extreme event)

6.4.5.1.1 Present condition

To have a comparison of the results, initially the present situation has been simulated without introducing any groyne. Figure 6.9 shows the water depth contour and velocity vector map of the study area. Directions of velocity vectors indicate that water is striking the south bank in several locations. Figure 6.10 shows the speed contour map of the present condition. Speed contour has revealed high speed near the south bank indicating flow concentration towards south bank. Thus the model has satisfactorily simulated the flow revealing the fact that high flow velocity in the near bank channel and its direction of attack are the triggering causes of bank failure in the study area.

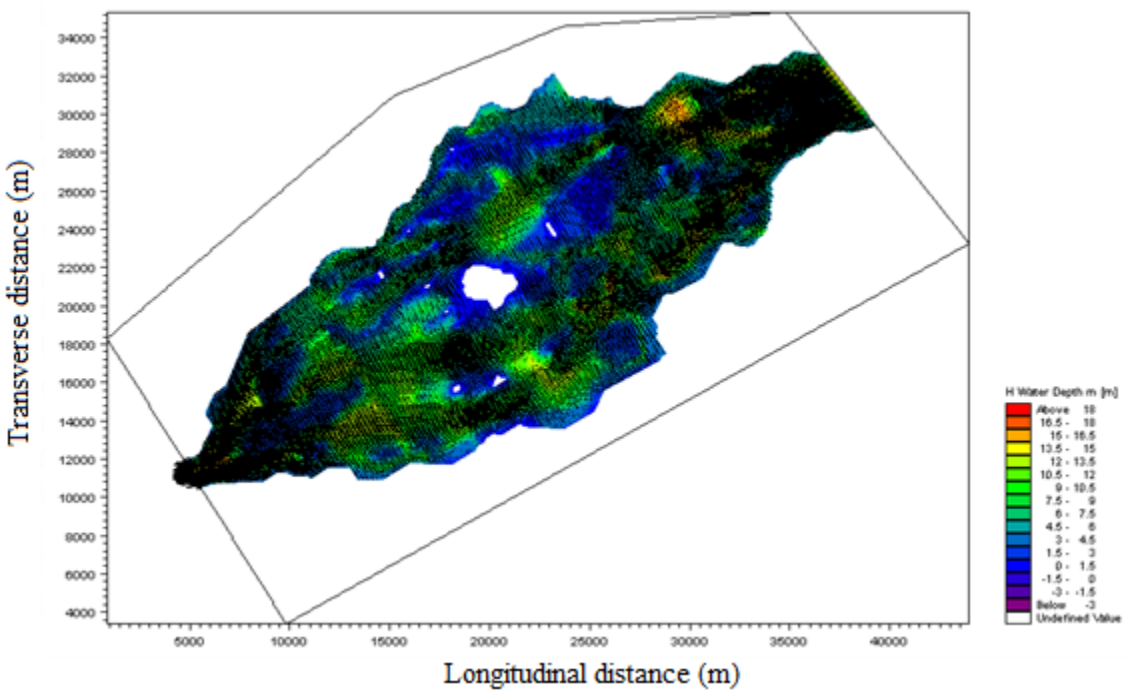

Figure 6.9 Water depth contour and velocity vector for present condition with 60000 cumec

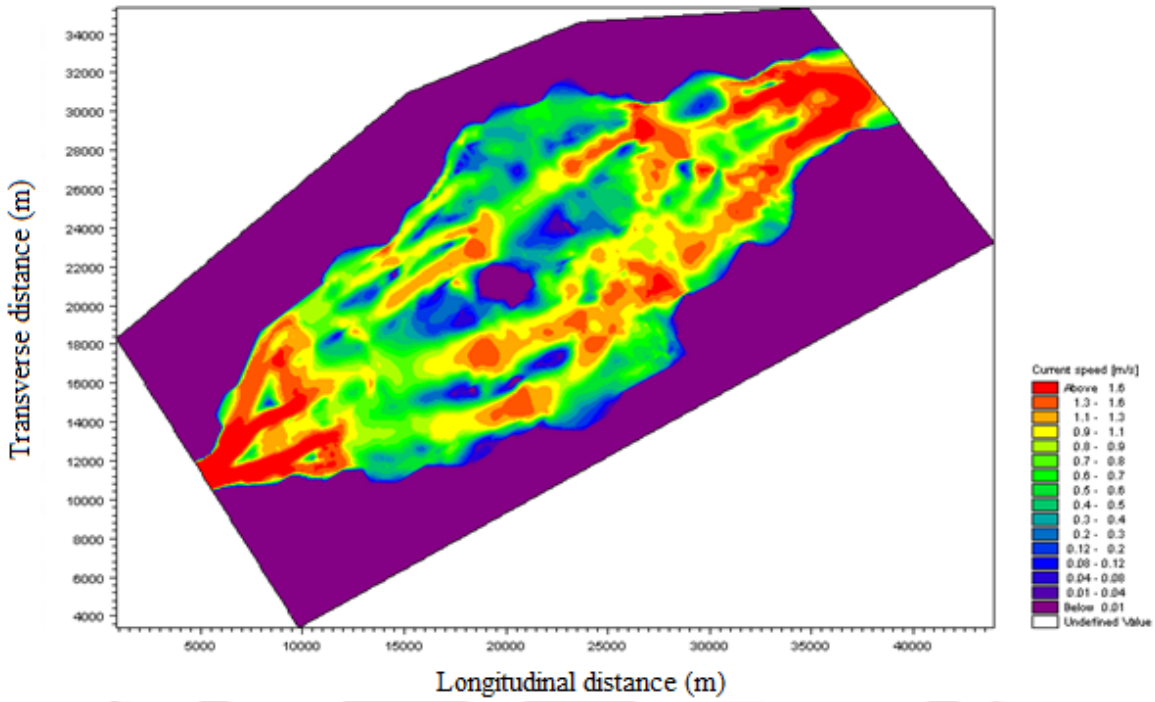

Figure 6.10 Speed contour for the present condition with 60000 cumec

6.4.5.1.2 Simulation with different alternatives

Based on experience, Water Resources Department proposed construction of 11 numbers of groynes to prevent this active erosion. Therefore, effect of providing 11 numbers of groyne varying in dimension and direction, as shown in figure 6.11 are analysed first for a flow discharge of 60000 cumec. Careful observation of velocity vector of figure 6.11 has revealed that the flow will move away from the bank once it strikes the groynes. This will also generate a very low speed zone near the vulnerable bank (figure 6.12) and thus will promote deposition of finer sediment in those areas.

To explore possibility of a more economic and efficient solution, several alternative combinations of groynes are then employed to observe the changes in flow characteristics. The different alternative combinations of groynes are considered based on expert judgment. The combinations tested are:

1. Combination of 9 groynes placed at suitable locations
2. Combination of 8 groynes placed at suitable locations
3. Combination of 7 groynes placed at suitable locations

4. Combination of 6 groynes along with dredging of river bed
5. Combination of 9 groynes along with dredging of river bed

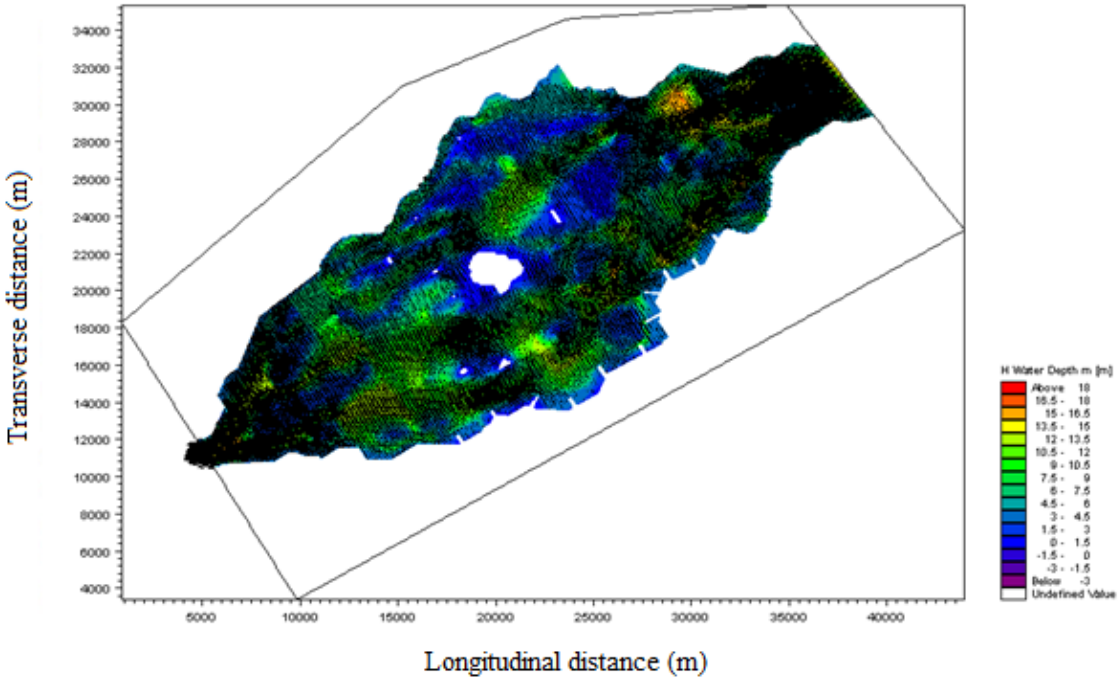

Figure 6.11 Water depth contour and velocity vector with 11 groynes

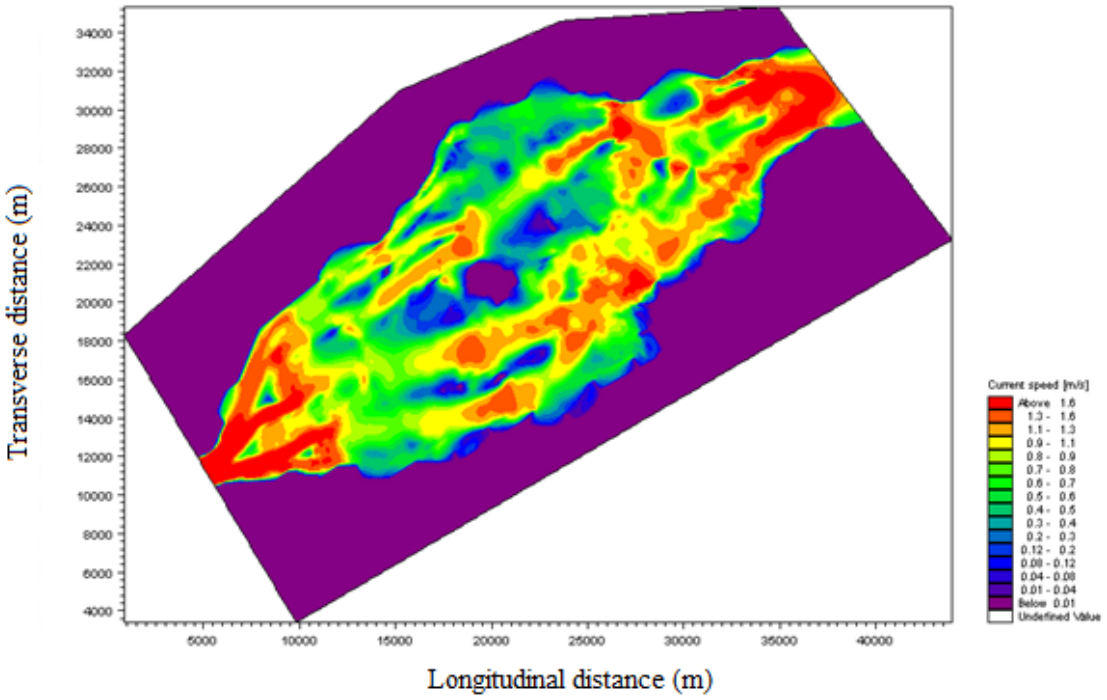

Figure 6.12 Speed contour with 11 groynes

6.4.5.2 Analysis for moderately high discharge (40000cumec)

During moderately high discharge, flow concentration may occurs in the near bank channels in case of braided river and it may therefore, generate more near bank flow velocity causing under cutting of the bank. Thus, there is chance of bank erosion at moderate discharge as well. For this purpose, all the alternative combinations are also tested with 40000 cumec.

6.4.5.3 Comparison of near bank velocity for different alternatives

For comparing performances of different alternative measures, near bank flow velocity is used as an index. As shown in figure 6.13, eight near bank points are taken as observation points on which water speed is evaluated for all the alternatives.

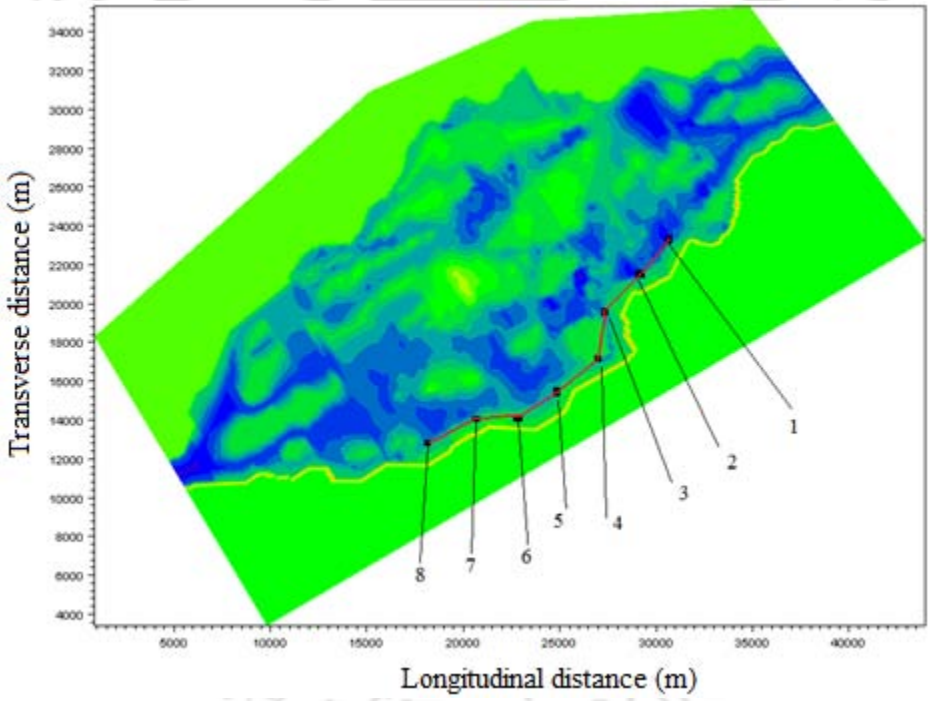

Figure 6.13 Study area with observation points

Figures 6.14 and 6.15 show the comparison of flow speed between all the alternatives for discharge values of 60000 cumec and 40000 cumec respectively. From these figures it can be clearly observed that, the combination of 9 groynes along with dredging of river bed is giving desired flow speed in the order of 0.5 m/s on the vulnerable area for both the values of discharge.

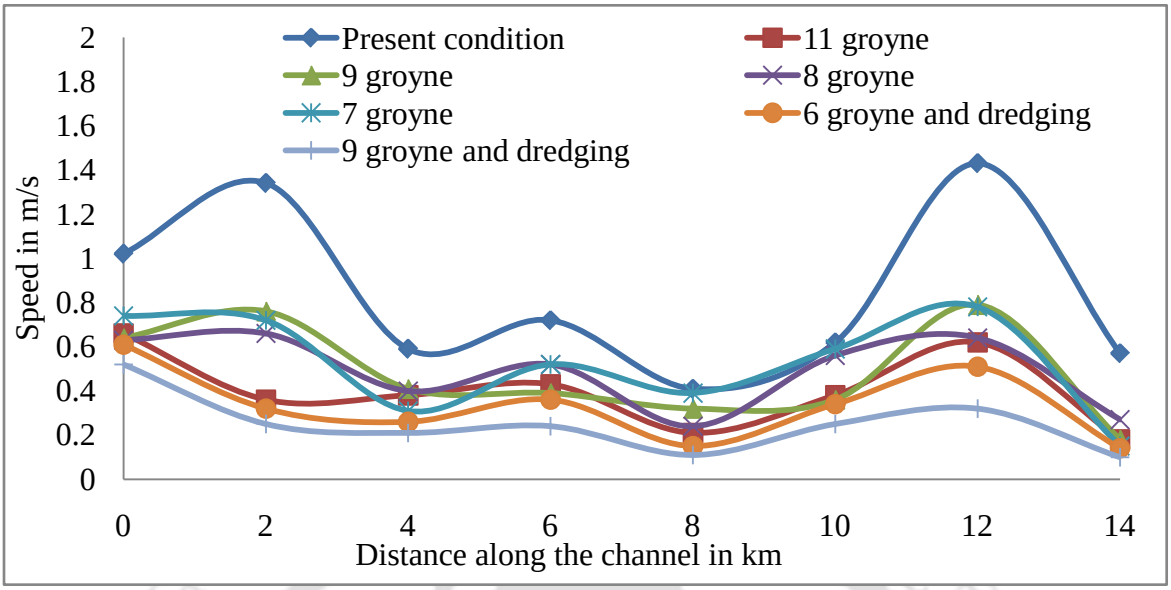

Figure 6.14 Comparison of speeds between alternatives for discharge of 60000 cumec

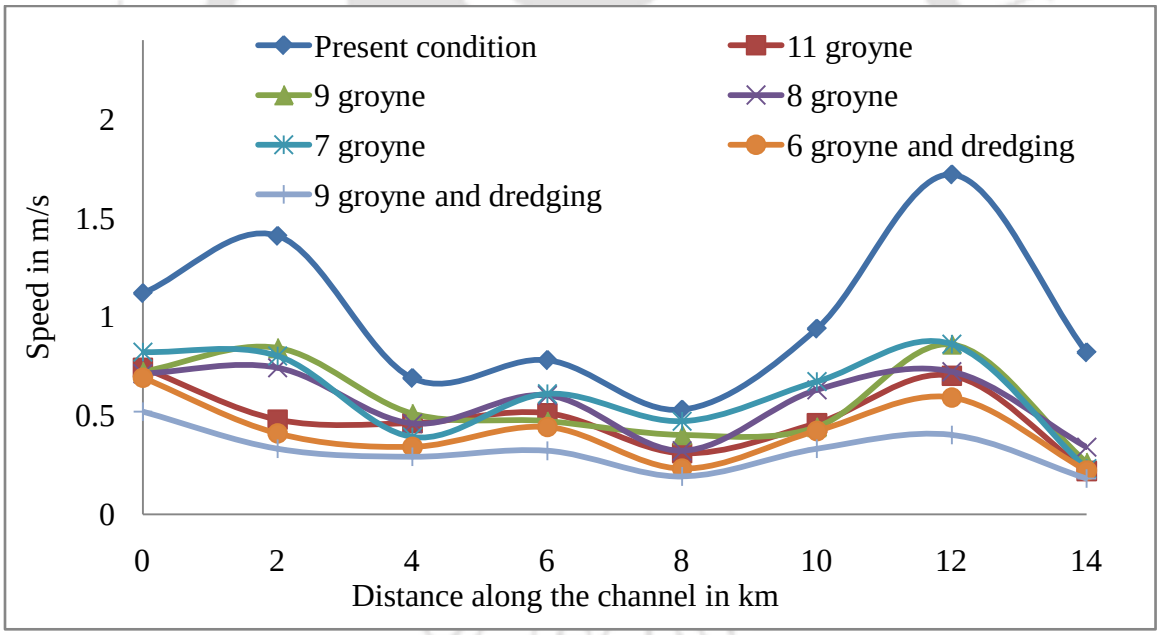

Figure 6.15 Comparison of speeds between alternatives for discharge of 40000 cumec

6.4.5.4 Details of the optimum combination

The best combination of groynes found out from all the combinations given from user side is shown in figure 6.16. In the same figure, the proposed position of river bed dredging is also shown. Table 6.1 shows the details of the groynes.

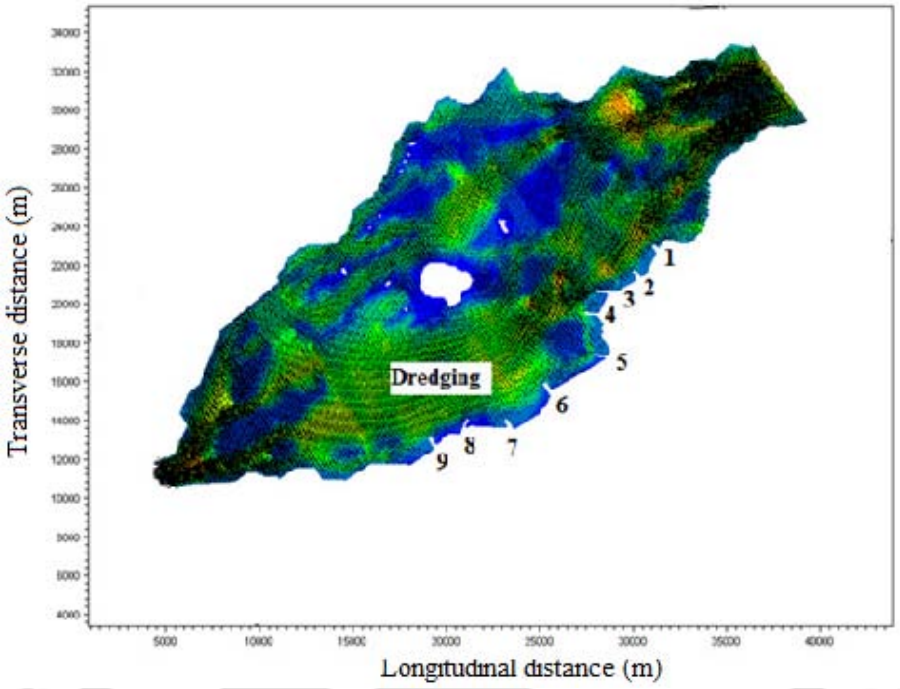

Figure 6.16 Proposed optimal combination of groynes with the proposed area of dredging

Table 6.1 Details of the optimal combination of groynes

Groyne no	Length of the groyne in meter	Bearing of the groyne in WCB degree	Geographical co-ordinate	
			Latitude	Longitude
1	470	330	26^0 22’ 48.20’’	92^0 11.52’ 55’’
2	610	330	26^0 22’ 0.46’’	92^0 11.16’ 38’’
3	870	275	26^0 21’ 35.86’’	92^0 10’ 23.2’’
4	870	277	26^0 20’ 56.5’’	92^0 10’ 1.92’’
5	860	273	26^0 19’ 50’’	92^0 10’ 19’’
6	650	329	26^0 18’ 47’’	92^0 8’ 26’’
7	650	328	26^0 17’ 49’’	92^0 7’ 5.3’’
8	800	22	26^0 17’ 54’’	92^0 5’ 37’’
9	650	328	26^0 17’ 19’’	92^0 4’ 36’’

6.5 Application of linked simulation-optimization model

The proposed linked simulation-optimization model is applied to obtain optimal combination of groynes for this river reach. As this proposed model simulates the hydrodynamic process several times depending on number of generation and initial population of the GA, a boundary fitted grid is generated with judiciously selected grid size to reduce computational time. The entire study channel has been divided in grids using grid size of 100×50. Figure 6.17 shows the generated grid for this river reach and the proposed low speed zone near the vulnerable bank.

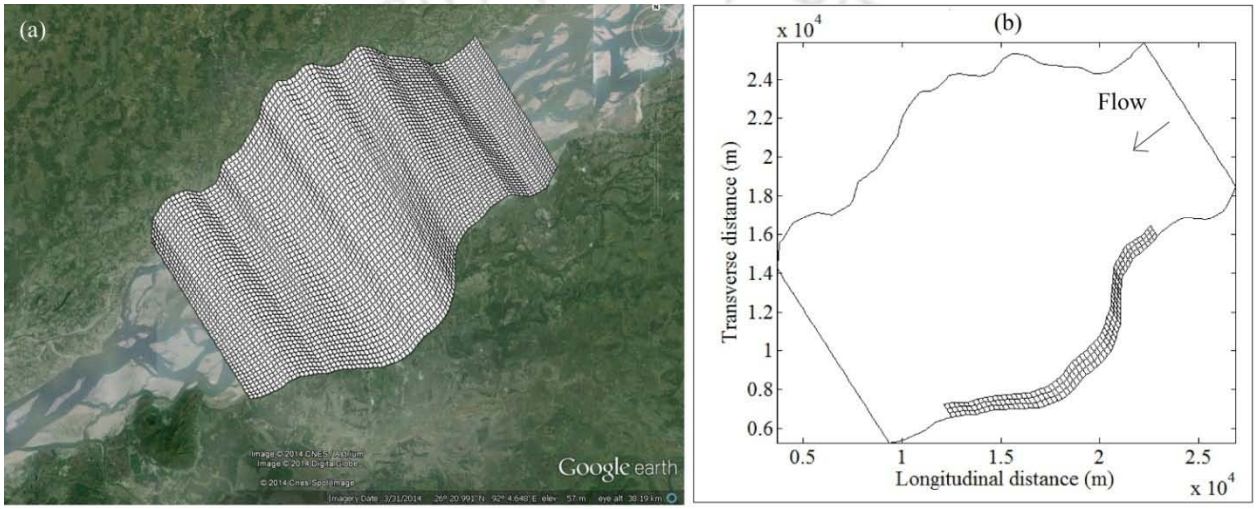

Figure 6.17 Study area along with low speed zones for the river reach of Brahmaputra: (a) study area with computational grid: (b) Low speed zone near the vulnerable bank

In the simulation study of iterative approach, it was established that the bank become more vulnerable for moderately high discharge of 40000 cumec, as compared to a discharge of 60000cumec. Therefore the hydrodynamic model in this linked simulation-optimization model is run with a discharge of value 40000 cumec and comparison is made accordingly. It is also observed that, dredging of the channel reduces the flow speed significantly and iterative approach give the optimal solution for the dredged situation. Therefore in this linked simulation-optimization model the dredged bathymetry is considered so that most optimal solution obtained in the iterative approach can be compared with the optimal solution obtained by linked simulation-optimization model. A CN value of 1.2, a CT value of 0.2 and a manning's roughness value of 0.031 are considered in the study.

In this channel, the area of speed reduction is on the left hand side of flow direction. Therefore, groynes are proposed on the left bank only. Decision variable, length of groyne (Llg) and position of groyne (Plg) are coded using binary string of length 3 and 7 respectively.

6.6 Results and discussions with linked simulation-optimization model

The main objective is to find out the number groynes which are to be placed on the reach so that the bank of the river can be protected. Initially, formulation I is considered where it is assumed that fund available is unlimited and the groynes can be placed at any location on the bank of the river. The main objective is the minimization of total construction cost while maintaining the flow speed at predefined value. In the first case, flow speed limit is considered as 0.6 m/sec. The maximum number of groynes considered is 7. Thus initial population is taken as 140. The values of Plg_{min} and Plg_{max} are considered as grid numbers 18 and 90 respectively and the values of Llg_{min} and Llg_{max} are considered as 0 and 5 respectively. The optimal solution shows that 5 numbers of groynes (Ng=5) are necessary for attaining the predefined target speed value. The lengths of these groynes are found as 440 m, 500 m, 260 m, 320 m and 1250m with corresponding positions on grid numbers 22, 32, 37, 59 and 87 respectively from upstream boundary. With this combination, the total construction cost required is ₹ 2.77×10^8. Figure 6.18 shows the velocity vector plot and speed contour map with the proposed combination of groyne for this case.

The present model also results in 5 number of groynes (Ng=5), to achieve another target speed of value 0.5 m/s on the predefined area. The lengths of these groynes are found as 1160 m, 1040 m, 320 m, 280 m and 1020 m with corresponding positions on grid numbers 26, 37, 61, 75 and 88 respectively from upstream boundary. Due to the increase in length of groynes, the total construction cost has increased to ₹ 3.82×10^8. Figure 6.19 shows the velocity vector plot and speed contour map with the proposed combination of groyne. Due to large number of initial populations for this formulation, a high simulation time of 200 hr was required by the present model.

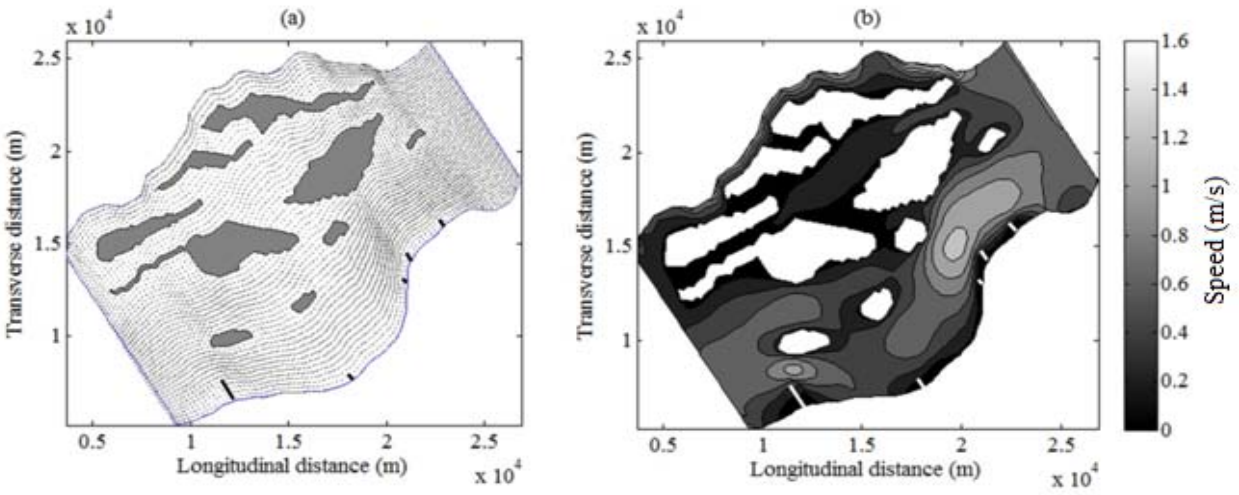

Figure 6.18 Optimal combination of groynes in vulnerable reach of river Brahmaputra by formulation I with target speed value of 0.6 m/s: (a) velocity vector; (b) speed contour

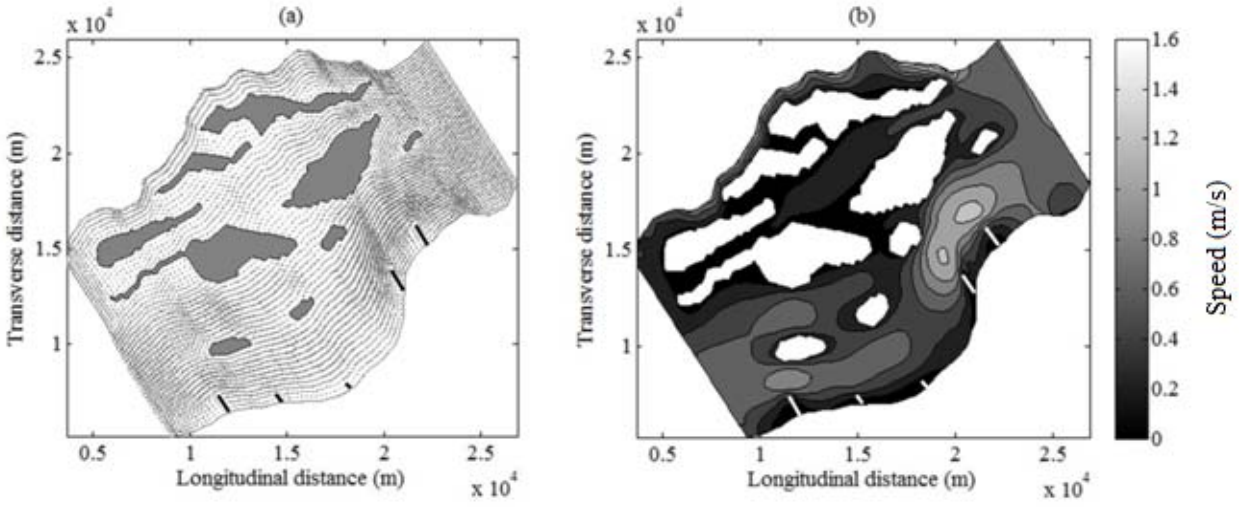

Figure 6.19 Optimal combination of groynes in vulnerable reach of river Brahmaputra by formulation I with target speed value of 0.5 m/s: (a) velocity vector; (b) speed contour

The formulation II is also applied to this reach of river Brahmaputra. In this case, it is assumed that the groynes can be placed at grid numbers 18, 27, 36, 45, 54, 63, 72, 81 and 90 from upstream boundary. The initial population is taken as 90. The values of Llg_{min} and Llg_{max} are 0 and 5 respectively. The proposed model is run to find the required lengths of groynes on those positions to achieve a target speed value of 0.6 m/s. For this case, the present model results in 6 number of groynes (Ng=6). The optimal position of these 6 groynes are found on grid numbers

18, 27, 36, 72, 81 and 90, having optimal length of 200 m, 720 m, 800 m, 300 m, 500 m and 260 m respectively. The total construction cost is found as ₹ 2.78×10^8. Figure 6.20 shows the velocity vector plot and speed contour map for this combination.

With a target speed value of 0.5 m/s on the predefined area, the present model results in 7 number of groynes (Ng=7). The optimal position of these groynes are found on grid numbers 18, 27, 36, 54, 63, 81 and 90, having optimal length of 200 m, 960 m, 800 m, 340 m, 330 m, 1000 m and 260 m respectively. Due to the increase in the length of groynes, the total construction cost has also increased to₹ 3.89×10^8. Figure 6.21 shows the velocity vector plot and speed contour map for this scenario. For formulation II the simulation time required was 128 hr.

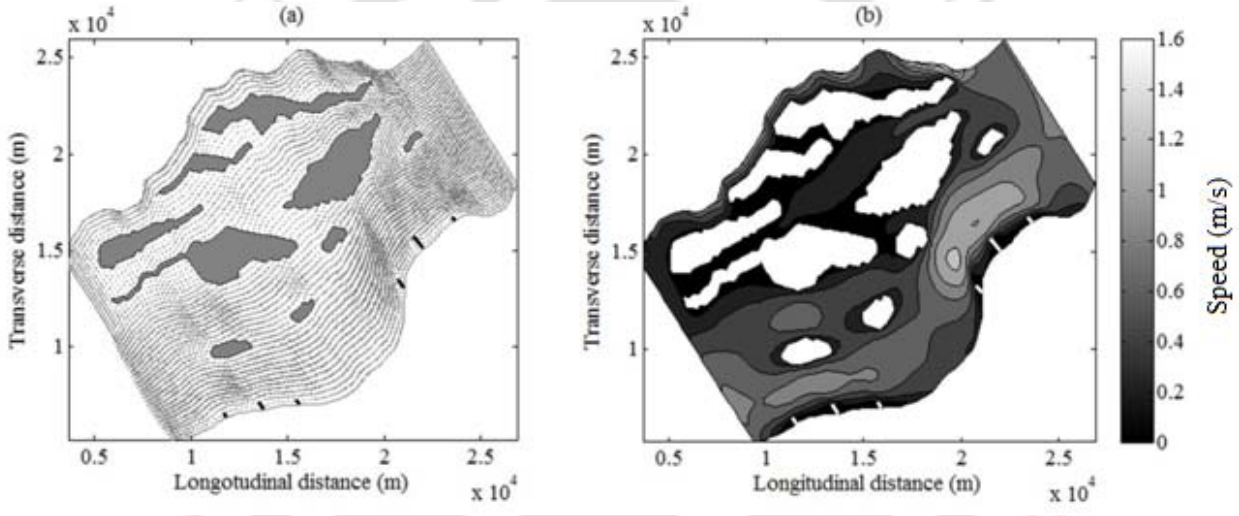

Figure 6.20 Optimal combination of groynes in vulnerable reach of river Brahmaputra by formulation II with target speed value of 0.6 m/s: (a) velocity vector; (b) speed contour

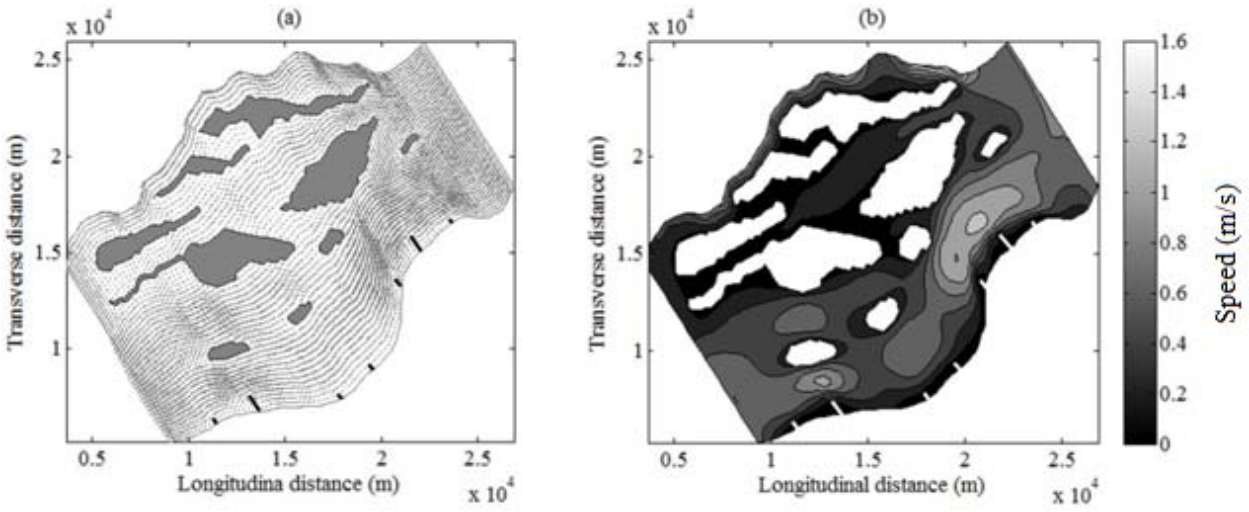

Figure 6.21 Optimal combination of groynes in vulnerable reach of river Brahmaputra by formulation II with target speed value of 0.5 m/s: (a) velocity vector; (b) speed contour

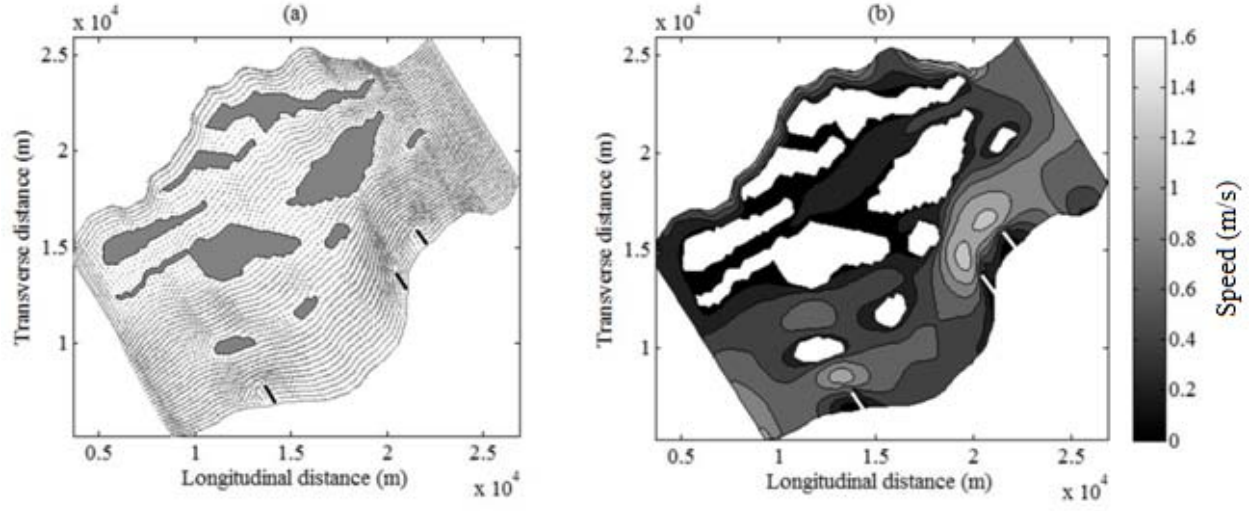

Figure 6.22 Optimal combination of groynes in river Brahmaputra by formulation III with three groynes of length 1000 m each: (a) velocity vector; (b) speed contour

In formulation III, it is assumed that fund for only three groynes of 1000 m length is available with the department. Therefore, the objective of the model is to place these groynes at optimal locations so that minimum spped can be achieved. Initial population of 30 is taken in this scenario. The values of Plg_{min} and Plg_{max} are taken as 18 and 90 respectively. The resulting positions given by the present model are grid numbers 9, 19 and 61. The optimal positions of these 3 groynes can minimize the flow speed on the predefined area up to 0.6021 m/s. Figure 6.22 shows the velocity vector plot and speed contour map with the proposed combination of

groynes for this case. Another experiment with 2 groynes is also conducted. In this case initial population of 20 is considered. The resulting positions given by the model are 13 and 57 which can reduce the flow speed on the predefined area to 0.8156 m/s. Figure 6.23 shows the velocity vector plot and speed contour map for this case. Low value of simulation time was required by the present model for the above two cases (43 hr with 3 groynes and 29 hr with 2 groynes), as the number of alternative solutions to be checked is lesser than the other formulations.

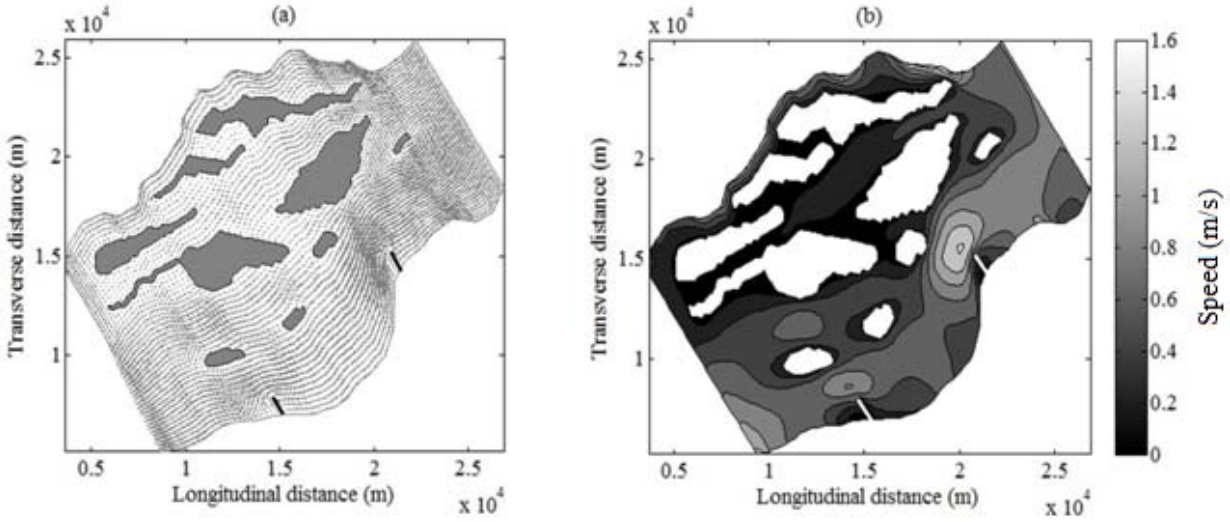

Figure 6.23 Optimal combination of groynes in river Brahmaputra by formulation III with two groynes of length 1000 m each: (a) velocity vector; (b) speed contour

6.7 Comparison with the results obtained by iterative approach

The results obtained by the proposed model are compared with the results obtained by using iterative approach. The total construction cost of groyne system obtained by using linked simulation-optimization model for achieving a target speed value of 0.5 m/s on the predefined area for the reach of river Brahmaputra is ₹ 3.82×10^8. However, by iterative approach with MIKE21C, the combination of 9 groynes along with dredging of river bed is leading to a speed of 0.5 m/s on the same area. The associated total cost of this system is ₹ 6.43×10^8.

In MIKE21C for the best combination of groyne i. e. 9 groynes along with river bed dredging, the groynes are placed uniformly. However in the simulation of the present condition without any groyne, it is observed that, in the mid portion of the vulnerable area there is already less speed (figure 6.10). In the linked simulation-optimization model, the groynes are placed

automatically in a way that the flow speed on the entire vulnerable area comes below permissible limit of 0.5 m/s. It is interesting to note that, the required speed could be achieved without putting any groyne in the mid portion of the vulnerable area, which in fact has got eroded in the past (figure 6.19). That has reduced the construction cost drastically in the proposed model than that of iterative approach.

In case of iterative approach, it is not possible to evaluate all the alternative solutions of the problem. Thus the solution obtained is always a sub-optimal solution. With this evaluation, it can be concluded that the proposed models have the capability to find out the optimal combination of groyne system required in a river reach for protecting the bank from erosion.

6.8 Conclusions

A comparative study between iterative approach and linked simulation-optimization approach for determining optimal combination of groynes is carried out to identify their advantages and limitations. From the study following conclusions are drawn,

1. 2D hydrodynamic softwares like MIKE21C can be used for determination of best combination of groynes from some chosen alternatives. However, this approach is cumbersome as it requires resetting of bathymetry every time for incorporating different alternative protection measures.
2. In the iterative approach of determining optimal combination of groynes, it is not possible to evaluate all the alternative solutions of the problem and hence the solution obtained never guarantee a true optimal solution.
3. By applying the proposed model in the river reach of Brahmaputra located between Nagaon and Marigaon district of Assam in India, it is observed that, the total construction cost required to achieve a target speed is significantly less than that of cost obtained using iterative approach.

CHAPTER 7

CONCLUSION, GENERAL DISCUSSION AND RECOMMENDATIONS FOR FURTHER STUDIES

7.1 Introduction

Although brief conclusions have been presented at the end of each of the previous chapters, a comprehensive conclusion followed by an overall discussion on the works performed in this study is presented in this chapter. Scope for future extension of this work is also suggested.

7.2 General discussions and conclusions

Review of literature has revealed that, solution of the governing equations of unsteady free surface flows remains a topic of continued interest since its development. A large number of studies have been conducted for solution of these equations for mathematical simulation of unsteady flow. This results in development of large number of in-house and commercially/freely available softwares for simulation of unsteady free surface flow. Efforts are still on for development of better numerical models capable of solution of these equations. However, it appears that, there is scope of doing a comparative study between different numerical schemes available for solution of these equations to have a detail comparison in terms of stability, computational complexity, computational time, accuracy and robustness. Considering this, extensive study on different numerical schemes has been carried.

Review of literature also revealed that, large number of studies have been conducted in the past for simulation of flow process around groynes both numerically and experimentally. A huge number of investigators have also applied different traditional and non-traditional optimization techniques for diverse fields of water resources engineering. Despite of large history of groyne simulation and water resources optimization studies, it is observed that, no study have been conducted for determination of cost effective combination of groynes for desired training of a river. This study is an attempt to develop a comprehensive simulation-optimization model, so that research gap in this area of engineering application can be addressed.

One of the important aspects for accurate simulation of unsteady free surface flow is the correct representation of the boundary conditions. Constant discharge or a flow hydrograph is generally used at upstream boundary depending on whether the flow is steady or unsteady. However, at the downstream boundary, extrapolation technique or characteristic equations may be adopted. Results computed by these two boundary conditions have revealed that extrapolation technique provides acceptable results for practical purpose with less computational effort, as compared to the use of characteristic equation.

Four different finite difference schemes namely, Lax diffusive, MacCormack predictor corrector, Modified predictor corrector and Beam and Warming have been investigated. Lax diifusive scheme is a relatively simple numerical scheme interms of computational complexities as it is an one step explicit scheme and therefore requires less computational time and computer space. However, due to the excessive dissipative nature associated with this scheme it can not reproduce the actual flow scenario around groynes. MacCormack predictor scheme applied in this study has the advantages of handling mixed subcritical-supercritical flow. Similarly, Modified predictor corrector scheme has a better capability of hadling mixed flow, as it avoid irroneous information from downstream by modifying the corrector step in case of supercritical flow. However, these two predictor corrector schemes also fail to simulate the flow behaviour near the groynes. Apart from these explicit schemes, Beam and Warming implict scheme has been found to be accurate not only in flow simulation around groynes but also in subcritical, supercritical and mixed flow regimes. Though this implicit scheme is computationaly complex and also takes larger computational time than the others, it remains stable for higher Courant number values, unlike the explicit schemes.

Another very important task in case of finite difference based hydrodynamic model is the discretization of the flow domain into finite difference grid. This may be achieved by using cartesian grid or boundary fitted grid. For accurate representation a curved channel using cartesian grid, a large number of grid is required. This results in larger computational time requirement. In case of boundary fitted grid, a curved boundary can be represnted accurately with lesser number of grid. To apply boundary fitted grid, 2D governing equations are transformed to a general coordinate system and its validity is proved for some experimental channel flows.

A GA based linked simulation-optimization model has been developed for evaluation of optimal combination of groynes leading to minimum construction cost. Due to the various advantages associated with Beam and Warming scheme, the hydrodynamic simulation model in this linked simulation-optimization model is developed using this scheme. The variables of this optimization model are number, position and length of groyne. The number of groyne is always an integer number. The other two variables are also integer in nature, as they are interms of some finite difference grids. To handle this integer nature of the variables in the optimization model effectively, binary coded GA is employed in this model. The proposed model has been applied for three different test problems including a hypothetical straight channel, a hypothetical bend channel and a hypothetical braided channel to establish its validity and applicability in different flow conditions. Successful application of the proposed model for these diverse cases has established its robustness.

To test the field applicability of the proposed linked simulation-optimization model, it is applied for a vulnerable reach of river Brahmaputra to determine the optimal combination of groynes. Final optimal groyne combination obtained from this model is compared with the groyne combination obtained by using traditional iterative approach. To have fair comparison, a widely used hydrodynamic software MIKE21C is used in the iterative approach in place of hydrodynamic model developed in this study. As the traditional iterative approach selects the best combination out of the chosen alternatives, scope of reaching a global optimal combination largely depends on the modeler's experience and is therefore subjective in nature. Because of this, the total construction cost by the proposed method has been found to be 40% less than that of iterative approach. This has clearly established merit of the proposed approach over the traditional approach.

Depending on the complexities of the channel and the grid size the simulation time varies. Time required for GA model also depends on the initial population and string length (number of variable). Therefore, for a large complex channel requiring a large number of groynes, the time required for the obtaining the final optimal results may be high. However, this may not be considered as a limitation, as number of alternatives tested during the computational procedure is enormous. Test of such large alternatives would have otherwise taken much more time and effort as compared to the time required by the model.

7.3 Future work possible

Following works may be taken as future extensions of the present works.

1. Though the numerical scheme presented in this study for simulation of unsteady free surface flow is quite efficient in handling wide varieties of flow types and also remains stable for larger Courant numbers, some other unconditionally stable scheme may also be used in the present simulation-optimization model to explore if more advantage can be obtained by doing so.

2. In this proposed model, it is assumed that, sedimentation can be promoted by lowering the flow speed on a defined portion within a river to prevent the bank erosion and hence the constraint is applied in the form of limiting flow speed. A detailed morphological model can be incorporated along with the hydrodynamic model to have a direct computation of sediment deposition, which can be used as a constraint for the optimization model.

3. All of the groynes considered in the present study are normal to the bank. The effect of oriented groyne on the results can also be studied.

4. The present study demonstrates the scope of applying linked simulation-optimization model in reducing flow speed in a defined zone within a channel flow. The concept can very well be used for other kinds of river training work. For example groynes can also be used for achieving minimum depth in a navigation channel. To achieve that in the proposed model, one needs to replace the constraint of target speed by constraint of target depth.

5. Some advanced optimization techniques such as Particle Swarm Optimization, Differential Evolution, and Simulated Annealing can also be considered for the present optimization model.

REFERENCES

Ackerman, C. T., and Brunner, G. W. (2006). “Dam failure analysis using HEC-RAS and HEC-GeoRAS.” *Proc. 3rd Federal Interagency Hydrol. Modeling Conf.*, Reno, Nevada.

Adams, T., Chen, S., Davis, R., Schade, T., and Lee, D. (2010). “The Ohio River community HEC-RAS model.” *Proc. World Environ. Water Resour. Cong.*, USA.

Aggett, G. R., and Wilson, J. P. (2009). “Creating and coupling a high-resolution DTM with a 1D hydraulic model in a GIS for scenario-based assessment of avulsion hazard in a gravel-bed river.” *J. geomorphology*, 113, 21-34.

Ahmed, H. S., Hasan, M. M., and Tanaka, N. (2010). “Analysis of flow around impermeable groynes on one side of symmetrical compound channel: An experimental study.” *Water Sci. and Eng.*, 3(1), 56-66.

Ahmed, J. A., and Sarma, A. K. (2005). “Genetic algorithm for optimal operating policy of a multipurpose reservoir.” *Water Resour. Manage.*, 19(2), 145-161.

Akanbi, A., and Katopodes, N. (1988). "Model for flood propagation on initially dry land." *J. Hydraul. Eng.*, 114(7), 689-706.

Akbari, G., and Firoozi, B. (2010). “Implicit and explicit numerical solution of Saint-Venant’s equations for simulating flood wave in natural rivers.” *Proc.5th National Cong. Civ. Eng.*, Ferdowsi University of Mashhad, Iran.

Alauddin, M., and Tsujimoto, T. (2012). “Optimum configuration of groynes for stabilization of alluvial rivers with fine sediments.” *Int. J. Sed. Res.*, 27(2), 158-167.

Alhan, C. M. K., and Medina, M. A. J. (2007). “Kinematic and diffusion waves: analytical and numerical solutions to overland and channel flow.” *J. Hydraul. Eng.*, 133(2), 217-228.

Ali, M. M., and Steffler, P. (2012). “Effect of friction on spurious oscillations in open channel modeling with variable bathymetry or roughness.” *J. Hydraul. Eng.*, 138(8), 695-706.

Alnahhal, S., Afifi, S., Qahman, K., Dentoni, M., and Lecca, G. (2010). "A simulation/optimization approach to manage groundwater resources in the Gaza aquifer (Palestine)." *Proc. Int. Conf. on Water Resour.*, Barcelona, Spain.

Ambrosi, D., Corti, S., Pennati, V., and Saleri, F. (1996). "Numerical simulation of unsteady flow at Po River delta." *J. Hydraul. Eng.*, 122(12), 455-462.

Anastasiou, K., and Chan, C. T. (1997). "Solution of the 2D shallow water equations using the finite volume method on unstructured triangular meshes." *Int. J. Numer. Methods Fluids*, 24, 1225–1245

Anderson, D. A., Tannehill J. D., and Pletcher, R.H. (1984). "*Computational Fluid Mechanics and Heat Transfer*." McGraw-Hill, New York.

Barros, M. T. L., Tsai, F. T. C., Yang, S. L., Lopes, J. E. G., and Yeh, W. W. G. (2003). "Optimization of large-scale hydropower system operations." *J. Water Resour. Plann. Manage.*, 129(3), 178-188.

Beam, R. M., and Warming, R. F. (1976). "An implicit finite difference algorithm for hyperbolic systems in conservation law form." *J. Comput. Phys*., 22, 87-110.

Beck, J. S., and Basson, G. R. (2008). "Klein River estuary (South Africa): 2D numerical modelling of estuary breaching." *Water S. A*., 34(1), 33-38.

Begnudelli, L., and Sanders, B. F. (2007). "Simulation of St. Francis dam-break failure." *J. Eng. Mechanics*, 133(11), 1200–1212.

Bellos, C. V., and Sakkas, J. G. (1987). "1-D dam-break flood-wave propagation on dry bed." *J. Hydraul. Eng*., 113(12), 1510–1524.

Bellos, C. V., Soulis, J. V., and Sakkas, J. G. (1991). "Computation of two dimensional dam break induced flows." *Adv. Water Resour.*, 14(1), 31-41.

Bellos, V., and Hrissanthou, V. (2011). "Numerical simulation of dam break flood wave." *European Water*, 33, 45-53.

Bhallamudi, S. M., and Chaudhry, M. H. (1992). “Computation of flows in open channel transitions.” *J. Hydraul. Res.*, 30(1). 77-93.

Bhattacharjya, R. K. (2006). “Optimal design of open channel section incorporating critical flow condition.” *J. Irrig. Drain. Eng.*, 132(5), 513–518.

Blade, E., Valentin, M. G., Juny, M. S., and Dolz, J. (2008). “Preserving steady-State in one-dimensional finite-volume computations of river flow.” *J. Hydraul. Eng.*, 134(9), 1343-1347.

Bo, Y. C., Kuan, C. Y., Chuan, B. Y., and Dan, Z. Z. (2002). “Numerical simulation of separated flow near groyne.” *J. Hydrodynamics*, Ser. B, 22, 47-52.

Bradford, S. F., and Katopodes, N. D. (2001). “Finite volume model for non level basin irrigation.” *J. Irrig. Drain. Eng*., 127(4), 216-223.

Bradford, S. F., and Sanders, B. F. (2002). “Finite-Volume model for shallow-water flooding of arbitrary topography.” *J. Hydraul. Eng.*, 128(3), 289-298.

Cat, V. U., and Duong, B. D. (2007). “Application of MIKE package to asses hydraulic regimes and flood mapping when construction of thermal power at the Mong Duong estuary.” *Japan-Vietnam Estuary Workshop*, Hochiminh, Vietnam.

Chang, J. X., Bai, T., Huang, Q., and Yang, D. W. (2013). “Optimization of water resources utilization by PSO-GA.” *Water Resour. Manage*., 27(10), 3525-3540.

Chaudhry, M. H. (2008). “*Open channel flow*.” 2nd edn. Prentice-Hall Inc, Englewood Cliffs.

Chen, J., Steffler, P. M., and Hicks, F. E. (2007). “Conservative formulation for natural open channels and finite-element implementation.” *J. Hydraul. Eng.*, 133(9), 1064-1073.

Cho, J. H., Sung, K. S., and Ha, S. R. (2004). “A river water quality management model for optimizing regional wastewater treatment using a genetic algorithm.” *J. Environ. Manage.*, 73, 229-242.

Cubanova, L. (2009). “Modeling of fish passes in conditions of Slovak Streams.” *Int. Symp. Water Manage. Hydraul. Eng*., Bratislava, Slovak Republic.

Danish Hydraulic Institute. (2006). *MIKE21C, Morphological Module and Grid generator, user's guide and reference manual*. Denmark.

Danish Hydraulic Institute. (2009). *MIKE11, user's guide and reference manual*. Denmark.

Das, A. (2000). "Optimal channel cross section with composite roughness." *J. Irrig. Drain. Eng.*, 126(1), 68–72.

Deb, K. (1999). "An introduction to genetic algorithms." *Sadhana*, 24(4-5), 293-315.

Dehghani, A. A., Azamathulla, H. M., Najafi, S. A. H., and Ayyoubzadeh, S. A. (2013), "Local scouring around L-head groynes." *J. Hydrol*., 504, 125-131.

Dressler, R. F. (1952), "Hydraulic resistance effect upon the dam-break functions." *J. Res. of the National Bureau of Standards*, 49(3), 217-225.

Duan, J. G., Wang, S. Y. and Jia, Y. (2001). "The applications of the enhanced CCHE2D model to study the alluvial channel migration processes." *J. Hydraul. Res*., 39(5), 469-480.

Duan, J. G., and Nanda, S. K. (2006). "Two-dimensional depth-averaged model simulation of suspended sediment concentration distribution in a groyne field." *J. Hydrol.*, 327, 426–437.

Duan, J. G., He, L., Fu, X., and Wang, Q. (2009). "Mean flow and turbulence around experimental spur dike." *Adv. Water Resour.*, 32, 1717–1725.

Farsirotou, E. D., Soulis, J. V., and Dermissis, V. D. (2002). "A numerical method for 2-D bed morphology calculations." *Int. J. Comput. Fluid Dynamics*, 16(3), 187–200.

Fazli, M., Ghodsian, M., and Neyshabouri, S. A. A. S. (2008). "Scour and flow around a spur dike in a 90^0 bend." *Int. J. Sed. Res.*, 23(1), 56-68.

Fennema, R. J., and Chaudhry, M. H. (1986). "Explicit numerical schemes for unsteady free-surface flows with shocks." *Water Resour. Res*., 22(13), 1923-1930.

Fennema, R. J., and Chaudhry, M. H. (1987). "Simulation of one-dimensional dam-break flows." *J. Hydraul. Res.*, 25(1), 41-51.

Fennema, R. J., and Chaudhry, M. H. (1989). “Implicit methods for two dimensional unsteady free-surface flows,” *J. Hydraul. Res*., 27(3), 321-332.

Fennema, R. J., and Chaudhry, M. H. (1990). “Explicit methods for 2-D transient free-surface flows.” *J. Hydraul. Eng.*, 116(8), 1013-1034.

Fiedler, F. R., and Ramirez, J. A. (2000). “A numerical method for simulating discontinuous shallow flow over an infiltrating surface.” *Int. J. Numer. Methods Fluids*, 32, 219-240.

Fredrik, H., Hermjan, B., Nicholas, P., Jonathan, R., Henk, E., and Andries, P. (2013). “Optimizing design of river training works using 3-dimensional flow simulations.” *Proc. 6th Int. PIANC-SMART Rivers Conf*., Liege, Netherland.

Ghostine, R., Mignot, E., Abdallah, M., Lawniczak, F., Vazquez, J., Mose, R., and Gregoire, C. (2010). “Discontinuous Galerkin finite-element method for simulation of flood in crossroads.” *J. Hydraul. Eng*., 136(8), 474-482.

Giri, S., Shimizu, Y., and Surajate, B. (2004). “Laboratory measurement and numerical simulation of flow and turbulence in a meandering-like flume with spurs.” *Flow Measurement and Instrumentation*, 15, 301-309.

Goldberg, D. E., and Kuo, C. H. (1987). ‘‘Genetic algorithms in pipeline optimization.’’ *J. Comp. Civ. Eng*., 1(2), 128–141.

Gorelick, S. M., Evans, B., and Ramson, I. (1983). “Identifying sources of groundwater pollution: An optimization approach.” *Water Resour. Res.*, 19(3), 779-790.

Guo, C. Y., and Hughes, W. C. (1984). “Optimal channel cross section with freeboard.” *J. Irrig. Drain. Eng.*, 110(3), 304-314.

Hall, W. A., and Buras, N. (1961). “The dynamic programming approach to water-resources development.” *J. Geophysical Res*., 66(2), 517-520.

Hasan, A. Z., Ghani, A. A., and Zakaria, N. A. (2007). "Application of 2-D modeling for Muda River using CCHE2D." *Proc. 2nd Int. Conf. on managing rivers in the 21st century: solution towards sustainable river basins*, River-side Kuching, Sarawak, Malaysia.

Hassan, K. I., and Dibike, Y. B. (2000). "Two-dimensional morphological modelling at the confluence of the Ganges and the Jamuna rivers for dredging and navigation study." *Proc. 4th Int. Conf. Hydroinf.*, Lowa, USA.

Hicks, F. E., and Steffler, P. M. (1992). "Characteristic dissipative Galerkin scheme for open-channel flow." *J. Hydraul. Eng.*, 118(2), 337-352.

Houghton, D. D., and Kasahara, A. (1967). "Nonlinear shallow fluid flow over an isolated ridge." *NCAR Rep. No. 259a*, National Center for Atmospheric Research, Boulder, Colorado.

Huang, J., and Charles, C. S. (1985). "Stability of dynamic flood routing schemes." *J. Hydraul. Eng*., 111(12), 1497-1505.

Hye, J. M. A., and Jahan, S. (2000). "Modeling response to flow and sediment regime changes due to construction of a bridge upstream of an existing bridge." *Proc. Int. Cong. Modeling and Simulation*, Canberra, Australia.

Isaacson, E., Stoker, J. J., and Troesch B. A. (1954). "Numerical solution of flood prediction and river regulation problems, Inst. Math. Sci., *Rept. No. IMM-NYU 205*, New York University, New York.

Jia, Y., Kitamura, T., and Wang, S. S. Y. (2001). "Simulation of scour process in plunging pool of loose bed-material." *J. Hydraul. Eng.*, 127(3), 219-229.

Jia, Y., and Wang, S. S. Y. (1999). "Numerical model for channel flow and morphological change studies." *J. Hydraul. Eng.*, 125(9), 924-933.

Jin, M., and Fread, D. L. (1997). "Dynamic flood routing with explicit and implicit numerical solution schemes." J. Hydraul. Eng., 123(3), 166-173.

Johnston, P. R., and Pilgrim, D. H. (1976). "Parameter optimization for watershed models." *Water Resour. Res*., 12(3), 477-486.

Kacimov, A. R. (1992). “Seepage optimization for trapezoidal channel.” *J. Irrig. Drain. Eng.*, 118(4), 520-526.

Kalkwijk, J. P. T., and Vriend, H. J. D. (1980). “Computation of the flow in shallow river bends.” *J. Hydraul. Res*., 18(4), 327–342.

Kassem, A. A., and Chaudhry, M. H. (1998). “Comparison of coupled and semi coupled numerical models for alluvial channels.” *J. Hydraul. Eng.*, 124(8), 794-802.

Kassem, A. A., and Chaudhry, M. H. (2005). “Effect of bed armoring on bed topography of channel bends.” *J. Hydraul. Eng.*, 131(12), 1136-1140.

Katopodes, N. D. (1984). “A dissipative Galerkin scheme for open-channel Flow.” *J. Hydraul. Eng.*, 110(4), 450-466.

Katopodes, N. D. (1984). “Two-dimensional surges and shocks in open channels.” *J. Hydraul. Eng.*, 110(6), 794-812.

Khan, A. A. (2000). “Modeling flow over an initially dry bed.” *J. Hydraul. Res*., 38(5), 383–388.

Kleinecke, D. (1971). “Use of linear programming for estimating geohydrologic parameters of groundwater basin.” *Water Resour. Res.*, 7(2), 367-374.

Klonidis, A. J., and Soulis, J. V. (2001). “An implicit scheme for steady two-dimensional free-surface flow calculation.” *J. Hydraul. Res.*, 39(3), 1-10.

Koopaei, K. B., Ervine, D. A., and Pender, G. (2003). “Field measurements and flow modeling of overbank flows in River Severn, U.K.” *J. Environ. Informatics*, 1 (1), 28-36.

Kuhnle, R. A., Alonso, C. V., and Shields, F. D. (1999). “Geometry of scour holes associated with 90^0 spur dikes.” *J. Hydraul. Eng.*, 125(9), 972-978.

Kuhnle, R. A., Alonso, C. V., and Shields, F. D. (2002). “Local scour associated with angled spur dikes.” *J. Hydraul. Eng*., 128(12), 1087-1093.

Kuiry, S. N., Sen, D., and Bates, P. D. (2010). “Coupled 1D–quasi-2D flood inundation model with unstructured grids.” *J. Hydraul. Eng*., 136(8), 493-506.

Lai, Y. G. (2010). “Two-dimensional depth-averaged flow modeling with an unstructured hybrid mesh.” *J. Hydraul. Eng*., 136(1), 12-23.

Lansey, K. E., and Mays, L. W. (1989). “Optimization model for water distribution system design.” *J. Hydraul. Eng*., 115(10), 1401-1418.

Liang, D., Falconer, R. A., and Lin, B. (2006). “Comparison between TVD-MacCormack and ADI-type solvers of the shallow water equations.” *Adv. Water Resour*., 29(12), 1833-1845.

Liang, D., Lin, B., and Falconer, R. A. (2007). “A boundary-fitted numerical model for flood routing with shock-capturing capability.” *J. Hydrol.*, 332, 477–486.

Liong, S. Y., Chan, W. T., and Ram, J. S. (1995). “Peak-flow forecasting with genetic algorithm and SWMM.” *J. Hydraul. Eng.*, 121(8), 613-617.

Leendertse, J. J. (1967). “Aspects of a computational model for long-period water-wave propagation.” *Rep. No. RM-5294-PR*, Hydraulic Research Division of the Delta Works, Netherlands.

Macchione, F., and Morelli, M. A. (2003). “Practical aspects in comparing shock-capturing schemes for dam break problems.” *J. Hydraul. Eng.*, 129(3), 187-195.

Mccoy, A., Constantinescu, G., and Weber, L. J. (2008). “Numerical investigation of flow hydrodynamics in a channel with a series of groynes.” *J. Hydraul. Eng.*, 134(2), 157-172.

Meier, W. L., and Beightler, C. S. (1967). “An optimization method for branching multistage water resource systems.” *Water Resour. Res*., 3(3), 645-652.

Miller, S., and Chaudhry, M. H. (1989). “Dam-break flows in curved channel.” *J. Hydraul. Eng.*, 115(11), 1465-1478.

Mingham, C. G., and Causon, D. M. (1998). “High-resolution finite-volume method for shallow water flows.” *J. Hydraul. Eng*., 124(6), 601-614.

Molls, T., Chaudhry, M. H., and Khan, K. W. (1995). “Numerical simulation of two dimensional flow near a spur dike.” *Adv. Water Resour*., 18(4), 221-236.

Molls, T., and Chaudhry, M. H. (1995). "Depth-averaged open-channel flow model." *J. Hydraul. Eng.*, 121(6), 453-465.

Molls, T., and Zhao, G. (2000). "Depth-averaged simulation of supercritical flow in channel with wavy sidewall." *J. Hydraul. Eng.*, 126(6), 437-445.

Mukherjee, A., and Sarma, A. K. (2010). "*2D flow simulation in alluvial river using MIKE software: a modeling approach*." Lambert Academic Publishing, Germany.

National Center for Computational Hydroscience and Engineering. (2005). *CCHE2D model, user's manual version 2.2*, University of Mississippi, USA.

Navarro, P. G., Alcrudo, F., and Saviron, J. M. (1992). "1-D open-channel flow simulation using Tvd-Mccormack scheme." *J. Hydraul. Eng.*, 118(10), 1359–1372.

Navarro, P. G., and Villanueva, A. F. I. (1999). "Dam-break flow simulation: some results for one-dimensional models of real cases." *J. Hydrol.*, 216, 227–247.

Negm, A. M., Abdulaziz, T., Nassar, M., and Fathy, I. (2010). "Prediction of life time span of high Aswan dam reservoir using CCHE2D simulation model." *Proc. 14th Int. Water Technol. Conf.*, Cairo, Egypt.

Nguyen, D. K., Shi, Y. E., Wang, S. S. Y., and Nguyen, T. H. (2006). "2D shallow-water model using unstructured finite-volumes methods." *J. Hydraul. Eng.*, 132(3), 258-269.

Nicolini, M., Giacomello, C., and Deb, K. (2011). "Calibration and optimal leakage management for a real water distribution network." *J. Water Resour. Plann. Manage.*, 137(1), 134-142.

Niyogi, P. (2009). "*Introduction to computational fluid dynamics*." Pearson Education Publications, India.

Nov, A., and Golany, P. (1979). "Optimization of a dam System for recharging runoff water into the ground." *Water Resour. Res*., 15(4), 891-898.

Ouillon, S., and Dartus, D. (1997). "Three-dimensional computation of flow around groyne." *J. Hydraul. Eng.*, 123(11), 962–970.

Pan, T. C., and Kao, J. J. (2009). “GA-QP model to optimize sewer system design.” *J. Environ. Eng.*, 135(1), 17-24.

Park, S. Y., Choi, J. H., Wang, S. and Park, S. S. (2006). “Design of a water quality monitoring network in a large river system using the genetic algorithm.” *J. Ecological Modeling*, 99, 289-297.

Qureshi, A. L., Khero, Z. I., and Lashari, B. K. (2012). “Optimization of irrigation water management: a case study of secondary canal, Sindh, Pakistan.” *Proc. 16th Int. Water Technol. Conf.*, Istanbul, Turkey.

Rahimpour, M., and Tavakoli, A. (2011). “Multi-grid Beam and Warming scheme for the simulation of unsteady flow in an open channel.” *Water SA*, 37(2), 229-236.

Rajaratnam, N., and Nwachukwu, A. (1983). “Flow near groin like structure.” *J. Hydraul. Eng.*, 109(3), 463-480.

Rashid, R. S., and Chaudhry M. H. (1995). “Flood routing in channels with flood plains.” *J. Hydrol.*, 171, 75-91.

Reis, L. F. R., Porto, R. M., and Chaudhry, M. H. (1997). “Optimal location of control valves in pipe networks by genetic algorithm.” *J. Water Resour. Plann. Manage*., 123(6), 317-326.

Rogers, B. D., Borthwick, A. G. L., and Taylor, P. H. (2003). “Mathematical balancing of flux gradient and source terms prior to using Roe’s approximate Riemann solver,” *J. Comput. Phys*., 192(2), 422-451.

Rossell, R. P., and Ting, F. C. K. (2013). “Hydraulic and contraction scour analysis of a meandering Channel: James River bridges near Mitchell, South Dakota.” *J. Hydraul. Eng.*, 139(12), 1286-1296.

Saikia, M. D. (2007). “Simulation of dam break hydraulics in natural flood plain topography." PhD thesis, Civ. Eng. Dept., Indian Institute of Technology Guwahati, Assam, India.

Saikia, M. D., and Sarma, A. K. (2006). “Analysis for adopting logical channel section for 1D dam break analysis in natural channels.” *ARPN J. Eng. Applied Sci*., 1(2), 46-54.

Saikia, M. D., and Sarma, A. K. (2007). “Numerical simulation model for computations of a dam break flood in natural flood plain topography.” *Dam Eng*., 17(1), 31-50.

Sarma, A. K. (1999). "A study of two-dimensional flow propagating from an opening in the river dike." PhD thesis, Civ. Eng. Dept., Guwahati University, Assam, India.

Schwanenberg, D., and Harms, M. (2004). “Discontinuous Galerkin finite-element method for transcritical two-dimensional shallow water flows.” *J. Hydraul. Eng.*, 130(5), 412-421.

Shahapure, S. S., Eldho, T. I., and Rao, E. P. (2011). “Flood simulation in an urban catchment of Navi Mumbai city with detention pond and tidal effects using FEM, GIS, and remote sensing.” *J. Waterway, Port, Coastal, Ocean Eng*., 137(6), 286-299.

Sharp, J. J., and Moore, E. (1976). “Analysis of unsteady flow in open channels.” *Int. J. Math. Educ. Sci. Technol*., 7(4), 377-393.

Simpson, A. R., Dandy, G. C., and Murphy, L. J. (1994). “Genetic algorithms compared to other techniques for pipe optimization.” *J. Water Resour. Plann. Manage*., 120(4), 423-443.

Singh, J., Altinakar, M. S., and Ding, Y. (2011). “Two-dimensional numerical modeling of dam-break flows over natural terrain using a central explicit scheme.” *Adv. Water Resour.*, 34, 1366-1375.

Singh, R. M., and Datta, B. (2006). “Identification of groundwater pollution sources using GA-based linked simulation optimization model.” *J. Hydrol. Eng.*, 11(2), 101-109.

Siviglia, A., Nobile, G., and Colombini, M. (2008). “Quasi-conservative formulation of the one-dimensional Saint-Venant–Exner model.” *J. Hydraul. Eng.*, 134(10), 1521-1526.

Sole, A., and Zuccaro, G. (2005). “New urban area flood model: a comparison with MIKE11-quasi2d.” *Adv. Geosci*., 2, 279–284.

Soleymani, M., and Delphi, M. (2012). “Comparison of flood routing models (Case Study: Maroon River, Iran).” *J. World Applied Sci*., 16 (5), 769-775.

Steffler, P., and Blackburn, J. (2002). *RIVER2D, user’s manual version 1.1*, University of Alberta, Canada.

Stronska, K., and Borowicz, A. (1999). "MIKE11 as flood management and flood forecasting tool for the Odra River, Poland." *Proc. 3rd DHI Software Conf.*, Helsingor, Denmark.

Tang, H. U., Xin, X. K., Dai, W. H., and Xiao, Y. (2010). "Parameter identification for modeling river network using a genetic algorithm." *J. Hydrodynamics*, Ser. B, 22(2), 246-253.

Tingsanchali, T., and Maheswaran, S. (1990). "2D depth-averaged flow computation near groyne." *J. Hydraul. Eng.*, 116(1), 71-86.

Tisdale, T. S., Scarlatos, P. D., and Hamrick, J. M. (1998). "Streamline upwind finite-element method for overland flow." *J. Hydraul. Eng.*, 124(4), 350-357.

Travis, Q. B., and Mays, L. W. (2008). "Optimizing retention basin networks." *J. Water Resour. Plann. Manage.*, 134(5), 432-439.

Tsakiris, G., and Bellos, V. (2014). "A numerical model for two-dimensional flood routing in complex terrains." *Water Resour. Manage.*, 28(5), 1277-1291.

US Army Corps of Engineers. (2008). *HEC-RAS, hydraulic user's manual version 3.3*, Hydrologic Engineering Center, Davis, CA.

Uijttewaal, W. (2005). "Effects of groyne layout on the flow in groyne fields: Laboratory experiments." *J. Hydraul. Eng.*, 131(9), 782–791.

Vaghefi, M., Ghodsian, M., and Neyshabouri, S. A. A. S. (2012). "Experimental study on scour around a T shaped spur dike in a channel bend." *J. Hydraul. Eng.*, 138(5), 471-474.

Vasquez, J. A., Millar, R. G., and Steffler, P. M. (2005). "Two-dimensional morphological simulation in transcritical flow." *River, Coastal and Estuarine Morphodynamics*, 253-258.

Wang, G. T., Yao, C., Okoren, C., and Chen, S. (2006). "4-point FDF of Muskingum method based on the complete St. Venant's equations." *J. Hydrol.*, 324, 339-349.

Wardlaw, R., and Sharif, M. (1999). "Evaluation of genetic algorithms for optimal reservoir system operation." J. Water Resour. Plann. Manage., 125(1), 25-33.

Wu, W. (2004). “Depth-averaged two-dimensional numerical modeling of unsteady flow and nonuniform sediment transport in open channels.” *J. Hydraul. Eng*., 130(10), 1013-1024.

Yazdi, J., Sarkardeh, H., Azamathulla, H. M., and Ghani, A. A. (2010). “3D simulation of flow around a single spur dike with free surface flow.” *Int. J. River Basin Manage.*, 8(1), 55-62.

Yossef, M. F. M., and Vriend, H. J. D. (2010). “Sediment exchange between a river and its groyne fields: Mobile-bed experiment.” *J. Hydraul. Eng.*, 136(9), 610-625.

Zarrati, A. R., Tamai, N., and Jin, Y. C. (2005). “Mathematical modeling of meandering channels with a generalized depth averaged model.” *J. Hydraul. Eng*., 131(6), 467-475.

Zhang, S., Xu, D., Li, Y., and Bai, M. (2013). “One-Dimensional Coupled Model of Surface Water Flow and Solute Transport for Basin Fertigation.” *J. Irrig. Drain Eng.*, 139(3), 181–192.

Zhao, D. H., Shen, H. W., Tabios, G. Q., Lai, J. S., and Tan, W. Y. (1994). “Finite volume two dimensional unsteady flow model for river basins.” *J. Hydraul. Eng.*, 120(7), 863-883.

PAPERS PRESNETED/PUBLISHED

1) **Kalita, H. M.,** Sarma, A. K., and Bhattacharjya, R. K. (2014), "Evaluation of Optimal River Training Work Using GA Based Linked Simulation Optimization Approach", Water Resources Management, Springer. Volume 28, Number 8, pp 2077-2092. (IF=2.259)

2) Sarma, A. K., **Kalita, H. M.** and Bhattacharjya, R. K. (2013), "Simulation-Optimization Linked model for Deciding Optimal River Training Work", International Workshop on Morphology of River Brahmaputra, held in Guwahati, India on 23-24 of October 2013.

3) **Kalita, H. M.,** and Sarma, A. K. (2012), "Efficiency and performances of finite difference schemes in the solution of Saint Venant's equation", International journal of civil and structural engineering, Integrated Publishing Association, Volume 2, Number 3, pp 941-949. (IF=0.289)

4) **Kalita, H. M.,** and Sarma, A. K. (2012), "Need of two-dimensional consideration for Modeling urban drainage", CD Proceedings of International conference on Environmentally Sustainable Urban Ecosystems (ENSURE 2012), held in IITGuwahati, India on 24-26 of February 2012.

5) Sarma, A. K., **Kalita, H. M.** and Bhattacharjya, R. K. (2011), "Mathematical model study for controlling bank erosion of Brahmaputra river", International Conference on the Status and Future of the World's Large Rivers, held in Vienna, Austria on 11-14 of April 2011.

6) **Kalita, H. M.,** and Sarma A. K. (2010), "2D Mathematical Modeling for Deciding Optimal Bank Protection Measures", International Conference organized by: Core Professional Group for the Brahmaputra (CPGB), held in Guwahati, India on 18-19 of December 2010.